Electronic Thesis and Dissertation Repository

4-13-2011 12:00 AM

Impact of Geomagnetically Induced Currents on Power Transformers

Jonathan E. Berge, *University of Western Ontario*

Supervisor: Dr. R. K. Varma, *The University of Western Ontario*
A thesis submitted in partial fulfillment of the requirements for the Doctor of Philosophy degree in Electrical and Computer Engineering
© Jonathan E. Berge 2011

Follow this and additional works at: https://ir.lib.uwo.ca/etd

 Part of the Other Earth Sciences Commons, and the Power and Energy Commons

Impact of Geomagnetically Induced Currents on Power Transformers

(Spine Title: Impact of GIC on Power Transformers)

(Thesis Format: Integrated-Article)

by

Jonathan (Jon) Eric <u>Berge</u>

Graduate Programme in Engineering Science

Department of Electrical and Computer Engineering

**Submitted in partial fulfillment
of the requirements for the degree of
Doctor of Philosophy**

**School of Graduate and Postdoctoral Studies
The University of Western Ontario
London, Ontario, Canada**

CERTIFICATE OF EXAMINATION

Supervisor

_____
Dr. Rajiv K. Varma

Co-Supervisor

_____
Dr. Luis Marti

Supervisory Committee

_____
Dr. Kazimierz Adamiak

_____
Dr. Lalu Mansinha

Examiners

_____
Dr. David Boteler

_____
Dr. Kamran Siddiqui

_____
Dr. Kazimierz Adamiak

_____
Dr. Anestis Dounavis

The thesis by

Jonathan (Jon) Eric Berge

entitled:

Impact of Geomagnetically Induced Currents on Power Transformers

is accepted in partial fulfilment of the
requirements for the degree of
Doctor of Philosophy

Date: _____   _____
                                          Chair of the Thesis Examination Board

Abstract

This thesis deals with the impact of Geomagnetically Induced Current (GIC) on power transformers in electrical power systems. A simulator to calculate the flows of GIC in an electrical power network, based on an assumed or measured induced geoelectric field is proposed. This simulator includes all needed mapping techniques to handle a system that covers a large geographical area.

A correlation between GIC and the reactive power absorbed in the core of the saturated transformer is proposed. That correlation is used to estimate GIC in a transformer utilizing existing reactive power measuring infrastructure within the electrical grid without the need for dedicated measurement equipment. This technique is validated by simulations with electromagnetic transients software, laboratory work and through data recorded during a GIC event on the Hydro One network. The slope correlating reactive power absorption to GIC from an electromagnetic transient model of the transformer may be used to predict GIC levels in the actual transformers.

The application of the technique correlating GIC with reactive power absorption is examined on a segment of a real 500 kV power transmission system. This technique allows GIC to be taken into account during load flow studies. Additionally, some benefits of increased visibility of GIC in the system are shown. A method to determine the frequency and magnitude of the harmonic currents generated by a saturated transformer is also proposed. It is expected that studies conducted in this thesis will be of value to utilities like Hydro One in planning mitigation measures against GICs.

Keywords: Geomagnetically Induced Current, Geomagnetism, Power system modeling, Power transmission meteorological factors, Transformer modeling

Co-Authorship

Publications originating from this thesis are listed below. The individual contributions of all members are listed.

Chapter 2

Article Title: A Software Simulator for Geomagnetically Induced Currents in Electrical Power Systems

Status: Published in *Proc. of the Canadian Conference on Electrical and Computer Engineering (CCECE 2009),* St. John's, Newfoundland, May 3-6, 2009. The version included in this thesis has been revised based on discussions originating at the conference and recent developments.

This work is supervised by Dr. R. K. Varma. The development of all models and algorithms is conducted by Jon Berge. The manuscript is written and prepared by Jon Berge with corrections by Dr. R. K. Varma. All figures are prepared by Jon Berge.

Chapter 3

Article Title: Determination of Geomagnetically Induced Current Flow in a Transformer from Reactive Power Absorption

Status: Final results will be submitted for publication in IEEE Transactions on Power Delivery.

This work is supervised by Drs. L. Marti and R. K. Varma, based on a concept proposed by Dr. L. Marti. The development of all models and algorithms is conducted by Jon Berge. All studies are preformed by Jon Berge. The manuscript is written and prepared by Jon Berge with corrections by Drs. L.

Marti and R. K. Varma. Dr. L. Marti contributed extensively to the introduction of the article. All figures are prepared by Jon Berge.

Chapter 4

Article Title: Laboratory Validation of the Relationship Between Saturating Current and Transformer Absorbed Reactive Power

Status: This work was performed exclusively for inclusion in this thesis, there is no intention to publish it elsewhere.

This work is supervised by Dr. R. K. Varma. All experiments are designed and conducted by Jon Berge. The manuscript is written and prepared by Jon Berge with corrections by Dr. R. K. Varma. All figures are prepared by Jon Berge.

Chapter 5

Article Title: Modelling and Mitigation of Geomagnetically Induced Currents on a Realistic Power System Network

Status: Final results will be submitted for publication in IEEE Transactions on Power Delivery.

This work is supervised by Drs. L. Marti and R. K. Varma. The development of all models and algorithms is conducted by Jon Berge. All studies are performed by Jon Berge. The manuscript is written and prepared by Jon Berge with corrections by Drs. L. Marti and R. K. Varma. All figures are prepared by Jon Berge.

Chapter 6

To Grandma and Grandpa,

It saddens me that your were not able to see me finish.

Acknowledgements

I would like to take the opportunity to show my sincere appreciation for my advisor, professor and mentor, Dr. Rajiv K. Varma. Dr. Varma, I am indebted to you not only for the support that you have given to me over my numerous years I have been your student, but also for the faith that you have unwaveringly shown in my abilities and the countless opportunities that you have opened for me.

I am indebted to Dr. Luis Marti, for posing a challenging topic and for taking the time and energy to supervise me. Dr. Marti, your insights and experience have proven invaluable, what I have learned working under you, I could not have replicated with a lifetime of study. Thanks are also owed to the staff with whom I worked at Hydro One for your friendship, advice and support, with special thanks to Dr. Afshin Rezaei Zare, who's perspectives on transformer modeling were tremendously valuable.

To my fellow students, all of you who I have know over the years, your names are too numerous to fill this page, but that does not mean that I do not value and remember what we have done together.

To my dear friends, again, your names and our stories are too many and too great for this humble page. I cherish you all.

Finally, to my parents, thank you so much, your invaluable love, support and guidance that has allowed me to achieve this and every thing that has come before it.

– Jon

Table of Contents

List of Tables

List of Figures

Chapter 1   Introduction

1.1 Background

Since the early days of long distance telegraph lines, the engineering community has been aware that at times geomagnetic disturbances have caused extremely low frequency currents to appear in long grounded electrical conductors such as those used in communications and electrical systems. This has come to be known as Geomagnetically Induced Current (GIC) [1-10]. These low frequency currents are typically in the order of 0.1 to 0.001 Hz, and for the purposes of electrical system analysis are considered DC. It is also possible for GIC to flow in ungrounded horizontal loops, where the magnetic field is non-uniform [1].

During disturbances, often accompanying a solar flare, the sun releases a cloud of plasma. If this cloud interacts with the Earth's magntic field electric currents are generated in the magnetosphere and ionosphere. These electric currents cause a short-term variation in the earth's magnetic field, which in turn creates an electric field at the surface of the affected region of the planet. GIC typically affects systems at auroral latitudes (regions near the earth's magnetic poles) and follows the 22 year solar cycle [11]. GIC activity peaks once during the 11 year half cycle [2, 3, 5]. While GIC events are more likely to occur during a peak, they are by no means limited to occurring at peak times.

From a geophysical perspective there are two indices used to measure the impact of a geomagnetic storm. While neither index is detailed enough to assess the specific impact of a given event on a power systems, they do give

an appreciation for the severity of a given storm. The *ap* index is a linear representation of the range of observed dB/dt at a given site for every three hour period. The *Ap* index is the average of the eight *ap* indices over the course of a day. The *K* index, ranges from 0 to 9 and is a quasi-logarithmic representation *ap* index compared to a quiet day reference. A global *Kp* index uses *K* indices from multiple observatories [12].

The Québec Blackout of March 13th, 1989 [13, 14] brought the potential for GIC to have catastrophic effects on the power system into the forefront of the minds of power engineers.

The process of understanding GIC can be divided into two distinct categories: geophysical and engineering. The underlying geophysical concepts are summarised by Boteler in [15]. The solution of the geophysical problem will typically yield an electric field over the earth's surface [15, 16]. This field is used to determine the currents induced in the electrical power system and ultimately the effect of those currents on the stability and security of the electrical power system. However, a review of the geophysics of GIC is beyond the scope of this chapter. GIC is ultimately dependent on the mutual inductance of three currents, the electro jet in the atmosphere, the telluric current in the earth, and GIC in manmade conductive networks. The impact of manmade conductive system is considered minimal on the electro jet and telluric currents and is neglected in calculating. The potential induced in manmade networks is dependant on the other two currents.

This review attempts to provide a comprehensive background of the engineering material published on the topic of GIC during the period 1990 to 2006. This time period covers the majority of work that originated in response to the March 1989 Blackout as well as some contemporary material.

Material published prior to 1990 is reviewed in [17]. Papers from other than IEEE publications are limited to those that are in the English language, and readily available for study.

During 1989 and the early 1990s there was a large amount of material published on GIC, including a 1989 EPRI conference dedicated to GIC. This was a direct response to Québec blackout and other power system problems that occurred on March 13th, 1989 and the sense of urgency it imparted on the power engineering community.

This chapter covers 6 general subtopics within the sphere of GIC. These topics ere: Effects of GIC, Measurement and Monitoring, Forecasting, Modelling, System Solution, and Mitigation. Of the 85 papers referenced in this review nearly one third of them cover effects of GIC on various components of electrical power systems, primarily transformers. The remaining papers treat the remaining topics fairly evenly.

1.1.1 Effects of GIC

The effect of GIC on an electrical power system is typically studied as constituent effects on individual subsystems and components. The areas which have received attention in the papers reviewed are protection systems, Static VAr Compensators, High Voltage Direct Current (HVDC) Transmission, transformers and generators.

The effects of GIC are seen primarily at higher latitudes. This is because the changes in magnetic field that cause GIC are greatest in these regions. In the northern hemisphere, the regions affected primarily by GIC are central and eastern Canada [14], the Scandinavian nations [18-21] and to a lesser extent, the north-eastern United States and the British Isles [18]. The

likelihood of a significant GIC event in north-western Eurasia is reduced because the earth's magnetic field is offset, the magnetic north pole is not located at the geographic North Pole, but rather in the Canadian arctic. The magnetic south pole is comparably skewed, in this case towards Australia. In the southern hemisphere, GIC, and associated transformer failures, have been reported in South Africa [20, 21]. Work is also being done to monitor GIC in the transmission system in China [22-29].

The net GIC impact on a system is dependent not only on the magnitude of the magnetic disturbance, but on its orientation. The induced current in a given conductor is proportional to both the magnitude of the field as well as the sine of the angle of the field relative to the conductor [30]. This is supported by studies performed in Québec [31, 32] where large (>1V/km) electrical fields were seen most often with either easterly or westerly orientations. Typically the field causing GIC is primarily east-west, because the electrojet follows lines of magnetic latitude.

1.1.1.1 Transformers

The main impact of GIC on electrical power systems is through the transmission transformers with grounded neutrals. The DC GIC causes the transformer core to saturate; which has detrimental effects on the transformer operation.

The magnetic flux in a transformer core is proportional to the integral of the voltage supplying the transformer [33]. The DC GIC will cause a DC component to this voltage. This DC voltage will cause the transformer core flux to increase as the GIC event continues. The magnetic history of the transformers is important in determining the effect of a given GIC event. If there is a pre-existing residual flux in the same direction as the GIC induced

flux the transformer will saturate sooner, conversely if the pre-existing flux opposes the GIC induced flux, transformer saturation will be delayed [34-37].

Because of the decreased slope of the transformer B-H curve in the saturated region, the required AC magnetizing current increases dramatically - often hundreds to thousands of times the normal magnetizing current [3, 38-43]. This increases the reactive power draw of the transformer drastically. In the knee region of the B-H curve, the AC magnetizing current is asymmetrical; this causes the draw of both odd and even harmonic currents [33, 34, 40-42, 44-48]. The large reactive and harmonic draws of GIC saturated transformer make proper operation of the power system difficult and tend to lead to power system instabilities.

Since the influence of GIC on a transformer is primarily through the saturation of its core, the construction of the transformer core is critical to understanding the impacts of GIC. Typical transformer core constructions are shown in Figure 1.1. The susceptibility of a transformer core to GIC saturation is dependent of the presence of DC flux paths [49, 50]. In the case of a three-phase three-leg transformer there is no complete DC flux path in the core. In these transformers, the DC flux must leak into the transformer tank. Typically all transformer types see some degree of flux leakage into the tank [46]. Because the transformer tank is not designed as a magnetic core, the tank can be very susceptible to damage due to heating.

Single-phase transformers are considered the most vulnerable to GIC [37]. Of the three-phase transformer constructions, they are generally ranked by susceptibility as follows [49, 50]:
1. shell-form (conventional) core – most susceptible
2. three-phase, seven-leg

3. three-phase, five-leg

4. three-phase, three-leg – least susceptible [51]

There will be variations in the susceptibility of individual transformers depending on their specific construction.
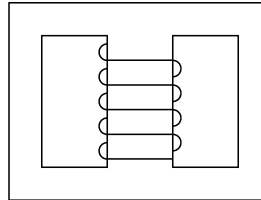
Single-phase
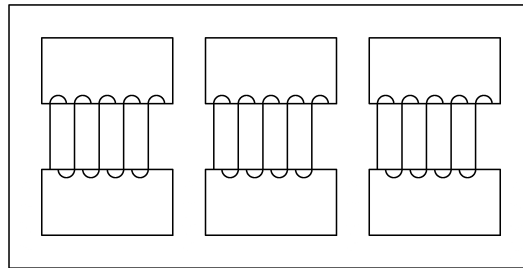
Three-phase shell-form
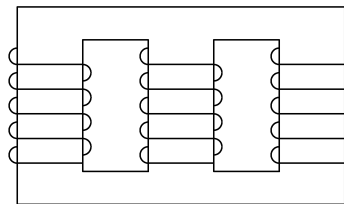
Three-phase three-leg
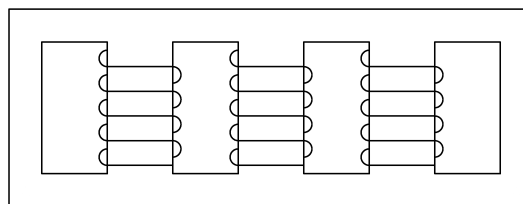
Three-phase five-leg
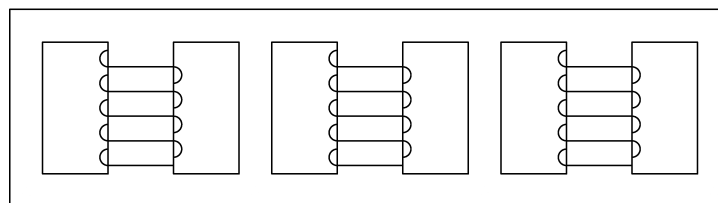
Three-phase seven-leg

Figure 1.1: Transformer core types

The increased magnetizing current drawn by the GIC saturated transformer results in substantially greater core losses in the transformer. These core losses result in increased heating both in the transformer core and in other metallic components because of flux leakage. This heating can severely reduce the lifespan of a transformer [40]. GIC induced transformer heating has been shown to cause the breakdown of transformer oil [39, 40]. During the 1989 geomagnetic storm that caused the Québec blackout a generator transformer at a nuclear station in New Jersey was destroyed due to overheating [6, 16]. In addition to the high cost of replacing the custom transformer, there was a significant lost revenue cost due to the 6 week downtime to source a replacement unit. Were a replacement not available, the lead time was estimate at one year.

1.1.1.2 Protection

GIC impacts protection systems in two ways: directly, due to the DC current induced in the lines, the other, is due to the large harmonic currents from saturated transformers. The presence of GIC itself should not be grounds for protective equipment to trip, however, the interaction with GIC can cause the misoperation of protective relays.

Traditional electro-mechanical relays are subject to additional relay torque from the harmonic components. This additional torque has been shown to account for upwards of 40% of the relay torque during a GIC event [52]. There is no relay torque caused by the DC current since electro-mechanical relay installations use traditional CTs and PTs which effectively block DC. Some effects have been documented on CTs [53].

In the case of microprocessor-based relaying, the effects of GIC are very much dependant on the relaying algorithms used. If a protective relay estimates

values based on either average or peak values, the measurements will be skewed by the presence of GIC induced harmonics [33, 52]. The use of a more sophisticated algorithm that would have the relay respond only to the fundamental would reduce the relay's vulnerability to misoperation due to GIC. When assessing the vulnerability to GIC of a protection scheme it is important to use a detailed model of the relay being used including the measurement algorithms [52].

Capacitor protection is impacted substantially by GIC. Capacitor banks present a low impedance path to the harmonic currents from saturated transformers. The flow of these harmonic currents can cause the capacitor overvoltage or overcurrent protection to trip [52, 54]. Additionally, capacitor neutral or unbalance protection may trip because of the asymmetrical nature of GIC-caused harmonics [33]. Current ANSI overvoltage limits for capacitor, which govern capacitor protective relay settings, are based on oil impregnated paper dielectric capacitors. Modern all film dielectric capacitors have a substantially greater capacity to withstand overvoltage conditions without sustaining damage [38]. This design improvement has not seen widespread adoption into relay settings, but would substantially reduce the likelihood of capacitor tripping during a GIC event. Because of the potential for voltage sags due to the increased reactive power demand of saturated transformers, it is of critical importance that capacitors be available during a GIC event to provide voltage support.

1.1.1.3 Static VAr Compensators

Static VAr Compensators (SVCs) allow the dynamic control of bus voltage in a power system by varying the reactance that they present to the bus to be controlled. This control improves system stability by allowing operators to regulate voltages at key buses to maintain load voltages, or modulate power

flow. A typical SVC uses a thyristor controlled reactor in parallel with either fixed or switched capacitor banks.

The introduction of a strong second harmonic at the terminals of an SVC can affect the thyristor firing controller such that there is an asymmetry in the reactor current. This asymmetry is essentially due to a DC current that will saturate the reactor, and needs to be mitigated. Conventional control methods for TCR balancing do not mitigate the second harmonic at the SVC terminals, but can in fact increase it depending on the system parameters [33]. When there is a foreseen need to mitigate second harmonic contamination, a TCR Balancing Controller is employed to eliminate TCR DC current [55].

1.1.1.4 High Voltage Direct Current Transmission

While little work has been done on the impact of GIC on High Voltage Direct Current (HVDC) systems, some effects have been observed at an HVDC substation in Québec [56]. In this case, the interaction between the saturated transformers at the generators and the converter station generated 5th and 7th harmonic currents on the AC side of the converter. These currents were amplified by the 6th harmonic filter on the DC side of the converter.

1.1.1.5 Generators

The proximity of generators to their step up transformers and the delta-wye design of those transformers ensure that no DC current due to GIC flows into generators. However the increased reactive, negative sequence and harmonic currents caused by the saturation of the generator step-up transformer on the high voltage side are injected into the generator. It has been found that these currents place stress on the generator windings, possibly causing over heating and in the case of harmonic currents, vibration [33, 42, 57].

1.1.2 Measurement and Monitoring

The generally accepted practice for measuring GIC in an electrical system is to install Hall-effect sensors on the neutral conductor of selected transformers. After appropriate filtering and conditioning, a measurement of the DC current in the transformer neutral is attained [58, 59]. The Sunburst system, developed by EPRI, uses this techniques and has been implemented in the United States, (primarily in the North East), Manitoba (on a feeder supplying Minnesota) [58], and in England and Wales [60]. The Minnesota power system also uses DC current measurement directly on a 500 kV phase conductor [61].

The principal disadvantage of this real time monitoring technique is that it does not provide warning necessary to enact changes necessary to protect the system [57, 58]. This drawback is common to any real time monitoring technique. Transformer neutral current monitoring has additional drawbacks; typically only selected neutrals will be monitored. This means that assumptions about the geo-electric field must be made in order to estimate the current in each line [62].

Transformer neutral currents are sometimes used to trigger events like dispatch alarms and fault recorders in order to facilitate the management and analysis of GIC incidents [13, 61, 63]. Parameters that are considered of interest with regard to the effects of GIC include system voltages and reactive power consumptions as well as, transformer tank temperature, transformer oil gassing, transformer noise and vibration [61, 63].

In order to better understand the cause of GIC, utilities and researchers are interested in electric and magnetic fields at the earth's surface. Magnetometers are used to measure and record magnetic field data [31, 61].

Electric fields have been measured using two methods, by either an isolated or grounded dipole [13, 31].

1.1.3 Forecasting

Real-time measurement of GIC is useful for understanding system status and for the after-the-fact analysis of events, because it provides a record of the GIC on the system. It has limited benefit to system operators in ensuring that a system survives a GIC event [62, 64]. In the absence of reasonably accurate GIC forecasts, the operating alternatives are to react to every potential GIC event. While this is a prudent measure, it typically leads to significant losses in revenue due to generation redistribution and reduction in power transfers [52, 64]. The less prudent measure is to ignore the possibility of GIC, but this mindset increases the possibility of a GIC event having catastrophic causes.

The simplest forecasting technique relies on an empirical relationship between ap index and GIC in a given power system segment [12]. This method has the disadvantages of not being adaptable because as the power system changes new empirical data must be gathered. Also, since the ap index is non directional, it does not account for the directional variability of the impact of geomagnetic fields variation on GIC.

A more sophisticated modelling technique uses a predicted auroral electrojet, the ionospheric current that is the principal cause of the magnetic field variations responsible for GIC. From this predicted electrojet, using Faraday's law:

$$V = -\int \frac{\partial B}{\partial t} \cdot ds \tag{1}$$

It is possible to calculate the electric field imposed by the geomagnetic event. Calculating GIC from this field is a relatively easy exercise. This calculation, however requires a good earth conductivity model [62, 67-69]

A computationally simpler alternative uses either an empirical or measured Earth *surface impedance* Z (representing the Earth response) to calculate the voltage field based on horizontal magnetic field [68, 69]. The impact of man made conductive networks is neglected in this calculation, because of the high grounding resistance of those networks when compared to Z.

$$-E_y = \frac{Z}{\mu_0} B_x \qquad (2)$$

The deployment of the ACE satellite to monitor incoming solar winds provides an opportunity to improve the accuracy of GIC forecasting by giving a one hour warning of a charged particulate stream destined for earth [64-66].

1.1.4 Modelling

Depending on the level of sophistication desired, it becomes necessary to model the earth and apply a magnetic field, as described above to calculate induced potentials. In order to appreciate the impact on reactive power flows, it is necessary to model the effects of the DC GIC on transformers.

The power system is typically modeled by its DC equivalent, taking the DC resistances of transmission lines and transformer windings [70]. The secondary side of distribution and generation transformers are often

neglected because it is assumed that no GIC is induced in the connected systems.

1.1.4.1 Earth Modelling

In order to calculate the electric field created by a given magnetic field, an electrical model of the earth is needed. Typically this model must be simplified based on assumptions in order to allow the model to be analysed given limited computing resources [71-75].

1.1.4.2 Field Modelling

It is simpler and often sufficient to model GIC using an assumed electric field instead of modelling the magnetic field and the earth. In this case the typical methods are to use a uniform electric field, or a piecemeal collection of uniform fields [76-79]. This option is computationally simple though not realistic. From the perspective of the electrical system model the electric filed is represented as line induced voltage (series sources in the transmission lines).

Realistic fields must follow the physics governing electric fields, as summarised in [76] and [35]. When using realistic fields, induced electric fields cannot be represented as earth surface potentials.

1.1.4.3 Transformer Modelling

The primary effect of GIC is the saturation of transformers. Because of this, accurate transformer modelling is critical to understanding GIC effect on a power system. It is necessary to model the low frequency and saturated behaviour of the transformer. This is typically done by modelling the detailed physics of the transformer core [35, 80], taking into account variables such as core geometry and winding construction [39].

1.1.5 System Solution

The method used for calculating the geomagnetically induced current in a power system based on a voltage field is essentially a DC load flow calculation. The DC resistance of the various components of the power system are represented in an admittance matrix. The ground resistance must also be considered. The induced voltages in the various transmission lines are represented, and the system may be solved for the GIC in each transmission line.

When solving for the GIC in a practical system, there may be actual field data, typically transformer neutral currents from selected stations, in addition to the estimated voltage field data. In this case, the system becomes overdetermined and special techniques must be used to solve it [81].

1.1.6 Mitigation

There are numerous possible strategies for mitigating the effects of GIC in electrical power systems. Typical operational GIC mitigation strategies used when a geomagnetic event is forecast include [13]:

- Increasing spinning reserve and more evenly distributing generation resources
- Reducing transmission line loading
- Cancelling maintenance and bringing all lines into service
- Minimizing switching operations
- Modifying or blocking protection systems prone to GIC interference

Another proposed mitigation strategy is to inject a DC current into transformer auxiliary winding to cancel the DC GIC [82]. The constant magnetic field induced in the transformer core by this compensating winding

would have to be opposite in sign and equal in magnitude to the GIC induced field.

GIC may be effectively blocked using capacitors. The insertion of series blocking capacitors directly into transmission lines is not feasible because of the costs of high voltage capacitors. If however, series capacitors are inserted for reasons of improving system stability, they do provide the side benefit of blocking GIC. The more common solution is to install DC blocking capacitors on transformer neutrals. This has been done both to block GIC as well as stray current from single-ended HVDC transmission [3, 83, 84].

Great care must be taken in the design of neutral blocking capacitors in order to prevent the capacitors from causing further problems in power system operation [3, 13, 83-85]. Neutral blocking capacitors can cause problems with:

- Insulation co-ordination
- Ferroresonance
- Resonance
- Relaying

These problems are typically avoided by employing a voltage limiting scheme on the neutral blocking capacitor. This can be done either with a spark gap [3, 85], varistor, or thyristor switch [83, 84].

1.2 Motivation

While it is well established that the primary effects of GIC on electrical power transmission systems centre around transformers, the relationship between GIC and the impacts on transformers is not quantified in a sufficient manner.

The ability to measure GIC, or the effects of GIC in electrical power networks is presently something that can only be achieved through the costly deployment of dedicated hardware. This has severely limited the deployment of GIC measurement equipment and basically leaves system operators in the position of attempting to manage GIC events without insight into how those events are affecting the system. Giving operators better visibility into a GIC event will improve their ability to asses and manage a GIC event.

While the historic impact of GIC on electrical power transmission networks has been limited to one large scale event, there is an increasing concern in the electrical power transmission energy about the detrimental effects of GIC. Utilities are presently preparing for the upcoming peak in solar activity expected late 2011 through 2013. As electrical transmission networks become more interconnected the consequences of a severe GIC event will be more widespread.

1.3 Objective

In very broad terms, this thesis seeks to define the relationship between GIC and its two principal effects on transformers, reactive power absorption and generation of harmonic currents. It will use the relationship between GIC and transformer reactive power absorption as a tool to measure GIC within an electrical network.

1.4 Outline

A brief outline of each thesis chapter is presented in this section. Chapter 2 presents a software GIC simulator to solve the DC model of the electrical grid. This will allow for the calculation of expecting GIC flows given a knowledge of induced electric fields within the network. Chapter 3 defines

the relationship between GIC and transformer reactive power absorption. This relationship will be used to measure the magnitude of the GIC in power transformers, by observation of the reactive power absorbed by those transformers. Chapter 4 illustrates a laboratory verification of the relationship between GIC and transformer absorbed reactive power. Chapter 5 presents a system study of GIC in a segment of a 500kV power transmission system. Using the principles developed in previous chapters, the impact of the GIC event on voltage profile is examined. The availability of the magnitude of GIC is explored from the perspective of an operator's ability to react to GIC and manage the network. Chapter 6 presents a mathematical examination of the harmonics generated by a transformer saturated by GIC. The conclusions of the thesis are presented in Chapter 7.

References

[1] R. Pirjola, "Geomagnetically induced currents during magnetic storms," IEEE Trans. Plasma Sci., vol. 28, pp. 1867-1873, 2000.

[2] D. H. Boteler, "Geomagnetic hazards to conducting networks," Nat. Hazards, vol. 28, pp. 537-561, 2003.

[3] V. Albertson, J. Kappenman and B. Damsky, "The influence of geomagnetically induced currents (GIC) on transmission systems," in Proceedings of the American Power Conference, 1990, pp. 311-15.

[4] T. S. Molinski, W. E. Feero and B. L. Damsky, "Shielding grids from Solar Storms," IEEE Spectrum, vol. 37, pp. 55-60, 2000.

[5] D. H. Boteler, R. J. Pirjola and H. Nevanlinna, "Effects of geomagnetic disturbances on electrical systems at the earth's surface," Advances in Space Research, vol. 22, pp. 17-27, 1998.

[6] J. G. Kappenman, "Geomagnetic Storms and Their Impact on Power Systems." IEEE Power Engineering Review, May 1996.

[7] J. G. Kappenman and V. D. Albertson, "Bracing for the geomagnetic storms," IEEE Spectrum, vol. 27, pp. 27-33, 1990.

[8] A. Vilianen and R. Pirjola, "Finnish geomagnetically induced currents project," IEEE Power Engineering Review, vol. 15, pp. 20-21, 1995.

[9] Q. Liu, Y. Wang and L. Liu, "Design and development on VxWorks-based GIC monitoring system", *2010 International Conference on Educational and Network Technology, ICENT 2010, June 25, 2010 - June 27,* p. 290-293, 2010.

[10] R. Pirjola, "Calculation of geomagnetically induced currents (GIC) in a high-voltage electric power transmission system and estimation of effects of overhead shield wires on GIC modelling", *J.Atmos.Solar Terr.Phys.,* vol. 69, no. 12, p. 1305-11, 2007.

[11] L. Trichtchenko, D. H. Boteler, " Response of Power Systems to the Temporal Characteristics of Geomagnetic Storms," in 2006 Canadian Conference on Electrical and Computer Engineering, 2006, pp. 4.

[12] L. Trichtchenko and D. H. Boteler, "Modeling geomagnetically induced currents using geomagnetic indices and data," IEEE Trans. Plasma Sci., vol. 32, pp. 1459-1467, 2004.

[13] L. Bolduc, "GIC observations and studies in the Hydro-Québec power system," J. Atmos. Solar Terr. Phys., vol. 64, pp. 1793-1802, 2002.

[14] D. H. Boteler, "Assessment of geomagnetic hazard to power systems in Canada," Nat. Hazards, vol. 23, pp. 101-120, 2001.

[15] D. H. Boteler, "Geomagnetically induced currents: present knowledge and future research," IEEE Trans. Power Del., vol. 9, pp. 50-58, 1994.

[16] R. Pirjola, "Space weather effects on technological systems on the ground," in Proceedings Asia-Pacific Conference on Environmental Electromagnetics. CEEM 2000, 3-7 may 2000, pp. 217-21.

[17] J. Kolawole, S. Mulukulta and D. Glover, "Effect of geomagnetic-induced-current on power grids and communication systems: A review," in Proc. of 22 Annual North-American Power Symposium, 1990, pp. 251-62.

[18] Risto J. Pirjola, David H. Boteler, "Geomagnetically Induced Currents in European High-Voltage Power Systems," in 2006 Canadian Conference on Electrical and Computer Engineering, 2006, pp. 1263-1266.

[19] R. Pirjola, A. Pulkkinen and A. Viljanen, "Studies of space weather effects on the Finnish natural gas pipeline and on the Finnish high-voltage power system," Advances in Space Research, vol. 31, pp. 795-805, 2003.

[20] J. Koen and T. Gaunt, "Geomagnetically induced currents in the Southern African electricity transmission network," in 2003 IEEE Bologna PowerTech, 23-26 June 2003, 2003, pp. 7 pp. Vol.1.

[21] C. T. Gaunt and G. Coetzee, "Transformer failures in regions incorrectly considered to have low GlC-risk", Power Tech 2007, p. 445-1, 1-5 July 2007.

[22] M. Cui, C. Liu, L. Liu and X. Zhang, "Preliminary study of the influence caused by solar storm on sichuan power grid", *2010 International Conference on Power System Technology: Technological Innovations Making Power Grid Smarter, POWERCON2010, October 24, 2010 - October 28,* p. IEEE Power Engineering Society (IEEE/PES); Chinese Society for Electrical Engineering (CSEE), 2010. 2010.

[23] C. Liu, L. Liu and X. Niu, "Disastrous space weather risk on large-scale power grid", *2010 5th International Conference on Critical Infrastructure, CRIS 2010, September 20, 2010 - September 22,* p. Institute of Electrical and Electronics Engineers (IEEE); Chinese Society for Electrical Engineering (CSEE), 2010.

[24] Q. Liu, Y. Wang and L. Liu, "Design and development on VxWorks-based GIC monitoring system", *2010 International Conference on Educational and Network Technology, ICENT 2010, June 25, 2010 - June 27,* p. 290-293, 2010.

[25] R. Pirjola, C. Liu and L. Liu, "Geomagnetically induced currents in electric power transmission networks at different latitudes", *2010 Asia-Pacific Symposium on Electromagnetic Compatibility, APEMC 2010, April 12, 2010 - April 16,* p. 699-702, 2010.

[26] J. Wang, Y. Wang and L. Liu, "Design of the web-based monitoring system architecture for geomagnetically induced current", *2010 International Conference on Educational and Network Technology, ICENT 2010, June 25, 2010 - June 27,* p. 244-247, 2010.

[27] Y. Wang, J. Wang and L. Liu, "Design and implementation of the web-based monitoring system for geomagnetically-induced current", *2010 IEEE International Conference on Intelligent Computing and Intelligent Systems, ICIS 2010, October 29, 2010 - October 31,* vol.3, p. 530-533, 2010.

[28] Chun-Ming Liu, Lian-Guang Liu and Y. Yang, "Monitoring and modeling geomagnetically induced currents in power grids of china", 2009 Asia-Pacific Power and Energy Engineering Conference, p. 4, 28-31 March 2009.

[29] F. He, X. Mu and L. Liu, "Wavelet de-noising and correlation analysis in gic signal during magnetic storm", *2008 International Workshop on Modelling, Simulation and Optimization, WMSO 2008, December 27, 2008 - December 28,* p. 3-6, 2008.

[30] D. H. Boteler, Q. Bui-Van and J. Lemay, "Directional sensitivity to geomagnetically induced currents of the Hydro-Quebec 735 kV power system," IEEE Trans. Power Del., vol. 9, pp. 1963-1971, 1994.

[31] L. Bolduc, P. Langlois, D. Boteler and R. Pirjola, "Study of geoelectromagnetic disturbances in Quebec, 1. General results," IEEE Trans. Power Del., vol. 13, pp. 1251-1256, 1998.

[32] L. Bolduc, P. Langlois, D. Boteler and R. Pirjola, "Study of geoelectromagnetic disturbances in Quebec, 2. Detailed analysis of a large event," IEEE Trans. Power Del., vol. 15, pp. 272-278, 2000.

[33] L. Bolduc, A. Gaudreau and A. Dutil, "Saturation time of transformers under dc excitation," Electr. Power Syst. Res., vol. 56, pp. 95-102, 2000.

[34] V. D. Albertson, B. Bozoki, W. E. Feero, J. G. Kappenman, E. V. Larsen, D. E. Nordell, J. Ponder, F. S. Prabhakara, K. Thompson and R. Walling, "Geomagnetic disturbance effects on power systems," IEEE Trans. Power Del., vol. 8, pp. 1206-1216, 1993.

[35] W. Chandrasena, P. G. McLaren, U. D. Annakkage and R. P. Jayasinghe, "Modeling GIC effects on power systems: The need to model magnetic status of transformers," in 2003 IEEE Bologna PowerTech, 23-26 June 2003, 2003, pp. 6 pp. Vol.2.

[36] R. A. Walling and A. H. Khan, "Characteristics of transformer exciting-current during geomagnetic disturbances," IEEE Trans. Power Del., vol. 6, pp. 1707-1714, 1991.

[37] A. P. S. Meliopoulos, G. J. Cokkinides and M. Rabinowitz, "Comparison of SS-GIC and MHD-EMP-GIC effects on power systems," IEEE Trans. Power Del., vol. 9, pp. 194-207, 1994.

[38] Y. You, E. F. Fuchs, D. Lin and P. R. Barnes, "Reactive power demand of transformers with DC bias," IEEE Ind. Appl. Mag., vol. 2, pp. 45-52, 1996.

[39] R. S. Girgis and C. Ko, "Calculation techniques and results of effects of GIC currents as applied to large power transformers," IEEE Trans. Power Del., vol. 7, pp. 699-705, 1992.

[40] R. S. Girgis, Chung-Duck Ko and D. J. Scott, "Analysis of transformer overheating due to geomagnetically induced currents," in Proceedings of the American Power Conference, 29 April-1 may 1991, 1991, pp. 1167-72.

[41] M. Lahtinen and J. Elovaara, "GIC occurrences and GIC test for 400 kV system transformer," IEEE Trans. Power Del., vol. 17, pp. 555-561, 2002.

[42] R. A. Walling and A. H. Khan, "Why solar storms can cause system havoc," Electr. World, vol. 204, pp. 39-40, 08. 1990.

[43] E. Mulasalihovic, H. Pfutzner, S. Traxler and H. Yamaguchi, "Effects of geomagnetically induced currents on the magnetic performance of transformer cores", *J Magn Magn Mater,* vol. 320, no. 20, p. 920-924, 2008.

[44] S. Lu, Y. Liu and J. D. L. Ree, "Harmonics generated from a DC biased transformer," IEEE Trans. Power Del., vol. 8, pp. 725-731, 1993.

[45] S. Lu and Y. Liu, "Study of power transformer excitation under GIC," in Proceedings of the 36th Midwest Symposium on Circuits and Systems, Aug 16-18 1993, 1993, pp. 879-882.

[46] P. R. Price, "Geomagnetically induced current effects on transformers," IEEE Trans. Power Del., vol. 17, pp. 1002-1008, 2002.

[47] X. Dong, Y. Liu and J. G. Kappenman, "Comparative analysis of exciting current harmonics and reactive power consumption from GIC saturated transformers," in 2001 IEEE Power Engineering Society Winter Meeting, Jan 28-Feb 1 2001, 2001, pp. 318-322.

[48] J. Yao, M. Liu, C. Li and Q. Li, "Harmonics and reactive power of power transformers with DC bias", *Asia-Pacific Power and Energy Engineering Conference, APPEEC 2010, March 28 - March 31,* 2010.

[49] S. Lu and Y. Liu, "FEM analysis of DC saturation to assess transformer susceptibility to geomagnetically induced currents," IEEE Trans. Power Del., vol. 8, pp. 1367-1376, 1993.

[50] N. Takasu, T. Oshi, F. Miyawaki, S. Saito and Y. Fujiwara, "Experimental analysis of DC excitation of transformers by geomagnetically induced currents," IEEE Trans. Power Del., vol. 9, pp. 1173-1182, 1994.

[51] M. A. S. Masoum and P. S. Moses, "Impact of balanced and unbalanced direct current bias on harmonic distortion generated by asymmetric three-phase three-leg transformers", *IET Electric Power Applications,* vol. 4, no. 7, p. 507-515, 2010.

[52] B. Bozoki, S. R. Chano, L. L. Dvorak, W. E. Feero, G. Fenner, E. A. Guro, C. F. Henville, J. W. Ingleson, S. Mazumdar, P. G. McLaren, K. K. Mustaphi, F. M. Phillips, R. V. Rebbapragada and G. D. Rockefeller, "Effects of GIC on protective relaying," IEEE Trans. Power Del., vol. 11, pp. 725-739, 1996.

[53] Changyun Li, Qingmin Li, Jinxia Yao, Min Liu, "The characteristics of electromagnetic current transformers with DC bias," International Conference on Sustainable Power Generation and Supply, 2009.

[54] R. P. Jayasinghe, P. G. McLaren and T. Gouldsborough, "Effect of GIC on overcurrent protection for filter banks," in 1993 IEEE Wescanex Conference, May 17-18 1993, 1993, pp. 36-42.

[55] The Electric Power Research Institute (EPRI) Report TR-100696, "Improved Static VAr Compensator Control." Final Report of Project 2707-01, Prepared by General Electric (GE) Company, Scanectity, NY, June 1992.

[56] D. L. Dickmander, S. Y. Lee, G. L. Desilets and G. L. Granger, "Ac/dc harmonic interactions in the presence of GIC for the Quebec-New England phase II hvdc transmission," IEEE Trans. Power Del., vol. 9, pp. 68-78, 1994.

[57] W. B. Gish, W. E. Feero and G. D. Rockefeller, "Rotor heating effects from geomagnetic induced currents," IEEE Trans. Power Del., vol. 9, pp. 712-719, 1994.

[58] R. L. Lesher, J. W. Porter and R. T. Byerly, "Sunburst - A network of GIC systems," IEEE Trans. Power Del., vol. 9, pp. 128-137, 1994.

[59] L. Lian-guang, Z. Hao, L. Chun-ming, G. Jian-hui and G. Qing-xiong, "Technology of detecting GIC in power grids and its monitoring device," in 2005 IEEE/PES Transmission and Distribution Conference and Exhibition: Asia and Pacific, Aug 15-18 2005, 2005, pp. 1546843.

[60] I. A. Erinmez, "Managing the impact of geomagnetically induced currents on the NGC transmission system," in Proceedings of 2001 Winter Meeting of the IEEE Power Engineering Society, 28 Jan.-1 Feb. 2001, 2001, pp. 336 vol.1.

[61] D. R. Fagnan, P. R. Gattens and F. D. Johnson, "Monitoring solar magnetic disturbances in power systems (a summary)," IEEE Power Engineering Review, vol. 10, pp. 4-6, 1990.

[62] I. A. Erinmez, J. G. Kappenman and W. A. Radasky, "Management of the geomagnetically induced current risks on the national grid company's electric power transmission system," J. Atmos. Solar Terr. Phys., vol. 64, pp. 743-756, 2002.

[63] T. H. Breckenridge, T. Cumming and J. Merron, "Geomagnetic induced current detection and monitoring," in Proceedings of 7th International Conference on Developments in Power Systems Protection (DPSP 2001), 9-12 April 2001, 2001, pp. 250-3.

[64] J. G. Kappenman, "Geomagnetic storm and power system impacts: Advanced storm forecasting for transmission system operations," in 1999 IEEE Power Engineering Society Summer Meeting, 1999, pp. 1187-91.

[65] R. Pirjola, D. Boteler, A. Viljanen and O. Amm, "Prediction of geomagnetically induced currents in power transmission systems," Advances in Space Research, vol. 26, pp. 5-14, 2000.

[66] A. Pulkkinen, M. Hesse, S. Habib, d. Z. van, B. Damsky, F. Policelli, D. Fugate, W. Jacobs and E. Creamer, "Solar shield: Forecasting and mitigating space weather effects on high-voltage power transmission systems", *Nat.Hazards,* vol. 53, no. 2, p. 333-345, 2010.

[67] J. G. Kappenman, W. A. Radasky, J. L. Gilbert and I. A. Erinmez, "Advanced geomagnetic storm forecasting: A risk management tool for electric power system operations," IEEE Trans. Plasma Sci., vol. 28, pp. 2114-2121, 2000.

[68] D. H. Boteler, "Calculating the voltages induced in technological systems during a geomagnetic disturbance," IEEE Trans. Electromagn. Compat., vol. 41, pp. 398-402, 1999.

[69] R. Pirjola and D. Boteler, "Calculation methods of the electric and magnetic fields at the Earth's surface produced by a line current," Radio Sci., vol. 37, pp. 14-1, 2002.

[70] F. S. Prabhakara, L. N. Hannett, R. J. Ringlee and J. Z. Ponder, "Geomagnetic effects modelling for the PJM interconnection system--II: Geomagnetically induced current study results," IEEE Trans. Power Syst., vol. 7, pp. 565-571, 1992.

[71] J. N. Towle, F. S. Prabhakara and J. Z. Ponder, "Geomagnetic effects modelling for the PJM interconnection system--I: Earth surface potentials computation," IEEE Trans. Power Syst., vol. 7, pp. 949-955, 1992.

[72] F. S. Prabhakara, J. Z. Ponder and J. N. Towle, "Computing GIC in large power systems," IEEE Comput. Appl. Power, vol. 5, pp. 46-50, 1992.

[73] D. H. Boteler, L. Trichtchenko, R. Pirjola, J. Parmelee, S. Souksaly, A. Foss and L. Marti, "Real-time simulation of geomagnetically induced currents", *7th International Symposium on Electromagnetic Compatibility and Electromagnetic Ecology,* p. 261-4, 26-29 June 2007.

[74] R. Pirjola, "Calculation of geomagnetically induced currents (GIC) in a high-voltage electric power transmission system and estimation of effects of overhead shield wires on GIC modelling", *J.Atmos.Solar Terr.Phys.,* vol. 69, no. 12, p. 1305-11, 2007.

[75] A. Pulkkinen, M. Hesse, M. Kuznetsova and L. Rastatter, "First-principles modeling of geomagnetically induced electromagnetic fields and currents from upstream solar wind to the surface of the Earth", *Annales Geophysicae,* vol. 25, no. 4, p. 881-893, 2007.

[76] D. H. Boteler and R. J. Pirjola, "Modelling geomagnetically induced currents produced by realistic and uniform electric fields," IEEE Trans. Power Del., vol. 13, pp. 1303-1308, 1998.

[77] D. H. Boteler and R. J. Pirjola, "Nature of the geoelectric field associated with GIC in long conductors such as power systems, pipelines, and phone cables," in Proceedings of International Symposium on Electromagnetic Compatibility, 21-23 may 1997, 1997, pp. 68-71.

[78] R. Pirjola, "Fundamentals about the flow of geomagnetically induced currents in a power system applicable to estimating space weather risks and designing remedies," J. Atmos. Solar Terr. Phys., vol. 64, pp. 1967-1972, 2002.

[79] M. Zou and L. Liu, "GIC calculation in power grid based on layered earth mode", *2010 5th International Conference on Critical Infrastructure, CRIS 2010, September 20, 2010 - September 22,* p. Institute of Electrical and Electronics Engineers (IEEE); Chinese Society for Electrical Engineering (CSEE), 2010.

[80] W. Chandrasena, P. G. McLaren, U. D. Annakkage and R. P. Jayasinghe, "An improved low-frequency transformer model for use in GIC studies," IEEE Trans. Power Del., vol. 19, pp. 643-51, 2004.

[81] A. A. Trichtchenko, D. H. Boteler and A. Foss, "GIC modelling for an overdetermined system," in 2006 Canadian Conference on Electrical and Computer Engineering, 2006, pp. 4.

[82] W. C. Viana, R. J. Micaleff, S. Young, F. P. Dawson and E. P. Dick, "Transformer design considerations for mitigating geomagnetic induced saturation," IEEE Trans. Magn., vol. 35, pp. 3532-3534, 1999.

[83] M. A. Eitzmann, R. A. Walling, M. Sublich, A. H. Khan, H. Huynh, M. Granger and A. Dutil, "Alternatives for blocking direct current in AC system neutrals at the Radisson/LG2 complex," IEEE Trans. Power Del., vol. 7, pp. 1328-37, 07. 1992.

[84] L. Bolduc, M. Granger, G. Pare, J. Saintonge and L. Brophy, "Development of a DC current-blocking device for transformer neutrals," IEEE Trans. Power Del., vol. 20, pp. 163-168, 2005.

[85] J. G. Kappenman, S. R. Norr, G. A. Sweezy, D. L. Carlson, V. D. Albertson, J. E. Harder and B. L. Damsky, "GIC mitigation: A neutral blocking/bypass device to prevent the flow of GIC in power systems," IEEE Trans. Power Del., vol. 6, pp. 1271-1281, 1991.

Chapter 2   A Software Simulator for Geomagnetically Induced Currents in Electrical Power Systems

2.1 Nomenclature

The various symbols used in this chapter are described below.

φ	Latitude in degrees
λ	Longitude in degrees
$\rho(\varphi)$	Radius of a given latitude line
R	Radius of the earth
N	Number of stations
n	Station number
M	Max. number of transformers per station
m	Transformer number (within a given station)
y_{gnd}	Ground conductance vector (Nx1)
Y_T	Transformer conductance matrix (NxM)
y_T	Transformer conductance vector (Nx1)
y_{stn}	Station conductance vector (Nx1)
Y_{line}	Line conductance data (NxN – symmetric)
$Y_{Tcoupling}$	Transformer coupling conductance (NxN – symmetric)
Y	System admittance matrix (NxN)
j	Equivalent current source vector (Nx1)
i	Calculated station GIC (Nx1)
I_T	Transformer GIC matrix (NxM)
V_{GIC}	Induced potential due to GIC (Nx1)

2.2 *Introduction*

Geomagnetically Induced Current (GIC) is the product of variations in the earth's magnetic field. These magnetic variations occur during geomagnetic disturbances produced by solar activity [1-9]. Solar activity follows an 11 year half cycle. During the peak of this cycle there is a marked increase in the probability of severe GIC. The next peak (cycle 24) is expected between late 2011 and 2013.

Hydro One in the province of Ontario, Canada, owns and operates one of the geographically largest transmission systems in North America. In the case of the Hydro One system there is little reliable historical GIC data available prior to 2005. The present GIC monitoring system was not fully deployed and calibrated prior to cycle 23 (2000). It is desirable to have an effective simulation tool to be able to examine many aspects of GIC including testing mitigation strategies and examining the impact of network modifications.

The concept for this simulator is based on a novel extension of the algorithm proposed in [10] and [11]. Where [10] and [11] only treat the analysis of a resistance network representative of a power system, this paper proposes a technique for modelling key power system components for GIC analysis as well as a technique for calculating the induced electric filed along an electrical power transmission system.

This chapter first presents the simulation method in section 2.3 including the modelling technique for each of the critical system components. Next, the calculation method is presented in section 2.4 and user interface in section 2.5. Results from the study systems are shown in section 2.6 and the application of the simulator to the Hydro One system is discussed in section

2.7. System data is not included for the portions of this paper that deal with Hydro One's system as Hydro One considers this data confidential. Discussions are presented in section 2.8 and conclusion in section 2.9.

2.3   Simulation Method

This chapter considers the case where the field of induced electric field in the electrical network is uniform and irrotational. The technique presented can be extended to consider non uniform fields. Because of the assumption of a uniform field, the induced potential in any given line will depend only on its terminal locations. Without this assumption it is possible that horizontal conduction loops will have GIC induced, these GICs will not be shown by models using this assumption. A field of induced potential (V_{GIC}) is applied across the area of interest to simulate these induced potentials. This simulator uses an admittance matrix based numerical method to simulate the effect of the induced potential imposed on the transmission network by a geomagnetic event. The induced potential is treated as a DC voltage field. While this is not strictly correct, it is a reasonable approximation [12], [13]. GIC is a time varying quantity with a period typically in the range of seconds to minutes.

The earth surface potential (ESP) method of modelling GIC generates a potential field over the surface of the earth. This field, which is typically recorded in volts per kilometre, results from applying either predicted or measured variations in the earth's magnetic field to a deep earth resistance model of the earth. A deep earth resistance model treats the earth as a thick (multiple km) layered sphere. The resistance of the earth model is far greater that that of the transmission lines and the effect of the transmission lines are neglected in this overall earth model [12], [13].

2.3.1 Mapping Transmission Station Locations

In order to calculate earth surface potential values for each network component, it is necessary to map the location of those components onto a flat plane kilometre grid. Once this is done, applying the volts per kilometre ESP is a simple matter. Any attempt to map spherical coordinates of equipment locations on to a flat linear grid introduces errors, especially when attempting to compute relative distances between multiple points, different mapping techniques can introduce variation of approximately 150 km, in the distance between two points at opposite ends of the province. A central reference point located at the algebraic mean of the latitude / longitude coordinates of the equipment of interest is selected to minimize this error. This central reference point serves as the origin of the flat plane linear map of the system. In the case of the Hydro One system, this point is located at 44.33192°N, 79.80532°W. This point is near the intersection of HWY 90 with Simcoe County Road 56, a few kilometres west of the city of Barrie, Ontario. Figure 2.1 shows four points of interest (A_1 through A_4) on a spherical plane. The locations of all points are calculated relative to a central origin by the method below. The final mapping is shown in Figure 2.2.

The procedure for locating a piece of equipment located at point A_1 (φ_1, λ_1), relative to the origin O (φ_0, λ_0), is illustrated in Figure 2.3. Two paths are considered, one, northward, parallel to the longitude lines (this is shown split as OB and CA_1) and one, eastward, parallel to the latitude lines, shows as BC. This line is located at the middle latitude between the two points O and A_1. For all calculations, the earth's radius R is assumed to be a constant 6371 km. The north (x) component of the mapped point is given as the arc length between O and A_1 in Figure 2.4, which depicts a cross sectional view of the earth:

$$x = R\frac{2\pi}{360}\left(\varphi_1 - \varphi_0\right)$$ (1)
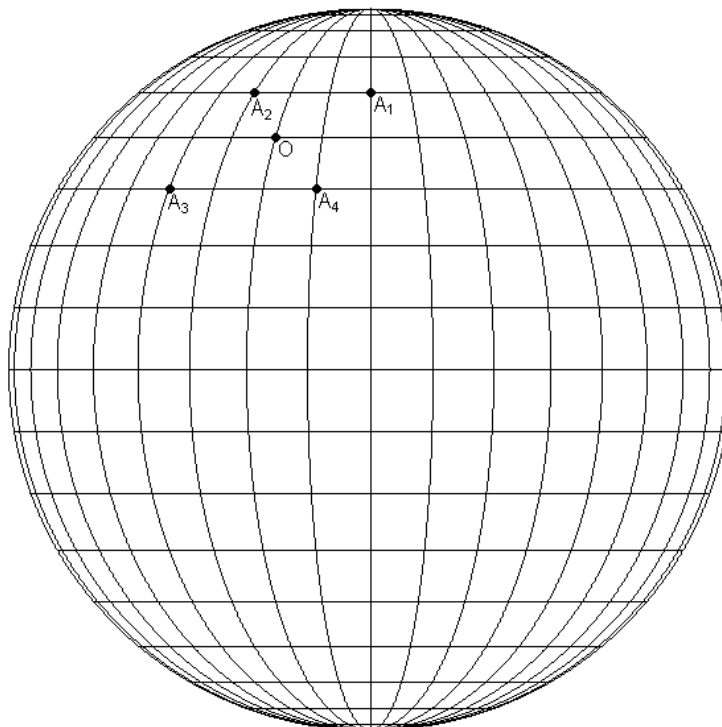
Figure 2.1: Points of interest on a spherical plane (earth)
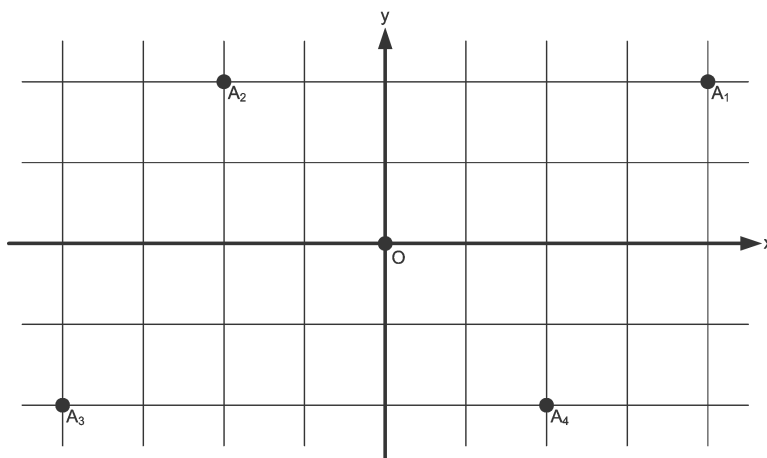
Figure 2.2: Points of interest mapped to a rectangular plane

The cross section of the earth along a latitude is illustrated in Figure 2.5. The east (y) component of the mapped point is given as the arc length between B and C in Figure 2.5. It should be noted that this arc is on the middle latitude between O and A_1:

$$y = \rho(\varphi')\frac{2\pi}{360}(\lambda_1 - \lambda_0) \tag{2}$$

where:

$$\varphi' = \frac{\varphi_0 + \varphi_1}{2} \tag{3}$$

$$\rho(\varphi') = R\cos\varphi' \tag{4}$$

Applying the ESP field to the station locations calculated above yields ESP values for each station.
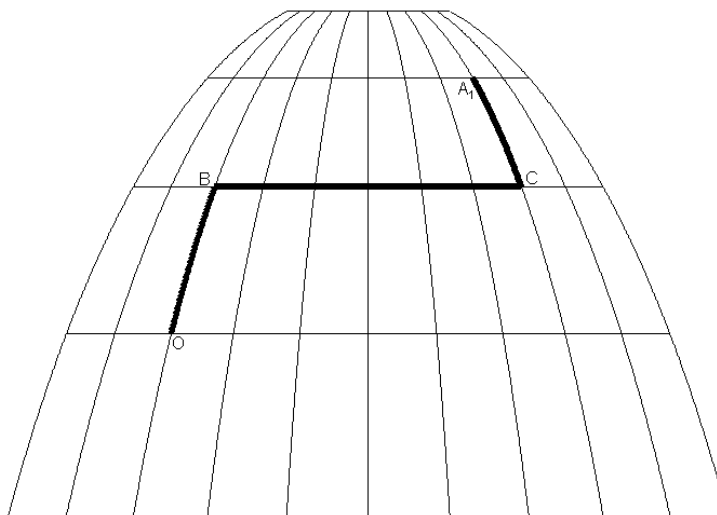
Figure 2.3: Connecting Points on a Sphere
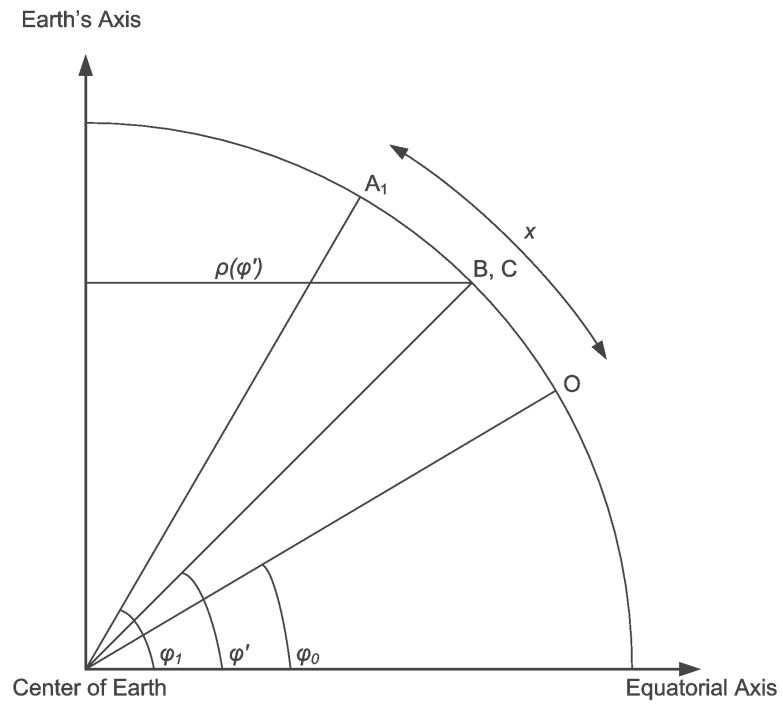
Figure 2.4: Axial cross section of the earth
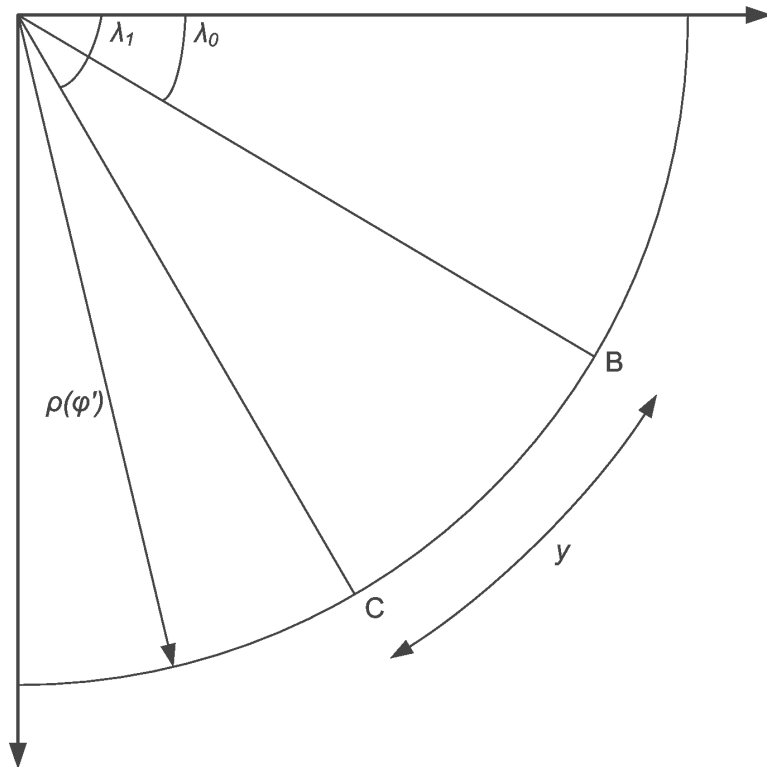
Figure 2.5: Cross section of the earth taken along latitude φ'

2.3.2 Modeling of Network Components

The model of the electrical transmission system needed for the GIC simulator is developed below. GIC is treated as a DC phenomenon and therefore, it is only necessary to model the DC resistance of the components considered. In the case of the Hydro One system, only 500 kV and 230 kV transmission networks are modeled. This is done because the other transmission elements form short, high resistance, radial networks which do not contribute significantly to GIC. It is assumed that the GIC in each of these networks is negligible.

This simulator uses a system model that treats all three phases in parallel, as they appear to the induced electric filed. Transmission lines are modeled by their conductor resistance. Transformers are modeled by their winding resistances, where they are wye connected and grounded, ungrounded transformers are treated as open circuits. Where an autotransformer couples two buses, its resistance is divided into a series resistance, coupling the two busses, and a resistance to the neutral terminal. It is also necessary to model the earth resistance for each station. A small representative study system having 5 buses is shown in Figure 2.6 and its model shown in Figure 2.7.
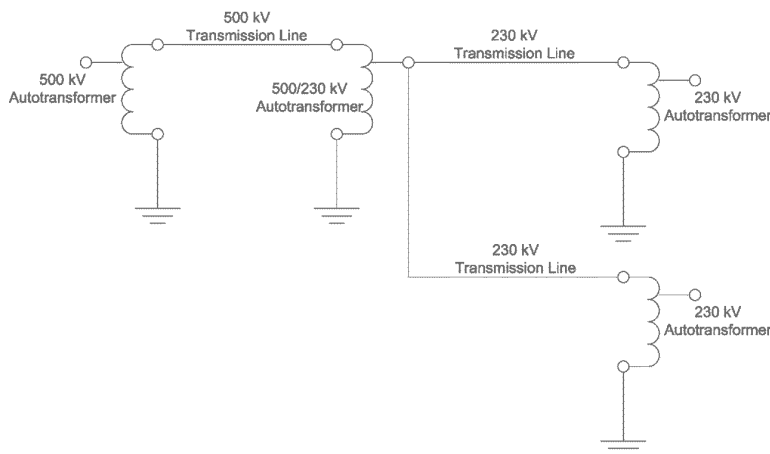
Figure 2.6: Study System
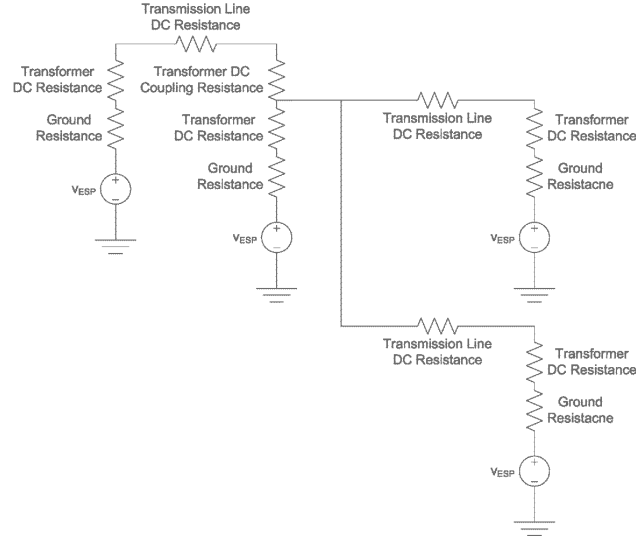
Figure 2.7: Equivalent DC Model of Study System

2.4 Calculation Method

The Geomagnetically Induced Currents are calculated as follows, based on the method presented in [10] and [11]. This algorithm is implemented as a MATLAB script, referred to as the *GIC Simulator* script. While any number of simulation engines could have been used to solve the DC circuit to determine GIC levels matlab was selected because of the author's easy access and familiarity. Autotransformer coils which couple multiple buses are treated the same as transmission lines connecting those buses. Earth Surface Potential (ESP) values are calculated by the method described in section 2.3.1. Steps represented by (9) through (12) are taken from [10] and [11].

Calculate transformer conductance vector (nx1):

$$y_{T_n} = \sum_{m=1}^{M} Y_{T_{n,m}} \tag{5}$$

Calculate station conductance vector (nx1):

$$y_{stn_n} = \frac{1}{\dfrac{1}{y_{T_n}} + \dfrac{1}{y_{gnd_n}}} \tag{6}$$

Any zero magnitude elements in this vector will yield a singular admittance matrix and the system will be unsolvable. After forming y_{stn} it is necessary to replace any zeros with trivially small values (10^{-8}).

Calculate system admittance matrix

$$Y'_{line} = Y_{line} + Y_{Tcoupling} \tag{7}$$

$$Y = diag(y_{stn}) + diag\left(Y'_{line} \bullet \vec{1}\right) - Y'_{line} \tag{8}$$

Convert ESP into Norton equivalent current source vector (nx1):

$$j_n = \sum_{x=1}^{N} \left(v_{GIC_n} - v_{GIC_x}\right) Y'_{line_{x,n}} \tag{9}$$

Calculate station voltage vector (1xn):

$$j = Yv_{stn} \tag{10}$$

$$v_{stn} = Y^{-1}j \tag{11}$$

Calculate the GIC in each station:

$$i_n = y_{stn_n} v_{stn_n} \tag{12}$$

If desired calculate the GIC in each station transformer:

$$I_{T_{n,m}} = i_n \frac{Y_{T_{n,m}}}{y_{T_n}} \tag{13}$$

While it is also possible to calculate the GIC in individual transmission lines this is not of interest here since the principal consequences on the electrical grid of GIC are transformer heating and harmonic current generation causing capacitor bank tripping, generator overheating, relay misoperation. Both of these phenomena are linked to the DC current in transformer windings [14]. Since GIC affects all three phases equally, the DC neutral current is indicative of the DC current in each of the phases.

2.5   User Interface

A detailed user interface has been developed to represent the system data on station location, transformer resistance and transmission lines using Microsoft Excel Worksheets.   These sheets are modifiable, lines and transformers may be added or removed. It is possible to add stations by simply creating a new listing in the station locations and transformer sheets and adding appropriate transmissions lines. All of the spreadsheets have provision to store station and line names, making for easy user interface with the system data.

These spreadsheets perform some data pre-processing and output files that are read into MATLAB by the GIC Simulator script. The GIC Simulator script performs the final processing of the input data, building the needed conductance matrices.

2.6   *Validation of Software Simulator*

In order to validate the proposed technique for GIC simulation, two case studies are performed. The first case study relates to a simple 5 bus system taken from [10, 11, 15]. The second case study is for the Hydro One 500 kV grid. Both systems are modeled in EMTP (using its steady state solver) and also solved using the GIC simulator. The calculated geomagnetically induced currents from both these methods are then compared.

2.6.1   Case Study 1: 5-bus system

This system, shown in Figure 2.5 consists of 5 buses in a straight line radial system. The line segments connecting two adjacent buses are modeled by their resistance, taken to be 5 ohms. The bus to ground resistance is 0.5 ohms, and the induced voltage in each line segment is 100 V. It was considered necessary to modify the topology of the system for simulation. The modified system is shown in Figure 2.9. The GIC in amperes as calculated from both the EMTP simulation and the developed tool are shown in Table 2-1.
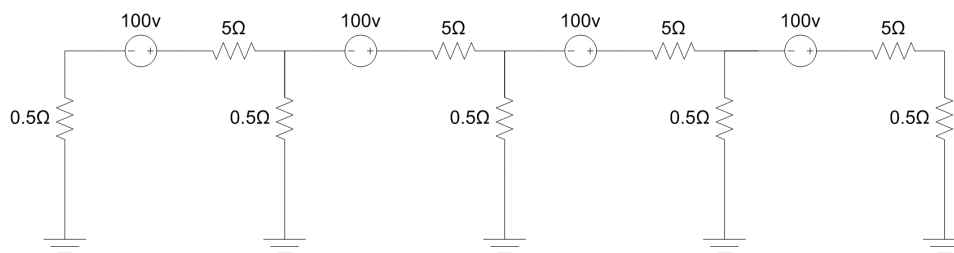
Figure 2.8: 5 bus system
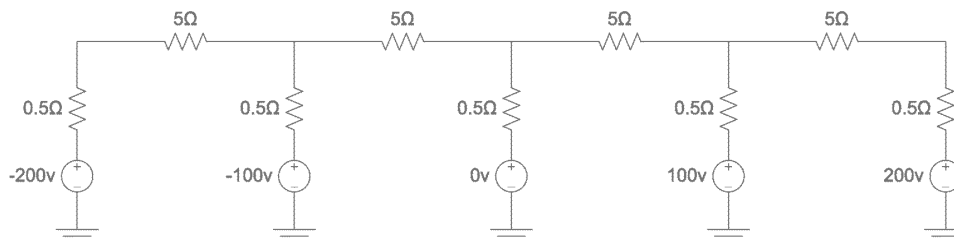
Figure 2.9: 5 bus system as modified to be simulated

Table 2-1: GIC (A) for 5 Bus System

	GIC_Sim	EMTP
A	-18.32	-18.32
B	-1.53	-1.53
C	0.00	0.00
D	1.53	1.53
E	18.32	18.32

In this small system, the GIC Simulator results match exactly those obtained from the EMTP.

2.6.2   Case Study 2: Hydro One 500 kV system

The data for this system is taken from internal Hydro One sources. A DC model of the system is developed. In this case study 19 nodes, and 40 connecting lines need to be modeled. This provides a very manageable system, with the benefit of using realistic system data. The results from this system should not be considered indicative of the actual system operations since the substantial GIC contribution of the much larger 230 kV system is not considered in this model. The GIC in amps as computed by the simulator and EMTP are comapred in Table 2-2.

The two modelling methods for the 500 kV system match very well. In both the case studies, the Simulator results are consistent with EMTP simulation.

2.7   *Application to Hydro One 500 kV and 230 kV System*

This study system simulates the entire 500 kV and 230 kV Hydro One transmission system (374 stations, 496 lines). So far, this simulation is being used to help guide specification for various new construction projects on the system, including the Nanticoke Static VAr Compensator.

Table 2-2: GIC (A) for Hydro One 500 kV System

	GIC_Sim	EMTP
Bowmanville SS	14.249	14.249
Bruce A TS	-23.774	-23.775
Bruce B SS	-38.888	-38.888
Cherrywood TS	0.192	0.192
Claireville TS	-13.501	-13.501
Essa TS	-0.571	-0.571
Hanmer TS	-13.780	-13.780
Hawthorne TS	46.827	46.827
Lennox TS	66.039	66.039
Longwood TS	-28.252	-28.251
Middleport TS	-7.313	-7.313
Milton SS	0.000	0.000
Nanticoke TS	10.136	10.136
Parkway TS C551VP	-3.766	-3.766
Parkway TS C550VP	-3.766	-3.766
Pinard TS	-5.544	-5.543
Porcupine TS	-0.708	-0.708
Trafalgar TS M573T	1.209	1.209
Trafalgar TS M5732T	1.211	1.211

2.7.1 System Overview

In Ontario the majority of the load and generation is concentrated along a primarily east-west corridor near the US border. Lines extend from this corridor to service areas to the north and east. The approximate configuration of this system is shown in Figure 2.10. Some stations as indicated on this diagram are in fact groups of nearby stations.

2.7.2 GIC Results

Simulation results are shown in Table 2-3 for a representative geomagnetic storm event of magnitude of 1V/km in both northerly and easterly directions. The impact of an actual geomagnetic event can be extrapolated based on these results, depending on the magnitude of the geoelectric voltage in either direction.
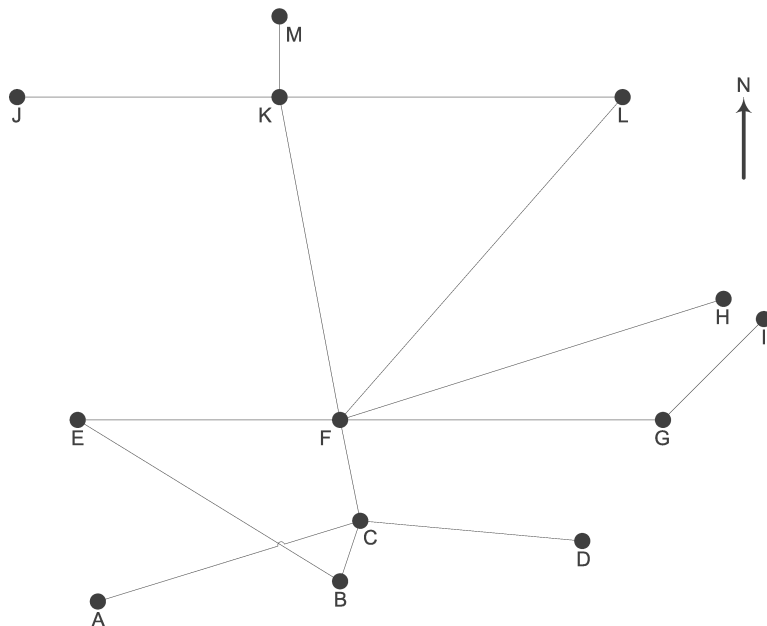
Figure 2.10: Major Line Groups in Hydro One (not to scale)

Table 2-3: GIC (A) for Generalized Hydro One 500 kV System

	North	East
A	-22.01	-51.87
B	-52.89	-2.81
C	-47.29	12.97
D	-19.10	101.11
E	98.82	-117.47
F	-108.23	34.72
G	-43.83	38.89
H	23.38	13.50
I	53.54	69.88
J	47.31	-199.93
K	69.80	2.41
L	32.76	45.19
M	37.99	10.72

2.8   Discussion

This GIC simulator provides the ability to easily and accurately predict GIC flows within an electrical power transmission system, given an accurate estimate of the induced potential.   This offers three principal benefits to electrical power engineers: the ability to understand GIC flows in their existing systems, the ability to see the impact of proposed system modifications on GIC flows and the ability to assess the effect of service outages and dispatch strategy on GIC flow.

In addition to the mapping technique discussed in section 2.1, the simulation method presented in this chapter offers a key advantage over EMTP simulation. The proposed method requires only the ESP field as an input, where in the case of EMTP simulation it is necessary to externally calculate the induced voltage in each line segment and input those values into the EMTP. Since the ESP values are continually changing, this streamlined interface will dramatically increase usability of the simulator.

Understanding the flow of GIC in an electrical power system is essential to judging the preparedness of the system in question, for an event as well as for directing the specification of new equipment to ensure sufficient GIC withstand capability.   This is especially important for equipment that is sensitive to harmonics such as Static VAr Compensators.

2.9   Conclusion

A novel software Simulator for predicting Geomagnetically Induced Currents in electrical power transmission systems has been developed and tested successfully on two test systems, including real electrical power transmission systems, with results supported by steady state simulation from the EMTP.

This simulator utilizes a new technique to map the locations of transmission equipment, and simulate autotransformers. The developed simulator offers great ease of use for working with GIC, as the geoelectric filed and system parameters are easily modifiable.

References

[1] R. Pirjola, "Geomagnetically induced currents during magnetic storms*," IEEE Trans. Plasma Sci.*, vol. 28, pp. 1867-1873, 2000.

[2] D. H. Boteler, "Geomagnetic hazards to conducting networks," Nat. Hazards, vol. 28, pp. 537-561, 2003.

[3] V. Albertson, J. Kappenman and B. Damsky, "The influence of geomagnetically induced currents (GIC) on transmission systems," in Proceedings of the American Power Conference, 1990, pp. 311-15.

[4] T. S. Molinski, W. E. Feero and B. L. Damsky, "Shielding grids from Solar Storms," IEEE Spectrum, vol. 37, pp. 55-60, 2000.

[5] D. H. Boteler, R. J. Pirjola and H. Nevanlinna, "Effects of geomagnetic disturbances on electrical systems at the earth's surface," Advances in Space Research, vol. 22, pp. 17-27, 1998.

[6] J. G. Kappenman, "Geomagnetic Storms and Their Impact on Power Systems." IEEE Power Engineering Review, May 1996.

[7] J. G. Kappenman and V. D. Albertson, "Bracing for the geomagnetic storms," IEEE Spectrum, vol. 27, pp. 27-33, 1990.

[8] A. Vilianen and R. Pirjola, "Finnish geomagnetically induced currents project," IEEE Power Engineering Review, vol. 15, pp. 20-21, 1995.

[9] L. Trichtchenko and D. H. Boteler, "Response of power systems to the temporal characteristics of geomagnetic storms," in 2006 Canadian Conference on Electrical and Computer Engineering, 2007.

[10] A. A. Trichtchenko, D. H. Boteler and A. Foss, "GIC modelling for an overdetermined system," in 2006 Canadian Conference on Electrical and Computer Engineering, 2006.

[11] A. A. Trichtchenko, D. H. Boteler and A. M. Foss, "GIC modelling for an overdetermined system," in 7th International Symposium on Electromagnetic Compatibility and Electromagnetic Ecology, 2007, pp. 254-6.

[12] D. H. Boteler, "Geomagnetically induced currents: present knowledge and future research," IEEE Trans. Power Del., vol. 9, pp. 50-58, 1994.

[13] R. Pirjola, "Space weather effects on technological systems on the ground," in Proceedings Asia-Pacific Conference on Environmental Electromagnetics. CEEM 2000, 3-7 may 2000. pp. 217-21.

[14] L. Bolduc, A. Gaudreau and A. Dutil, "Saturation time of transformers under dc excitation," Electr. Power Syst. Res., vol. 56, pp. 95-102, 2000.

[15] D. H. Boteler, L. Trichtchenko, R. Pirjola, J. Parmelee, S. Souksaly, A. Foss and L. Marti, "Real-time simulation of geomagnetically induced currents," in 7th International Symposium on Electromagnetic Compatibility and Electromagnetic Ecology, 2007, pp. 261-4.

Chapter 3   Determination of Geomagnetically Induced Current Flow in a Transformer from Its Reactive Power Absorption

3.1 Introduction

Solar disturbances release a clioud of high energy particles into space. If this plasma cloud crosses the earth's path it interacts with the earth's magnetic field to produce geomagnetic disturbances. A key feature of geomagnetic disturbance is and increase in the auroral electrojets in the boreal and austral zones. The electrojet can be visualized as a conductor suspended 100 km above the surface of the earth with a width of 600 km, and currents up to 2000 kA. Durring geomagnetic disturbances variations in the electroject (in the order of 1 to 100 mHz) produce magnetic field variations that induce voltages in relatively long conductors at ground level. This is a Solar magntic Disturbance (SMD). If these conductors, for instance the wires of an HV transmission line, are grounded through the neutral connection of transformers at the ends of the line, a closed loop or return path is formed and currents will circulate. These currents are commonly referred to as Geomagnetically Induced Currents (GIC) [1, 2].

The electrojet normally resides in regions near the earth's magnetic poles. During an SMD, current density of the electrojet increases and its size extends away from the poles. During severe SMD events, the electroject can extend to latitudes below the 40° parallel. On September 1st, 1859, the Carrington event, which is considered to be the most severe geomagnetic

event in recent recorded history [3], the aurora could be seen in relatively low latitudes such as Florida and Southern California.

The frequency and intensity of SMD events tend to follow the 22 year solar cycle [4]. The frequency of sunspot activity peaks twice during this 22 year cycle [5-7]. While SMD events are more likely to occur during a peak or solar maximum, they are by no means limited to occurring at peak times.

Power transformers are designed to operate in the linear region of their magnetizing characteristic. When dc or low frequency currents such as GIC flow into a transformer winding, the operating point is shifted and half-cycle saturation takes place, as illustrated in Figure 3.1. When a transformer enters into dc biased or half-cycle saturation both odd and even harmonics are generated. Power apparatus such as transformers and capacitor banks are designed to operate with power frequency voltages and currents. Harmonic currents superimposed on power frequency currents can cause a number of undesirable effects such as spot heating in power transformers, overloading of capacitor banks, improper operation of certain types of protective relays, extraneous losses, and machine overheating, to name a few.

The Québec Blackout of March 13th, 1989 was triggered by the tripping of capacitor banks of key Static VAr Compensators (SVCs) and a cascading series of events that led to the voltage collapse of the 735 kV network [8, 9]. This incident highlighted in dramatic manner how extreme space weather events and GIC can cause cascading failures leading to massive disruption of electrical power service.
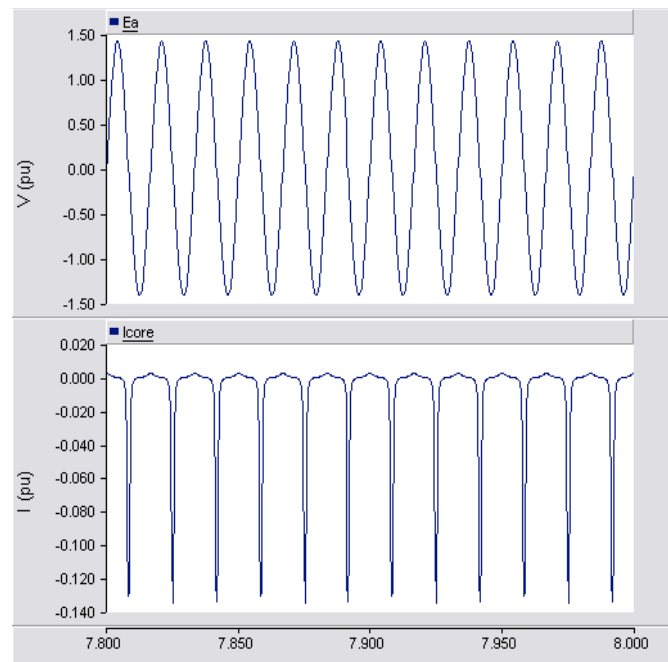
Figure 3.1: Terminal voltage and magnetizing current for a transformer under half cycle saturation

3.1.1 Simulation of GIC in Power Systems

There is a substantial body of research devoted to the analysis of GIC in HV transmission networks. In general, proposed techniques aim at determining the electrical field potential that causes GIC to circulate in transmission lines through the neutral grounding points of transformers [10].

Electric field potentials at ground level depend on many factors such as the properties of the earth resistivity over large geographical areas, as well as temporal and spatial variation of the induced electric field during an SMD event. Once the induced potentials on transmission circuits are assessed with varying degrees of uncertainty and simplifying assumptions, the GIC currents circulating in transmission lines and transformers are then calculated by modelling the power system as a dc network where the forcing functions (normally voltage sources) are estimated from the induced potentials [11].

Once the GIC currents are estimated, their potential effect on power apparatus has to be assessed. In the case of transformers, two main areas of concern are the heating effects of harmonics caused by half-cycle saturation, and the heating caused by stray flux as the core goes in and out of saturation. These effects depend heavily on the construction and type of transformer. For instance, banks of single-phase units are more susceptible than three-phase units, and three-leg core-type units are the least susceptible [12].

From the point of view of Protection and Control, susceptibility to GIC depends on the type and magnitude of harmonic currents caused by transformer saturation. Thus, even if the GIC circulating in the power network could be assessed with reasonable accuracy, the effect on the performance of the system and potential damage to equipment remains difficult to assess, especially in real time.

3.1.2 Measurement and Monitoring of GIC

Measuring GIC directly is a way to get around the difficulties and uncertainties in modelling it from fundamental principles (i.e., induced potentials at ground level). The generally accepted practice for measuring GIC on an electrical system is to install Hall-effect sensors on the neutral conductor of selected transformers. After appropriate filtering and conditioning, a measurement of the DC current in the transformer neutral is attained [13, 14]. The Sunburst system, developed by EPRI, uses this techniques and has been implemented in the United States, (primarily in the North East), Manitoba (on a feeder supplying Minnesota) [8], and in England and Wales [15]. The Minnesota power system also uses DC current measurement directly on a 500 kV phase conductor [16]. Hydro One has deployed an extensive GIC detection network [17]. In 2005 it had 12

monitoring stations transmitting real-time data directly to the operations and control centre. In preparation for the peak of sunspot cycle 24 (2011-2013) the number of GIC monitoring stations will be increased to 17.

Transformer neutral currents are sometimes used to trigger alarms and fault recorders in order to facilitate the analysis of GIC incidents [9, 16, 18]. Parameters that are considered of interest with regard to the effects of GIC include system voltages and reactive power consumption, as well as, transformer tank temperature, transformer oil gassing, transformer noise and vibration [16, 18]. The reactive power absorption of a transformer increases when that transformer's magnetic core is saturated. This relationship is almost linear and depends nearly entirely on the saturated reactance of the transformer [12].

The installation of real-time GIC monitors on every transformer, would be very useful but a rather expensive proposition. On the other hand, knowing the amount of GIC flowing in the winding of a transformer is not a direct indication of whether or not the transformer will enter into half-cycle saturation.

3.1.3 Requirements of the power system controlling authority

During an SMD event, the power system controlling authority (i.e., the system operator) needs to assess if any of the potential problems described earlier are, or will be taking place. Since the problems associated with GIC are caused by transformer saturation and the subsequent generation of harmonics, the notion of assessing these effects directly, rather than through simulations affected by different levels of uncertainty is quite attractive. Control room EMS (Energy Management Systems or SCADA) continuously measure and monitor real and reactive power in real time with the existing

infrastructure. A reliable relationship between measured reactive power loss in a transformer, harmonic currents, and GIC flowing through the windings would directly provide the information needed to make practical operational decisions in real time. The decisions could range from taking equipment at risk out of service, to re-configuring the network to reduce GIC impact.

This paper proposes an approach to obtain the relationships between transformer reactive power loss and GIC from EMS reactive power measurements. Unlike earlier work that acknowledged the correlation between GIC and reactive power absorption [12], this paper seeks to define that relationship, and validates it using both simulation and field data. Finally, it uses the newly defined relationship to estimate GIC levels from measured reactive power loss.

Section II presents the proposed concept of employing transformer reactive power absorption to determine its saturation level and consequently the GIC. Section III shows an application of the technique on a simulation of a bank of single phase autotransformers modeled in the Electromagnetic Transients Program EMTDC/PSCAD [19]. In Section IV the effect of the path of the flow of GIC through the transformer windings is examined. Section V presents a case study using GIC and reactive power measurements of the Hydro One network obtained during an SMD event that took place on May 2005. Conclusions are presented in section VI.

3.2 Proposed Technique

Consider the simplified transformer representation shown in Figure 3.2. The core magnetization and core losses can be represented by a shunt reactance X_m and resistance R_c. Saturation effects can be taken into account by assuming X_m to be a nonlinear inductance, as shown in Figure 3.3 (a). Since

the phenomenon under consideration is a quasi steady-state one, we introduce the additional simplification of ignoring hysteresis and lumping all core losses into R_c.
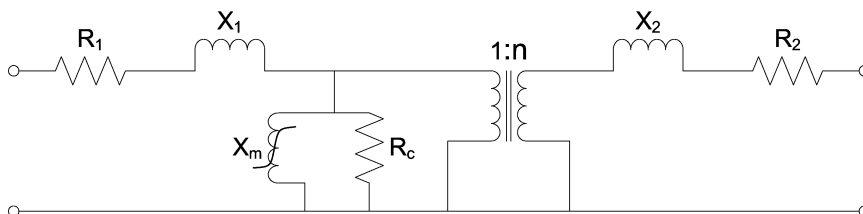
Figure 3.2: Transformer Model
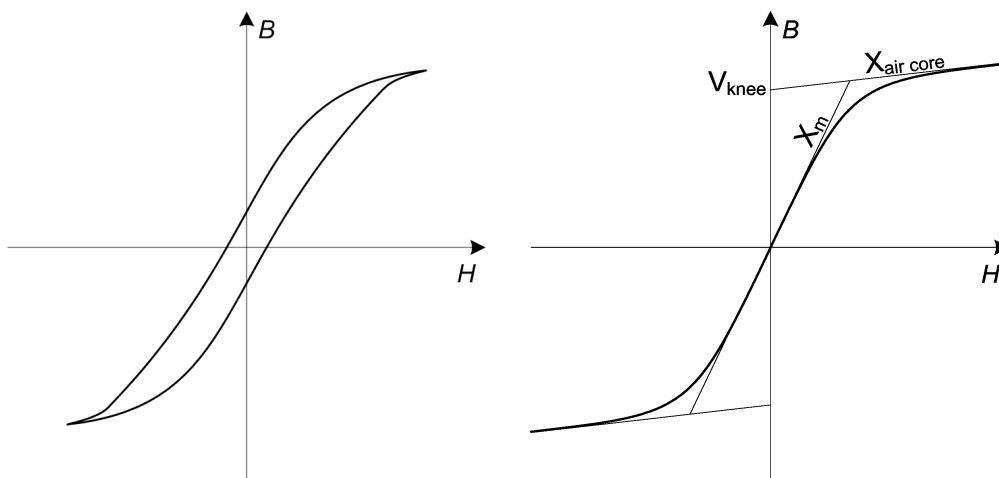
Figure 3.3 (a): Typical B-H curve, (b): Simplified B-H curve

With this assumption, the core characteristic is depicted in Figure 3.3 (b). In the saturated region, the apparent shunt impedance of the transformer becomes small and more reactive power is drawn. When the transformer is exposed to GIC the flow of quasi-DC current to ground through the transformer causes a DC voltage to appear across the non-linear core reactance over a relatively long period of time (minutes to hours). The *V-I* characteristic of the non-linear element is shown in a simplified manner in Figure 3.4.
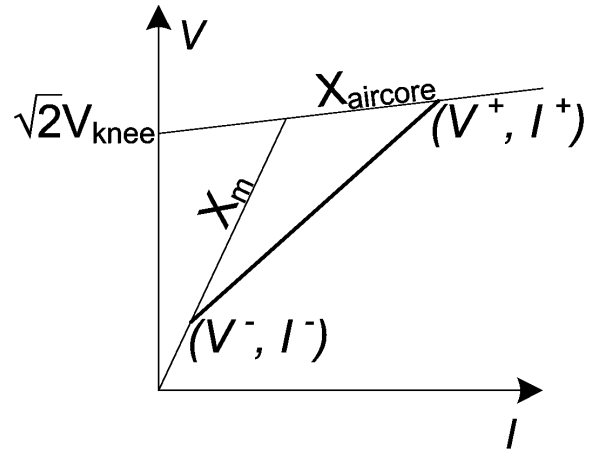
Figure 3.4: Transformer core reactance V-I characteristic
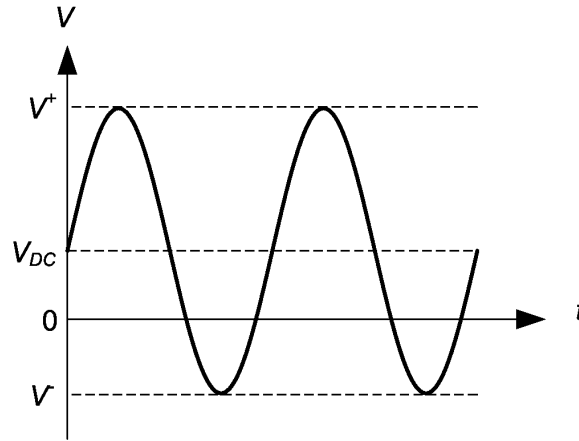
Figure 3.5: Voltage imparted on transformer core

Figure 3.5 shows the voltage seen across the core reactance in the transformer model, in this case a *V-I* model of the transformer core is used. V_{DC} is the voltage imparted on the core caused by the saturating GIC. The 60 Hz AC voltage is offset by a DC voltage due to the GIC. The positive peak voltage is labeled V^+ and the negative peak, V^-. The transformer's operating region (V^+ to V^-), with an AC rms voltage of 1 pu, for a given level of saturation V_{DC} is defined by:

$$V^+ = V_{DC} + \sqrt{2} \tag{1}$$

$$V^- = V_{DC} - \sqrt{2} \tag{2}$$

Assuming that the transformer is operating partly in the saturated region:

$$V^+ > V_{knee} \tag{3}$$

$$-V_{knee} < V^- < V_{knee} \tag{4}$$

The current limits of the transformer's current operating region, defined by I^+ and I^- (as seen in Figure 3.4) are then given as:

$$I^+ = B_{aircore}\left(\left(V_{DC} + \sqrt{2}\right) - \sqrt{2}V_{knee}\left(1 - \frac{B_m}{B_{aircore}}\right)\right) \tag{5}$$

$$I^- = B_m\left(V_{DC} - \sqrt{2}\right) \tag{6}$$

The effective susceptance of the transformer can be determined by:

$$B_{effective} = \frac{I^+ - I^-}{V^+ - V^-} \tag{7}$$

Using the voltages defined in (1) and (2) and the currents defined in (5) and (6):

$$B_{effective} = \frac{V_{DC}\left(B_{aircore} - B_m\right) + \sqrt{2}\left(B_{aircore} + B_m\right) + \sqrt{2}V_{knee}\left(B_m - B_{aircore}\right)}{2\sqrt{2}} \tag{8}$$

Since the air core susceptance $B_{aircore}$ is much larger than the magnetizing susceptance B_m, the magnetizing susceptance is assumed to be 0, giving:

$$B_{effective} = \left[V_{DC} + \sqrt{2}\left(1 - V_{knee}\right) \right] \frac{B_{aircore}}{2\sqrt{2}} \tag{9}$$

The reactive power absorbed in the magnetizing branch of the transformer is given by:

$$\begin{aligned}
Q_{tr} &= VI \sin\theta \\
&= VI (\because \theta = 90°) \\
&= B_{effective} V^2 \\
&= B_{effective} (\because V \cong 1)
\end{aligned} \tag{10}$$

From the original assumptions, (8), (9) and (10) are only valid when (3) and (4) are true.

Given that the saturation characteristic parameters ($B_{aircore}$ and B_m) of the transformer are constant for a given transformer, the effective reactance ($B_{effective}$) varies linearly with the saturating current through the transformer core. If the assumption that the terminal voltages are maintained at a constant value of 1.0 pu is true, the reactive power absorbed by the transformer will increase linearly with the saturating current in the transformer as shown by (9).

Based on measured reactive power levels for the transformer and a knowledge of the expected transformer reactive power absorption for a given power flow level, it is possible to estimate the magnitude of the saturating current utilizing the behaviour of the transformer in saturated conditions. Through existing EMS-based data acquisition, the transformer loading and its reactive power absorption are known. From this information, it is possible to determine the magnitude of GIC using the proposed technique illustrated in Figure 3.6, as follows: The difference between the reactive power flow into the transformer (Q_1) and the reactive power flow out of the transformer (Q_2)

is taken to be the reactive power absorbed by the transformer (Q_{tr}). The load current (I_2) of the transformer is used along with a model of the transformer under unsaturated conditions to determine the expected reactive power absorbed by the transformer (Q_{trL}). The difference between the expected and actual reactive power absorption is attributed to GIC (Q_{trGIC}). Finally, a predetermined characteristic is used to calculate I_{GIC} - the magnitude of GIC. In this paper, the predetermined characteristic has been taken from electromagnetic transient simulation using PSCAD. For practical implementation it is recommended that studies be performed during transformer pre-commissioning testing to determine the needed characteristic.
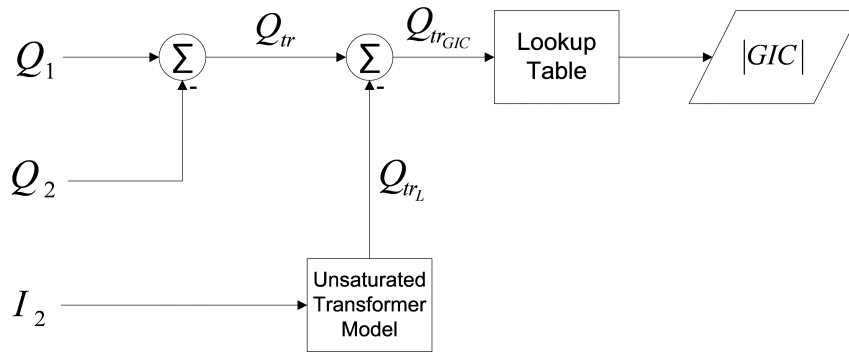
Figure 3.6: Technique for determining GIC with transformer power flows

3.3 Case Study I: Simulation of a Single-Phase Autotransformer Bank

3.3.1 Study System

The study system is shown in Figure 3.7. The transformer of interest T_1 is a three-phase bank that consists of three single-phase autotransformers. This transformer bank is supplied by an ideal voltage source V_1 behind a delta-connected ideal transformer T_2 which serves to block DC currents from the source V_1. A DC current source I_1 injects current in each primary phase to simulate GIC, and a second source I_2 may be used to inject GIC in the

secondary windings, in both directions. The low voltage side of the transformer T_1 supplies a constant power load of 100 MW (the transformer's rated capacity). This load is isolated from the flow of low frequency current again with a delta-connected ideal transformer T_3. This system is simulated in PSCAD. The current at the ground terminal (I_{ground}) of the transformer bank is monitored, as are the input and output real and reactive powers. The transformer input power (P_1, Q_1) and output power (P_2, Q_2), respectively, are measured directly.
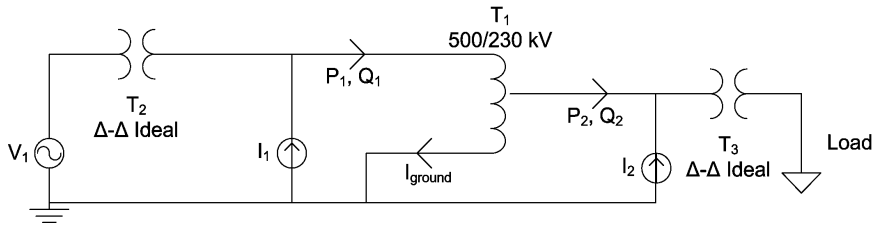
Figure 3.7: Single Phase Transformer Study System

3.3.2 GIC flow from HV Terminal to Ground

This case considers the flow of saturating current from the high voltage terminal of the transformer into the ground. This would be the case of a transformer whose low voltage terminal is supplying a practically ungrounded system with little or no GIC flow.

To examine the effects of saturation caused by the injection of a DC current, 100A per phase of GIC is selected. Although this is at the high end of GIC values observed in HV networks, it is used to illustrate the effect of GIC on the transformer. The most severe effect of the saturation of the transformer is the increased transformer reactive power consumption. In this case reactive power draw increases more than tenfold from approximately 10 MVAr to nearly 120 MVAr. Figure 3.8 shows the average reactive power consumption with increasing GIC levels.

Transformer Reactive Power Draw
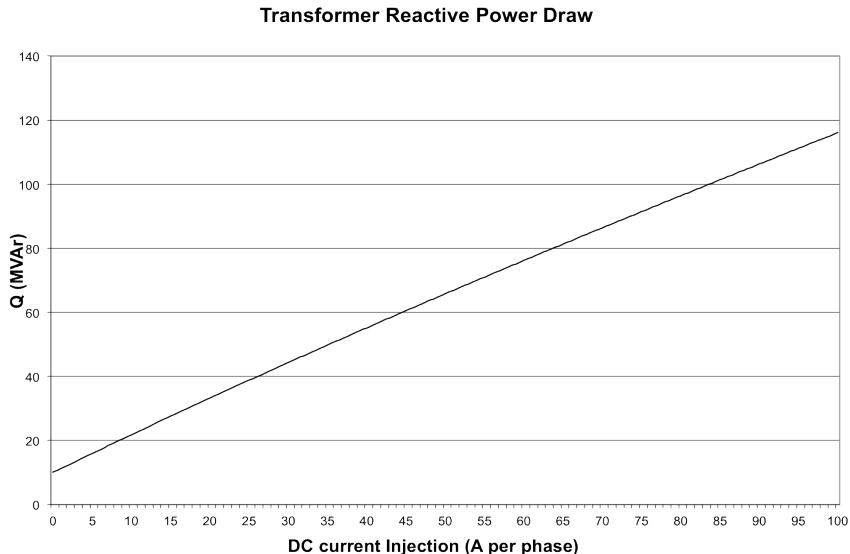
Figure 3.8: Transformer reactive power consumption with variation DC current injection

3.4 Effect of GIC Flow Path in an Autotransformer

The previous section considered an autotransformer where the GIC flow was set from the HV terminal to ground. However, in a system where the LV network is grounded, the distribution of DC current through HV, LV and neutral terminals depends on a number of factors such as orientation of lines connected to HV and LV buses, induced electric field orientation, and other circuit parameters such as line and neutral grounding resistances.

The level of saturation in an autotransformer depends on the net DC flux in the core, which in turn depends on the current in the HV and common windings. Since GIC monitors normally measure neutral current, GIC measurements in an autotransformer only reflect directly the flux contribution from the common winding.

The net DC magnetic field induced in the core (H_{GIC}) is a product of the ampere-turns of DC current. Since the number of turns on each winding is

not readily available, it can be represented as a constant (k) times the nominal rated voltage at the terminal in question.

For a GIC flow of 100A from the HV (500kV) terminal to the LV (240 kV) terminal, the injected GIC is:

$$H_{GIC} = 100(500k) - 100(240k) \tag{11}$$

The nonlinear behaviour of a saturated transformer is dependent on the DC flux offset. The path which GIC takes through the transformer to create this offset has no bearing on the effects seen by the transformer. The transformer reactive power consumption can be used as an indicator of the net DC flux in the transformer. Given this knowledge and an understanding of general GIC flow pattern in a given transformer, it is possible to use transformer reactive power consumptions as an indicator of system GIC levels.

3.5 Case Study II: Hydro One Essa TS Transformer, May 15, 2005 SMD Event

On May 15, 2005, the Hydro One GIC detection network recorded the effects of a relatively mild SMD event. During this event, there was no interruption of service, protective equipment malfunction, or nuisance equipment tripping. The neutral GIC currents monitored in the neutral of a 500kV/230kV/28kV, 750 MVA autotransformer at Essa TS reached 30 A (10 A per phase). The transformer bank consists of three-single-phase units.

The analysis presented in this section is based on Hydro One's historical records from the GIC EMS records, which stores measurements from 12 GIC monitoring network. The technique proposed here takes into consideration instrument calibration drift.

3.5.1 Modified Technique

3.5.1.1 Nomenclature

This nomenclature is used exclusively for this case study to describe a modified technique needed to condition the real system data.

$I_{GICn_{MEAS}}$ Measured transformer neutral current

$\bar{I}_{GICn_{MEAS}}$ Mean transformer neutral current (taken during a period with no GIC activity)

$I'_{GICn_{MEAS}}$ Measured transformer neutral current with instrument drift error corrected

$Q_{1_{MEAS}}$ Measured transformer primary winding reactive power

$Q_{2_{MEAS}}$ Measured transformer secondary winding reactive power

ΔQ_{MEAS} Measured transformer reactive power absorption

$\Delta Q'_{MEAS}$ Measured transformer reactive power absorption with instrument drift error corrected

$Q_{1_{EST}}$ State-estimated transformer primary winding reactive power

$Q_{2_{EST}}$ State-estimated transformer secondary winding reactive power

ΔQ_{EST} State-estimated transformer reactive power absorption

ΔQ_{CAL} Calibration factor for transformer reactive power absorption

ΔQ_{GIC} Transformer reactive power absorption attributed to GIC

3.5.1.2 Measurement of GIC

Hydro One GIC monitoring stations consist of a Hall Effect sensor located on the neutral to ground connection of the transformer's wye windings [14]. The analog signals from these sensors are digitized and filtered to remove power frequency and higher frequency components. Hence, this signal is expected to correspond to GIC only. The most prevalent error in this signal is an offset

caused by calibration drift of the sensor's DC offset. This error can be corrected by calculating a calibration factor during a period where there is no GIC activity, as shown:

$$I'_{GICn_{MEAS}} = I_{GICn_{MEAS}} - \bar{I}_{GICn_{MEAS}} \tag{12}$$

Figure 3.9 shows measured neutral terminal GIC over the duration of the SMD event. In all figures in this section the time axis is labelled in minutes from midnight May 13, 2005. The data is presented for March 14th and 15th (minutes 0 to 2879).
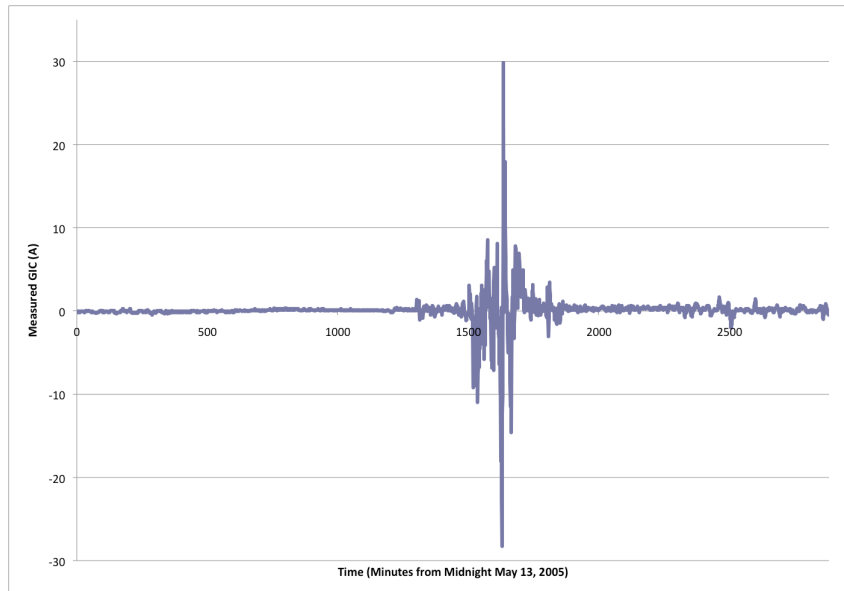
Figure 3.9: Measured Transformer Neutral Current with Error Corrected

3.5.1.3 Calculation of Transformer Reactive Power Absorption

Through the use of bus CVTs and transformer bushing CTs, the real and reactive power flows through each transformer are recorded. In the case of Essa TS 18T4, since no load or reactive compensation is connected to the tertiary winding, the net transformer reactive power absorption is calculated as the difference between the reactive power flows in the primary and secondary terminals:

$$\Delta Q_{MEAS} = Q_{1_{MEAS}} - Q_{2_{MEAS}} \tag{16}$$

Any possible measurement or calibration error in the measured quantities will also be seen in the calculated ΔQ_{MEAS}, and will need to be compensated for.

The Hydro One EMS system also uses a state estimator [20, 21, 22]. When modelling the operation of a transformer the state estimator takes into account only the series winding reactance of the transformer, neglecting the core reactance. By taking the difference between the estimated reactive power flows, the reactive power absorption due to the series element (calculated by the winding currents) can be determined as:

$$\Delta Q_{EST} = Q_{1_{EST}} - Q_{2_{EST}} \tag{17}$$

When no GIC is present, ΔQ_{EST} and ΔQ_{MEAS} should be equal except for the small amounts of reactive power absorbed by the unsaturated transformer magnetizing current. So long as the terminal voltage of transformer remains constant, the magnitude of this current remains constant. Also, if there is an error in the measured transformer reactive power levels, that error will contribute to the difference in these quantities. A calibration error correction factor is taken during a period with no GIC present. This gives an error corrected value:

$$\Delta Q'_{MEAS} = \Delta Q_{MEAS} - \Delta Q_{CAL} \tag{18}$$

Taking the calibration error correction into account, any difference between the estimated and measured reactive power levels is attributed to GIC:

$$\Delta Q_{GIC} = \Delta Q'_{MEAS} - \Delta Q_{EST} \tag{19}$$

Figure 3.10 shows the error corrected reactive power absorption $\Delta Q'_{MEAS}$, the state estimated reactive power absorption ΔQ_{EST}, and the transformer neutral current $I'_{GIC_{MEAS}}$. A clear correlation between the magnitude of GIC and the difference between the measured and error-corrected transformer reactive power absorption is seen.

3.5.1.4 Calculation of the Magnitude of GIC

In this case the magnitude of GIC can be calculated using a ratio obtained from simulation work, since field testing of the transformer was not possible. In electromagnetic transient simulation, the ratio has been found to be:

$$\frac{\Delta Q_{GIC}}{I'_{GICn_{MEAS}}} = 0.367 \tag{20}$$
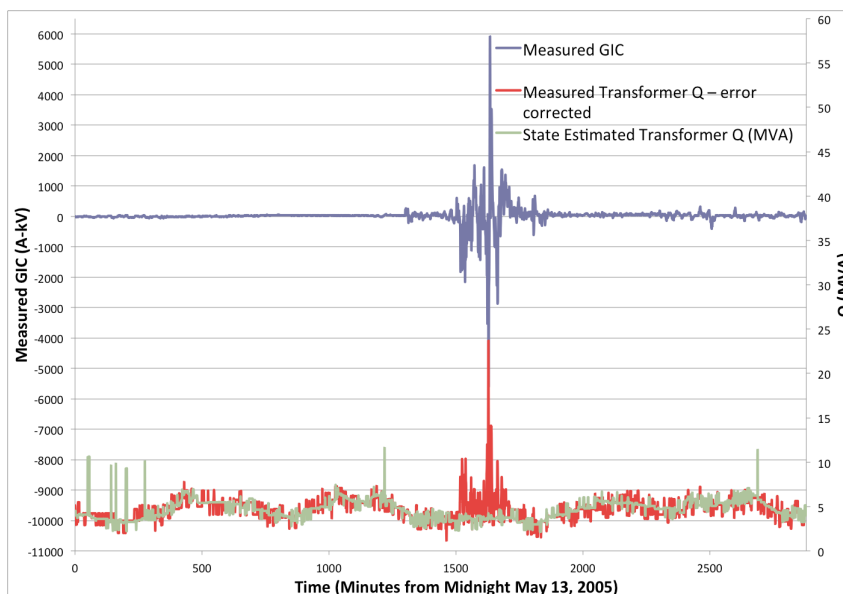
Figure 3.10: Transformer Reactive Power Absorption

3.5.2 Results

ΔQ_{GIC} is calculated for each time sample using (20). The absolute magnitude of GIC ($I'_{GICn_{MEAS}}$) is calculated employing (20). This calculated value of GIC is shown along with the magnitude of the GIC level in Figure 3.11. The results seem to follow the shape however the magnitude of the predicted GIC is approximately 33% greater than the recorder data. The calculation is based on the assumption that all GIC flows from the HV terminal to ground (the native slope), in this case there is likely additional flow out of the LV terminal that are affecting the results. In order to allow an assessment of the correlation between the calculated GIC and observed GIC Figure 3.12 shows the calculated GIC multiplied by 0.75, a factor designed to accommodate for the GIC that flows out the LV terminal. This factor was calculated based on the angle of the event and an analysis of the flow of GIC within the entire network using the simulator presented in Chapter 2. This figure shows a good correlation between the predicted and observed values.
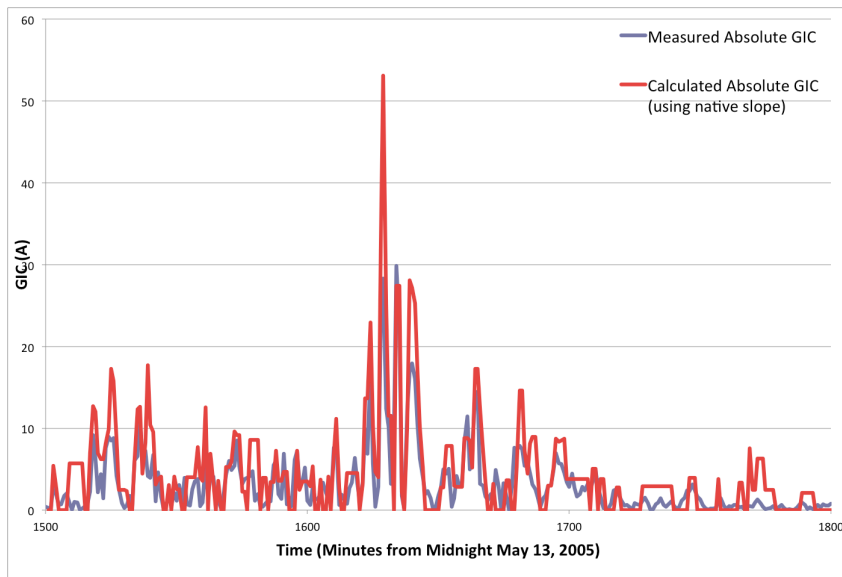
Figure 3.11: Magnitudes of Actual and Calculated GIC Levels
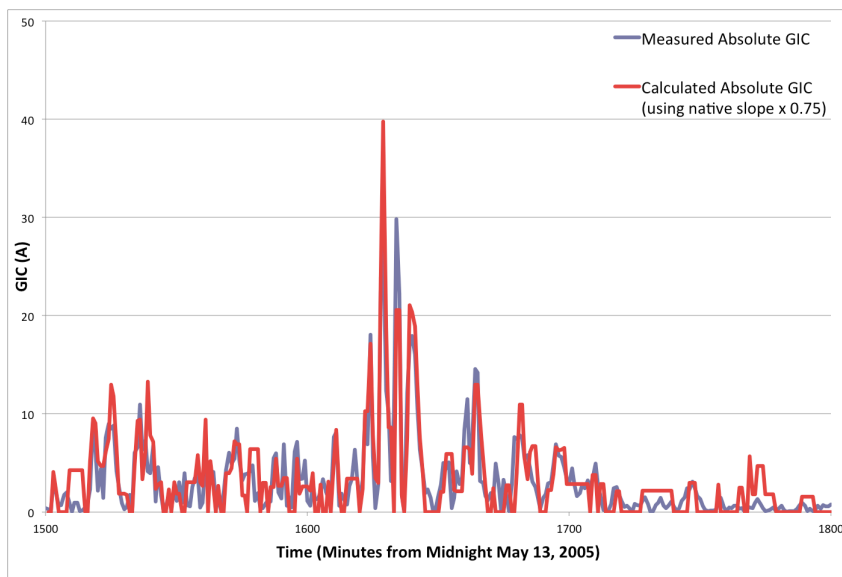
Figure 3.12: Magnitudes of actual and adjusted calculated GIC levels
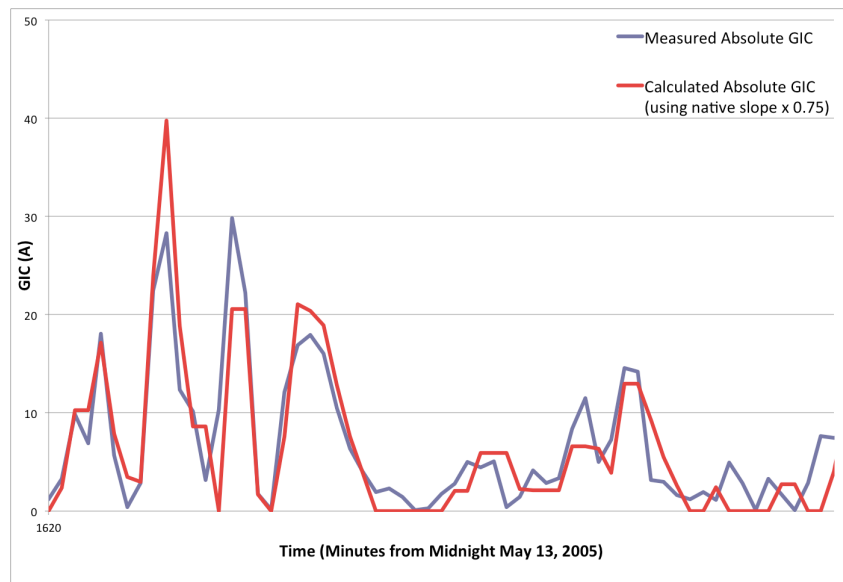
Figure 3.13: Magnitudes of actual and adjusted calculated GIC levels, close up of 1620 to 1680 minutes

A close-up of the plot showing a smaller timeframe is shown in Figure 3.13. A good correlation is seen between the predicted and measured GIC.

3.6 Conclusions

This paper introduces a technique to estimate the flow of GIC in HV transformer based on its reactive power absorption that can be computed from available measurements of power flows at the terminals of the transformer. While previous work [12] has, through simulation, noted a correlation between reactive power absorption and GIC, this paper not only defines that relationship, but proposes its application to measure GIC using existing infrastructure in place to measure reactive power.

Reactive power flow is monitored in real time on most modern EMS/SCADA systems by the power system controlling authority. Therefore, in principle, the GIC flows on every transformer in the system due to an SMD event can be determined in real time without additional GIC monitoring equipment and

without direct knowledge of the electric field or ground characteristics of the HV transmission network.

This proposed technique is consistent with simulations carried out with commercially available EMTDC/PSCAD software. Field measurements retrieved from historical records of the May 2005 SMD event show a very good correlation between calculated GIC and measured values on a transformer with a dedicated GIC monitor. This level of agreement is very encouraging considering the relatively low GIC currents measured during the event and the relatively low time resolution of historical records.

While the example presented in this paper is for an autotransformer and is therefore complicated by the multiterminal flow of GIC, it should be noted that in the case of two winding transformers, there is only a single GIC flow path in each winding. In this case the calculation of GIC is very simple. Even in the case of autotransformers the net DC flux is easily computed with the presented technique. It is ultimately the net DC flux that causes undesired effects in the electrical grid.

If the GIC flowing through every transformer are known, it is relatively simple to estimate the flows in transmission lines. This would in turn allow the estimation of the induced electric field spatially as well as temporally. This information would be valuable in the validation and improvement of traditional field-based GIC estimation techniques.

Validation of the proposed technique with measurements of a relatively mild SMD event could be considered as a good starting point. As more measurements become available during the maximum period of solar cycle 24, it will be possible to obtain data from more SMD events to validate and/or

refine this technique for broader application outside the Hydro One HV transmission network.

References

[1] R. Pirjola, "Geomagnetically induced currents during magnetic storms," IEEE Trans. Plasma Sci., vol. 28, pp. 1867-1873, 2000.

[2] D. H. Boteler, "Geomagnetic hazards to conducting networks," Nat. Hazards, vol. 28, pp. 537-561, 2003.

[3] "A Super Solar Flare," Science News, NASA Science: 2008. Available online: science.nasa.gov.

[4] L. Trichtchenko, D. H. Boteler, "Response of Power Systems to the Temporal Characteristics of Geomagnetic Storms," in 2006 Canadian Conference on Electrical and Computer Engineering, 2006, pp. 4.

[5] D. H. Boteler, "Geomagnetic hazards to conducting networks," Nat. Hazards, vol. 28, pp. 537-561, 2003.

[6] V. Albertson, J. Kappenman and B. Damsky, "The influence of geomagnetically induced currents (GIC) on transmission systems," in Proc. of the American Power Conference, 1990, pp. 311-15.

[7] D. H. Boteler, R. J. Pirjola and H. Nevanlinna, "Effects of geomagnetic disturbances on electrical systems at the earth's surface," Advances in Space Research, vol. 22, pp. 17-27, 1998.

[8] L. Bolduc, "GIC observations and studies in the Hydro-Québec power system," J. Atmos. Solar Terr. Phys., vol. 64, pp. 1793-1802, 2002.

[9] D. H. Boteler, "Assessment of geomagnetic hazard to power systems in Canada," Nat. Hazards, vol. 23, pp. 101-120, 2001.

[10] D. H. Boteler, "Geomagnetically induced currents: present knowledge and future research," IEEE Trans. Power Del., vol. 9, pp. 50-58, 1994.

[11] D. H. Boteler, L. Trichtchenko, R. Pirjola, J. Parmelee, S. Souksaly, A. Foss and L. Marti, "Real-time simulation of geomagnetically induced currents", *7th International Symposium on Electromagnetic Compatibility and Electromagnetic Ecology,* p. 261-4, 26-29 June 2007.

[12] R.A. Walling, A.H. Khan, "Characteristics of Transformer Exciting-Current during Geomagnetic Disturbances." IEEE Trans. Power Del., vol. 6, no 4, pp. 1707-1714, 1991.

[13] R. L. Lesher, J. W. Porter and R. T. Byerly, "Sunburst - A network of GIC systems," IEEE Trans. Power Del., vol. 9, pp. 128-137, 1994.

[14] L. Lian-guang, Z. Hao, L. Chun-ming, G. Jian-hui and G. Qing-xiong, "Technology of detecting GIC in power grids and its monitoring device," in 2005 IEEE/PES Transmission and Distribution Conference and Exhibition: Asia and Pacific, Aug 15-18 2005, 2005, pp. 1546843.

[15] I. A. Erinmez, "Managing the impact of geomagnetically induced currents on the NGC transmission system," in Proc. of 2001 Winter Meeting of the IEEE Power Engineering Society, 28 Jan.-1 Feb. 2001, 2001, pp. 336 vol.1.

[16] D. R. Fagnan, P. R. Gattens and F. D. Johnson, "Monitoring solar magnetic disturbances in power systems (a summary)," IEEE Power Engineering Review, vol. 10, pp. 4-6, 1990.

[17] L. Marti, Chun Li, "*Real-Time GIC Monitoring in the Ontario HV Network*". North American Transmission and Distribution Conference (NATD), Toronto, May 2005.

[18] T. H. Breckenridge, T. Cumming and J. Merron, "Geomagnetic induced current detection and monitoring," in Proc. of 7th International Conference on Developments in Power Systems Protection (DPSP 2001), 9-12 April 2001, 2001, pp. 250-3.

[19] "EMTDC/PSCAD User Manual", HVDC Research Center, Manitoba, 2003.

[20] F. C. Schweppe, J. Wildes, and D. B Rom. "Power system static state estimation I, II, III", IEEE Trans. PAS, Vol. PAS-89, No.1, 1970.

[21] T. Van Cutsem and M. Ribbens Pavella "Hierarchical methods for state estimation of electric power systems." IEEE Trans. PAS Vol. PAS-102, No. 10, pp. 3415-3424. 1983

[22] T. Van Cutsem and M. Ribbens Pavela "Critical survey of Hierarchical methods for state estimation of electric power systems," IEEE Trans. PAS, Vol. PAS-102, No.10, 1983.

Chapter 4 Laboratory Validation of the Relationship Between Saturating Current and Transformer Absorbed Reactive Power

4.1 Introduction

Geomagnetically induced currents are currents induced in large conductive networks, such as high voltage transmission lines, due the magnetic filed variations that occur during geomagnetic disturbances. These currents have frequencies in the range of (1 to 10mHz) and for the purposes of the analysis of power frequency (50 or 60 Hz) networks; GIC can be treated as direct current [1-9].

Power transformers are designed to operate in their linear regions. When low frequency currents such as GIC flow into the transformer windings the operating point is shifted partly into the saturated region. This shift reduces the effective core impedance and causes a corresponding increase in the reactive power absorbed by the transformer core.

The reactive power absorbed by a transformer in its core magnetization circuit increases if the transformer becomes saturated by a low frequency current [1]. It has been discovered that the relationship between saturating current and absorbed reactive power due to that current is linear and constant for a given transformer. In this thesis, the abovementioned relationship is proposed as the basis of a technique for measuring geomagnetically induced current (GIC) through a transformer core. Using the reactive power absorbed by existing transformers it is possible to, quickly

and at low cost, deploy a GIC monitoring network on an existing power system. This proposed GIC monitoring system will employ the infrastructure already in place to monitor power frequency voltage, current and power levels. Provided adequate signals are monitored and telemetered to observe the reactive power absorbed in the transformers of interest, and adequate models of those transformers are available, the proposed method can be implemented exclusively on a software level, without requiring the deployment of specialized sensors.

This chapter seeks to validate the relationship between GIC and reactive power absorbed by the transformer in a laboratory environment. In Chapter 3, the relationship was established using electromagnetic transient simulation software PSCAD/EMTDC, and was validated using observed data taken from a minor event on a Hydro One 500/230 kV autotransformer located in Barrie, Ontario, Canada. In this chapter, laboratory experiments are conducted under various loading and saturating current conditions to illustrate and validate the above relationship. While the lab transformer is not designed to be an analog to a practical power transformer, the general core characteristic will be the same, though the impedances will be different. It is expected that the lab transformer will show the same properties when saturated as a large power transformer.

Section 4.2 presents the test circuit with a discussion of its design. Results under various loads are shown in section 4.3. Finally, Conclusions are presented in section 4.4.

4.2 Test Circuit

In this chapter, a two winding transformer is considered. Since a power supply was not available that could inject both AC (at 60 Hz) and DC into the

transformer under study, it was necessary to utilize a two winding transformer to provide galvanic isolation between the AC and DC supplies.

The test circuit, shown in Figure 4.1, consists of two identical antiparallel connected single-phase transformers (T1 and T2), of which T1 is the transformer of interest. This transformer configuration was selected because the secondary voltage of one branch will be 180° out of phase with the other. This in combination with an equal load on both transformer secondary circuits, results in zero current in the neutral conductor. The zero neutral current allows components to be inserted into the neutral conductor without affecting the circuit as it appears to 60 Hz AC. A DC source is inserted in the neutral conductor to supply the saturating current. Since each antiparallel branch is identical it is presumed that the DC current splits equally between the two transformers. If there is a slight unbalance in the two loads (indicated by Z) the unbalance current will also flow through the capacitor.
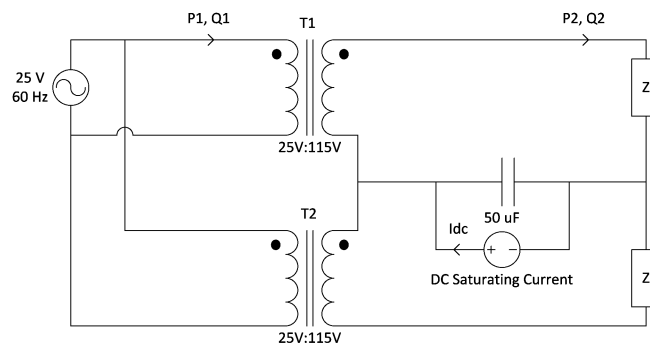
Figure 4.1: Test Circuit

The load *Z* consists of a resistance in parallel with a DC choke reactor, which consumes reactive power and will not saturate due to the injected DC current. This type of reactor has an extremely high knee point so that it will not become saturated in the presence of the DC saturating current.

The transformer of interest is a 115V:25V, 37.5 VA power supply transformer model number 166K25 by Hammond Engineering. The AC source is set to the rated voltage of the transformer. Two loads with widely differing power factors are considered. These are 25+j10VA and 30+j26VA.

The transformer real and reactive power (P_1 and Q_1, respectively) are measured at the primary terminals of the transformer T1. P_2 and Q_2 are the real and reactive power, respectively, measured at the load terminals. The DC saturating current (I_{dc}) is utilized to simulate GIC and is measured at the DC source. The DC saturating current (I_{GIC}) in each transformer winding is taken to be ½ I_{dc}.

4.3 Results

Studies are performed for two loads by varying the injected GIC and recording the power levels. The results of these studies are compiled in Table 4-1. The relationship between the reactive power absorbed by the transformer Q_{trGIC} and the dc current simulating GIC I_{GIC} is illustrated in Figure 4.2. The computation of Q_{trGIC} is performed as per the following relationships, repeated from Chapter 3:

$$Q_{tr_{GIC}} = (Q_1 - Q_2) - (Q_1 - Q_2)\big|_{I_{GIC}=0} \tag{1}$$

The plot between GIC (I_{GIC}) and transformer reactive power absorption due to GIC (Q_{trGIC}) is shown to be linear and almost the same for both loading conditions having widely different power factors. The linear relationship is approximated by the solid line indicated in Figure 4.2. For the transformer studied a correlation between GIC (I_{GIC}) and transformer reactive power absorption due to GIC (Q_{trGIC}) is found (through linear regression) to be:

$$Q_{tr_{GIC}} = 120(I_{GIC} - 0.01)$$

(2)

Table 4-1: Experimental Results

I_{DC}	I_{GIC}	P_1	Q_1	P_2	Q_2	Q_{tr}	Q_{trGIC}
Load #1: 25+j10VA − pf = 0.93							
0	0	38.9	23.1	25.9	8.9	14.2	0.0
0.107	0.0535	39.3	28.3	26.4	10.0	18.3	4.1
0.170	0.085	40.5	32.6	25.0	9.3	23.3	9.1
0.221	0.1105	40.7	35.7	24.3	9.6	26.1	11.9
0.275	0.1375	42.2	39.7	24.3	9.9	29.8	15.6
0.319	0.1595	42.8	42.6	25.5	10.1	32.5	18.3
0.363	0.1815	43.8	45.5	24.1	10.2	35.3	21.1
0.427	0.2135	44.9	50.0	26.1	10.6	39.4	25.2
0.47	0.235	45.9	53.0	25.8	10.6	42.4	28.2
0.518	0.259	46.9	56.2	25.6	10.6	45.6	31.4
Load #2: 30+j26VA − pf = 0.76							
0	0	47.3	43.5	31.4	26.5	17.0	0.0
0.083	0.0415	48.4	47.0	31.1	26.3	20.7	3.7
0.150	0.075	48.4	50.5	31.0	26.1	24.4	7.4
0.211	0.1055	50.7	54.5	30.5	25.8	28.7	11.7
0.276	0.138	51.5	57.8	30.1	25.5	32.3	15.3
0.316	0.158	51.8	60.0	29.9	25.4	34.6	17.6
0.376	0.188	53.4	63.3	29.0	25.0	38.3	21.3
0.418	0.209	54.4	65.6	29.0	25.0	40.6	23.6
0.488	0.244	55.9	69.0	28.0	24.0	45.0	28.0
0.537	0.2685	57.3	71.4	28.0	24.0	47.4	30.4
0.593	0.2965	58.5	74.0	27.0	24.0	50.0	33.0
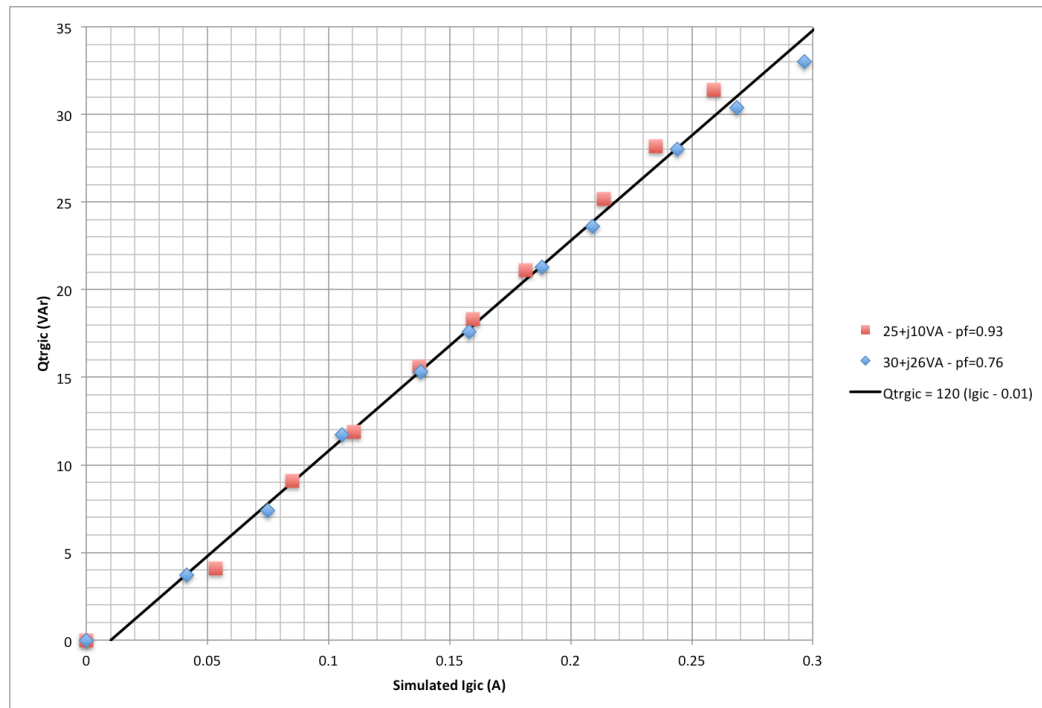
Figure 4.2: Transformer saturation under various loading conditions

4.4 Conclusion

For the studied transformer even when tested under diverse loading conditions, it is shown that the absorbed reactive power of a transformer is linearly proportional to the magnitude of the saturating current. This controlled laboratory test serves to affirm the work performed in Chapter 3, which was done in both electromagnetic transient simulation and verified using historic operating data from Hydro One.

References

[1] R. Pirjola, "Geomagnetically induced currents during magnetic storms*," IEEE Trans. Plasma Sci*., vol. 28, pp. 1867-1873, 2000.

[2] D. H. Boteler, "Geomagnetic hazards to conducting networks," Nat. Hazards, vol. 28, pp. 537-561, 2003.

[3] V. Albertson, J. Kappenman and B. Damsky, "The influence of geomagnetically induced currents (GIC) on transmission systems," in Proceedings of the American Power Conference, 1990, pp. 311-15.

[4] T. S. Molinski, W. E. Feero and B. L. Damsky, "Shielding grids from Solar Storms," IEEE Spectrum, vol. 37, pp. 55-60, 2000.

[5] D. H. Boteler, R. J. Pirjola and H. Nevanlinna, "Effects of geomagnetic disturbances on electrical systems at the earth's surface," Advances in Space Research, vol. 22, pp. 17-27, 1998.

[6] J. G. Kappenman, "Geomagnetic Storms and Their Impact on Power Systems." IEEE Power Engineering Review, May 1996.

[7] J. G. Kappenman and V. D. Albertson, "Bracing for the geomagnetic storms," IEEE Spectrum, vol. 27, pp. 27-33, 1990.

[8] A. Vilianen and R. Pirjola, "Finnish geomagnetically induced currents project," IEEE Power Engineering Review, vol. 15, pp. 20-21, 1995.

[9] L. Trichtchenko and D. H. Boteler, "Response of power systems to the temporal characteristics of geomagnetic storms," in 2006 Canadian Conference on Electrical and Computer Engineering, 2007.

Chapter 5   Modelling and Mitigation of Geomagnetically Induced Currents in a Realistic Power System Network

5.1 Introduction

During a solar magnetic disturbance that interacts with the earth, the electrojet increases in size and magnitude. This current in the ionosphere, causes short term variations in the earth's magnetic field, which in turn creates an electric field over the surface of the affected region of the planet. GIC typically affects systems at auroral latitudes (regions near the earth's magnetic poles) and approximately follows the 11 year sunspot half cycle [1]. GIC activity peaks during this 11 year half cycle [2-4]. While GIC events are more likely to occur during a peak, they are by no means limited to occurring at peak times.

The main impact of GIC on electrical power systems is through the transmission transformers with grounded neutrals. The GIC which is quasi DC causes the transformer core to saturate, which could potentially have detrimental effects on the transformer operation.

The increased magnetizing current drawn by the GIC saturated transformer and the increased harmonic content of the magnetizing current results in substantially greater core losses in the transformer. These core losses result in increased heating both in the transformer core and in other metallic components because of flux leakage. This heating can severely reduce the lifespan of a transformer. GIC induced transformer heating has been shown to cause the breakdown of transformer oil and insulation [5, 6]. During the

1989 geomagnetic storm that caused the Québec blackout a generator transformer at a nuclear station in New Jersey was destroyed due to overheating [8, 9]. In addition to the high cost of replacing the transformer, there was a significant lost revenue cost due to the time to install a replacement.

A linear relationship between the level of saturating GIC and the reactive power absorbed by the transformer has been established in Chapters 3 and 4, and can be used to determine the level of GIC flowing in a given transformer.

5.2 Modelling of Geomagnetically Induced Currents in Load Flow Studies

Comprehensive modelling of the interaction between geomagnetically induced currents and power system components typically requires a transient simulation engine capable of handling DC currents. Simulating realistic networks of even a few buses becomes computationally very intensive, and solutions are very slow, if they are attainable.

This chapter proposes a technique to model the impacts of GIC in a load flow application. With this technique established, this chapter explores the impact of GIC on a realistic system representing a portion of a larger high voltage transmission network. A number of mitigation strategies are examined.

5.2.1 Load Flow Model of a Saturated Transformer

Load flow studies consider only fundamental frequency (60 Hz) operation of the power system. The GIC levels must be calculated by a solver dedicated to them, such as the one presented in Chapter 2, which applies induced potentials on a model of the power network constructed based on the DC

resistance of the network components. For the purposes of these studies, an assumption is made that the networks connected to the secondary terminals of the transformers do not contribute GIC. Once the expected GIC levels are determined, the transformer reactive power absorption based on that level is determined by back calculating from the method presented in Chapter 3. In these studies, all transformers considered are 750 MVA autotransformers taken from a segment of the 500kV transmission network of Hydro One. The relationship between GIC and absorbed reactive power (due to GIC) is given in Figure 5.1. The data in this figure are taken from an electromagnetic transient simulation of the transformer in question using EMTDC/PSCAD software [10].
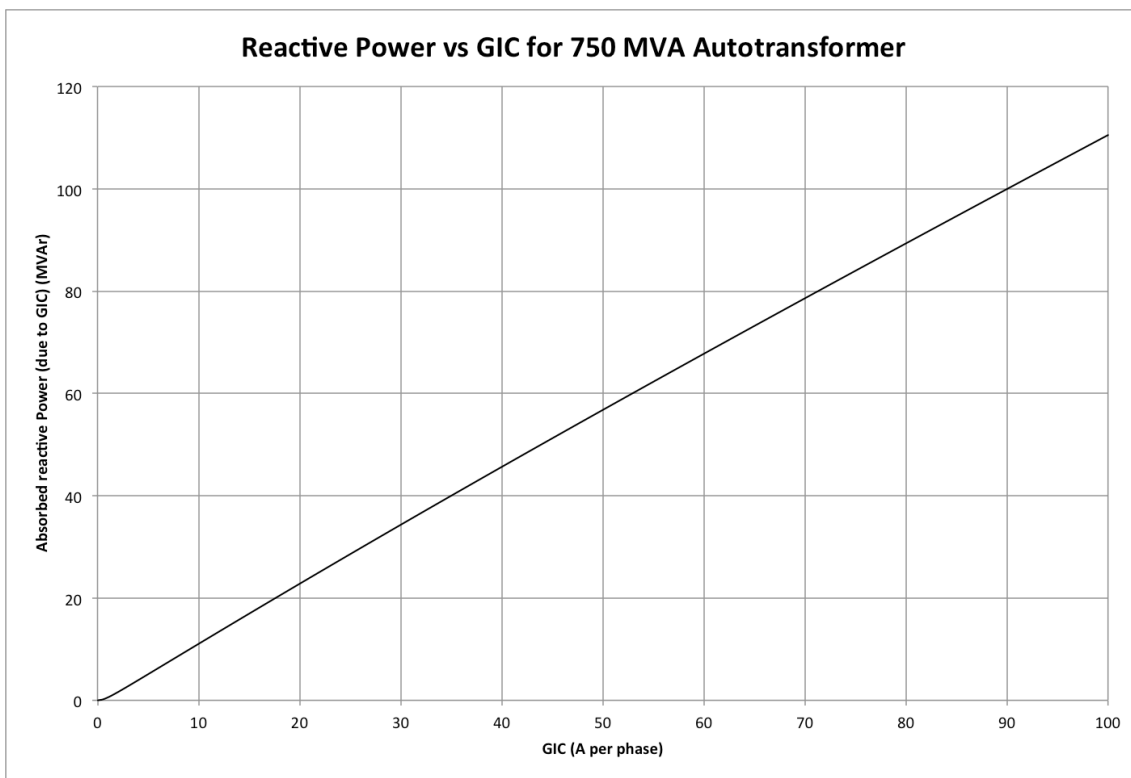
Figure 5.1: Absorbed reactive power versus saturating GIC

Once the expected reactive power absorption of each transformer due to the imposed GIC is determined, this is modelled as a constant (for a given GIC level) impedance load on the primary terminals of the transformer, the size of which is determined by the imposed GIC.

With this model it is possible to quickly determine the impact of GIC on the flow of power and bus voltages. Variations in bus voltage will affect the reactive power absorbed by saturated transformers. To allow for this the reactive power absorptions (calculated at 1 pu bus voltage) should be modeled as constant impedance loads.

5.2.2 Harmonic Distortion

The principal threat to electrical infrastructure during a GIC event is spot heating of the transformer core due to harmonic currents [5, 6]. Total Demand Distortion (TDD) is used in this chapter to represent the level or harmonic currents on each transformer. TDD is indicative of the ratio of aggregated harmonic currents to rated fundamental current. The use of Total Harmonic Distortion as a ratio with respect to actual fundamental current is deceiving if the transformer is lightly loaded, because it will over represent the level of harmonic currents present. When working in terms of currents THD and TDD are defined as:

$$THD = \sqrt{\sum_{h=2}^{N} \left(\frac{I(h)}{I(1)} \right)^2} \tag{1}$$

$$TDD = \sqrt{\sum_{h=2}^{N} \left(\frac{I(h)}{I_{rated}} \right)^2} \tag{2}$$

Hotspots caused by spot heating due to harmonic currents can degrade the insulation in a transformer and reduce its service life; in extreme cases spot heating may cause acute failure of the transformer [5, 6]. The extent to which harmonic currents cause spot heating, and the impact of that heating on transformer life vary depending on various factors including transformer construction and core type. The transformer owner or manufacturer can set guidelines for acceptable TDD levels based on temperatures of key spots within the transformer as determined by either experimental or simulation studies. Once limits have been established, these may be made known to system operators. The technique proposed in this chapter for mitigating the impact of GIC on transformer heating is predicated on the availability of above information with system operators.

The harmonic currents generated in a transformer core saturated by GIC are caused by the operation of the transformer in the non-linear operating region above the kneepoint. Since the operating region of a transformer saturated by GIC depends on the magnitude of the saturating current, the level of TDD will be proportional to the level of saturating GIC. EMTDC/PSCAD studies are performed to determine this relationship for the transformer used in these studies (detailed specifications are given in the Appendix), with the transformer loaded at its rated capacity. The results are illustrated in Figure 5.2.

TDD vs GIC for 750 MVA Autotransformer at Full Load

Figure showing TDD % on the y-axis (0.00 to 20.00) versus GIC (A per phase) on the x-axis (0 to 100), with a curve rising from near 0 to about 17.
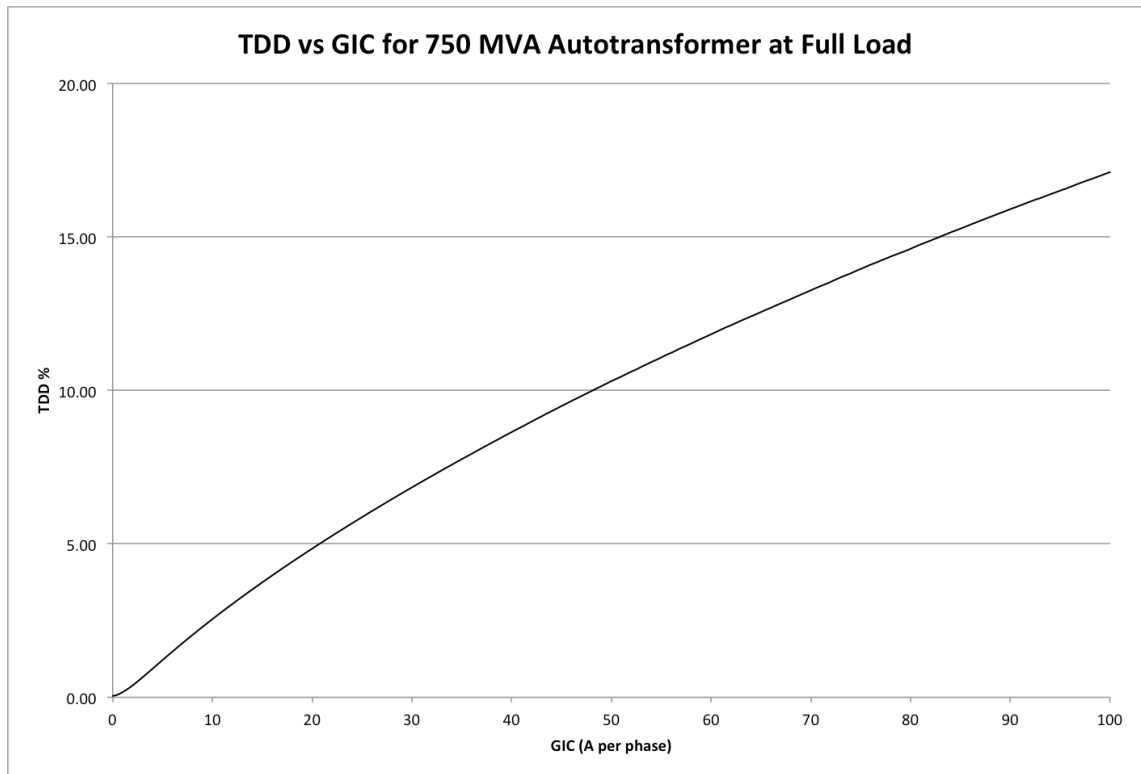
Figure 5.2: TDD versus saturating GIC

5.3 Study System

The Hydro One transmission system operates at 500 kV, 230 kV, and 115 kV, with sub-transmission at lower voltages. The 115 kV lines are typically not considered when modelling GIC as their contribution is assumed to be small because of their higher resistance. This leaves the 500 and 230 kV networks to be considered, which consist of 375 stations, interconnected by nearly 500 transmission circuits.

The study system considered is a segment of a Hydro One 500 kV transmission network which is mapped in Figure 5.3. The schematic is shown in Figure 5.4 Bus A is considered to be the slack bus for this radial network. Buses B1, B2, C, E and F each serve loads (modelled as a single PQ load on each bus). Bus D connects to a large generator, equipped with an

Automatic Voltage Regulator (AVR) that maintains the secondary voltage of the transformers at that bus at 1.06pu, and consequently provides dynamic reactive power support to the network. The slack bus A maintains a voltage of 1.05 pu. Full specifications for all lines and transformers are given in the appendix.

5.4 Impact of GIC on the System

Table 5-1 shows the load flow results for the study system described above. *Psec* and *Qsec* are the real and reactive power delivered to the load at each bus. *Vpri* is the per-unit bus voltage on the primary side of the transformer. *Imposed GIC* is the transformer saturating current for each station calculated using the GIC solver in Chapter 2. Each transformer's portion of this GIC is *GIC per transf.* *Expected TDD%* and *Qgic per transf* are calculated using the EMTDC/PSCAD results described previously in section 5.2.2 and 5.2.1, respectively. *Qgic* is the aggregate reactive power absorption due to GIC for the station. All scenarios shown are based on an event with a uniform electric field strength of 3 V/km in an eastward direction.

The first system study shows the system response to the GIC event, with no corrective action taken. As expected, the transformer stations at the east end of the line (E and F) carry the majority of the GIC, in excess of 50A in each transformer. At station E the TDD due to transformer saturation exceeds 10% and at station D, it approaches 10%. Depending on the limits of the transformers in question these units may be considered in distress due to excessive harmonic spot heating. Even if there is not a risk of eminent transformer failure due to spot heating, they will likely experience a decreased lifetime due to the damage caused to insulation.

Figure 5.3: Map of Study System
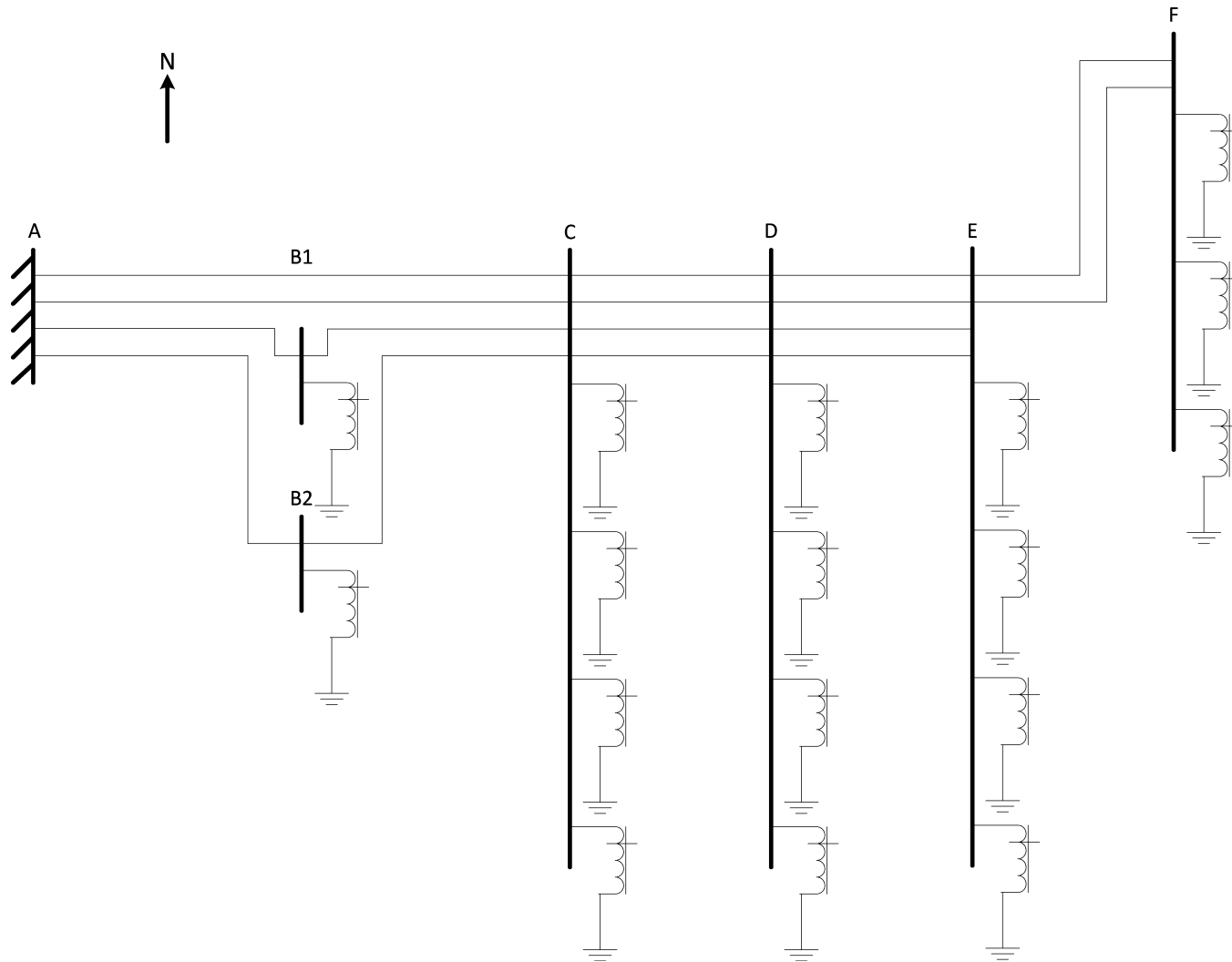
Figure 5.4: 500kV Study System

Table 5-1: Case Study Results

	Base Case With no GIC			With 3V/km GIC								
All equipment in service												
	Psec	Qsec	Vpri (pu)	Imposed GIC	GIC per transf	Expected TDD %	Qgic per transf	Qgic	Psec	Qsec	Vpri (pu)
A	303.47	-658.94	1.05						300.36	-881.97	1.05
B1	430	-25	1.044	-11.298	-11.298	2.8	12.6447216	12.6447216	430	-25	1.0419
B2	430	-25	1.044	-11.298	-11.298	2.8	12.6447216	12.6447216	430	-25	1.0419
C	740	760	1.038	0.5769	0.144225	0.09	0.16141662	0.64566648	740	760	1.0336
D	-2600	-533.74	1.0465	42.75	10.6875	2.67	11.96145	47.8458	-2600	-798.91	1.0382
E	260	75	1.035	198.12	49.53	10.3	55.433976	221.735904	260	75	0.9937
F	440	-75	1.0389	140.49	46.83	9.82	52.412136	157.236408	440	-75	0.9665

	Base Case With no GIC			With 3V/km GIC								
Transformer Tripped at E												
	Psec	Qsec	Vpri (pu)	Imposed GIC	GIC per transf	Expected TDD %	Qgic per transf	Qgic	Psec	Qsec	Vpri (pu)
A	303.5	-658.95	1.05						300.43	-880.2	1.05
B1	430	-25	1.044	-10.773	-10.773	2.8	12.0571416	12.0571416	430	-25	1.0419
B2	430	-25	1.044	-10.773	-10.773	2.8	12.0571416	12.0571416	430	-25	1.0419
C	740	760	1.038	1.7043	0.426075	0.27	0.47686314	1.90745256	740	760	1.0336
D	-2600	-533.74	1.0465	47.82	11.955	3.04	13.380036	53.520144	-2600	-796.99	1.0382
E	260	75	1.035	185.79	61.93	12.12	69.312056	207.936168	260	75	0.9946
F	440	-75	1.0389	144.39	48.13	9.98	53.867096	161.601288	440	-75	0.9699

Table 5-1: Case Study Results (continued)

	Base Case With no GIC			With 3V/km GIC							
						Transformer Tripped at F					
	Psec	Qsec	Vpri (pu)	Imposed GIC	GIC per transf	Expected TDD %	Qgic per transf	Qgic	Psec	Qsec	Vpri (pu)
A	303.53	658.96	1.05						300.2	-884.06	1.05
B1	430	-25	1.044	-11.277	-11.277	2.8	12.6212184	12.6212184	430	-25	1.0419
B2	430	-25	1.044	-11.277	-11.277	2.8	12.6212184	12.6212184	430	-25	1.0419
C	740	760	1.038	0.6234	0.15585	0.09	0.17442732	0.69770928	740	760	1.0336
D	-2600	533.74	1.0465	42.96	10.74	2.67	12.020208	48.080832	-2600	-801.69	1.0381
E	260	75	1.035	199.05	49.7625	10.3	55.69419	222.77676	260	75	0.9932
F	440	-75	1.0389	139.2	69.6	13.19	77.89632	155.79264	440	-75	0.9655

	Base Case With no GIC			With 3V/km GIC							
						Transformer Tripped at E and F					
	Psec	Qsec	Vpri (pu)	Imposed GIC	GIC per transf	Expected TDD %	Qgic per transf	Qgic	Psec	Qsec	Vpri (pu)
A	303.52	-661.15	1.05						300.36	-882.66	1.05
B1	430	-25	1.044	-10.749	-10.749	2.8	12.0302808	12.0302808	430	-25	1.0419
B2	430	-25	1.044	-10.749	-10.749	2.8	12.0302808	12.0302808	430	-25	10.419
C	740	760	1.038	1.7607	0.440175	0.27	0.49264386	1.97057544	740	760	1.0336
D	-2600	-536.63	1.0464	48.06	12.015	3.04	13.447188	53.788752	-2600	-800.26	1.0381
E	260	75	1.0345	186.72	62.24	12.12	69.659008	208.977024	260	75	0.994
F	440	-75	1.0346	143.07	71.535	13.47	80.061972	160.123944	440	-75	0.9655

Table 5-1: Case Study Results (continued)

	Base Case With no GIC			With 3V/km GIC							
	Psec	Qsec	Vpri (pu)	Imposed GIC	GIC per transf	Expected TDD %	Qgic per transf	Qgic	Psec	Qsec	Vpri (pu)
A	266.77	679.47	1.05						267.2	-583.61	1.05
B1	430	-25	1.0383	7.77	7.77	2.03	8.696184	8.696184	430	-25	1.0401
B2	430	-25	1.0383	7.77	7.77	2.03	8.696184	8.696184	430	-25	1.0365
C	740	760	1.0247	18.669	4.66725	1.07	5.2235862	20.8943448	740	760	1.0285
D	-2600	645.82	1.0429	-1.7148	-0.4287	0.09	0.47980104	1.91920416	-2600	-446.97	1.0491
E	260	75	1.0157	71.67	17.9175	4.42	20.053266	80.213064	260	75	1.0636
F	440	-75	1.0195	118.86	39.62	8.64	44.342704	133.028112	440	-75	1.0938

The table is headed "2 lines tripped (A to E)".

Qgic Values are assumed for bus voltages of 1pu, in simulations these are treated as constant impedance loads.

It is also of note that the increased reactive power absorption due to GIC causes the voltages at the unregulated buses to drop. This is of particular concern at bus F, where the voltage drops just below 0.97 pu. On it own this may not be a cause for concern, however if the event were to grow in severity as it progresses, or were the system to suffer a loss of VAr support, there is a risk that under voltage limits could be violated. Low bus voltages may potentially lead to stability problems within the system and should be managed carefully. It may be necessary to bring additional VAr support online at buses E or F. This will help improve the network's voltage profile. Capacitors banks may be helpful in providing voltage support, however, if grounded, they may be vulnerable to overcurrent tripping due to the high frequency harmonics generated by the transformers saturated by GIC.

Mitigating action to protect the system is advisable, especially if the event is expected to increase in severity.

5.5 Transformer Protection

When a transformer is at risk of damage, due to overheating or other factors, conventional protection wisdom would dictate that the transformer should be removed from service to protect the asset. Three system studies where transformer are removed from service are presented in the second, third and fourth blocks of Table 5-1.

The second system study considers the pre-emptive tripping of one of the transformers at station E, the station where the transformers are in the most distress. As seen in the net GIC levels in each station (*Imposed GIC*), removing a transformer from service has little impact. However, the GIC flow through that station is now shared across the windings of three instead

of four transformers. The increased GIC in each transformer increases the TDD generated by the saturated cores and places the transformers deeper into distress. This course of action could lead to a cascading need for action being taken on all transformers in the station.

The third system study shows a transformer tripping at station F, with similar results to the transformer tripping at station E. In the case of this station, the impact of the tripping is greater due to there being few transformers at the station. As in the last system study the transformers remaining in service are in greater distress due to harmonic spot heating than in the case with all transformers in service.

The fourth system study illustrates a trip of a transformer at station E and a transformer at station F. In this case the impact of both of the previous discussed system studies are seen at the same time. While taking distressed transformers out of service during a GIC event will protect those individual transformers, it does so at the cost of the equipment left in service.

5.6 System Protection by Line Tripping

GICs are induced in the system in the transmission lines. Furthermore, the typical DC resistance of a transmission line is an order of magnitude or more greater than the resistance of transformer windings. Knowing this, it can be concluded that the best way to influence GIC levels is to remove transmission lines from service.

The fifth system study presented in Table 1, shows a case where two of the four transmission lines connecting stations A to E are removed from service. This operating action results in severe reductions in the GIC levels seen at the vulnerable stations E and F. At station E, the most affected station in

the base case, the GIC per transformer drops from 49.53 to 17.92 A. This results in a drop in the TDD level to less than 4.5%. Station F sees a lower reduction from 46.83 to 39.62 A and a reduction in TDD to 8.64%. It is however of note that no mitigation was taken on the line into station F.

The system voltage profile sees a marked improvement by removing lines from service; none of the bus voltages fall below 1 per unit. With the reduced TDD from the transformers the risk of capacitor bank tripping is diminished and there is a better chance of the system surviving the event.

5.6.1 Impact of Line Tripping on Power Flow

When removing lines from service, there is a risk that the lines remaining in service will not be able to handle the power flow. In the scenario shown, the most heavily loaded line is the segment connecting the generator at Bus D to bus C. With only two (of four) lines in service, each line caries 960 MVA, which is close to the rated capacity of approximately 1000 MVA. Care must be taken to ensure that the line capacity is not exceeded.

If it is necessary the ten-hour overload capacity of the line can be used. If the GIC persists past ten hours, careful switching operations can bring one of the lines previously removed from service back online to replace a line reaching the end of its allowable time for overloaded operation. It may also be advisable to redistribute generation to reduce the power flow in line groups where lines have been tripped out to reduce GIC in the system. The load shedding option may also be considered as a final resort to avoid overloading of lines.

5.7 Conclusions

This Chapter presents a detailed analysis of the impact of GIC in a realistic network configured from the actual 500kV transmission network of Hydro One. Different cases of impact of GIC and corresponding mitigating measures are examined. As shown in the case studies presented, with an improved visibility of GIC within the system, system operation can make better informed decisions on how to act during a GIC event. This improved decision making ability can only serve to improve the system's ability to manage a GIC event.

Appendix

Transformer Specifications:

Transformer MVA:	750 MVA
Primary Voltage:	500 kV
Secondary Voltage:	230 kV
Leakage Reactance:	0.10 pu
Magnetizing reactance:	0.40 %
Air Core Reactance	0.20 pu
Knee Voltage:	1.10 pu

Transmission Line Impedances:

	X	R
A to B1	0.028	0.003
A to B2	0.028	0.003
B1 to C	0.039	0.004
B2 to C	0.039	0.004
A to C	0.066	0.007
C to D	0.066	0.007
D to E	0.261	0.027
E to F	0.273	0.028

All values are per-unit on a base of 750 MVA and 500 kV. Where a group consists of multiple parallel lines the given specifications are used for each line.

References

[1] L. Trichtchenko, D. H. Boteler, " Response of Power Systems to the Temporal Characteristics of Geomagnetic Storms," in 2006 Canadian Conference on Electrical and Computer Engineering, 2006, pp. 4.

[2] D. H. Boteler, "Geomagnetic hazards to conducting networks," Nat. Hazards, vol. 28, pp. 537-561, 2003.

[3] V. Albertson, J. Kappenman and B. Damsky, "The influence of geomagnetically induced currents (GIC) on transmission systems," in Proceedings of the American Power Conference, 1990, pp. 311-15.

[4] D. H. Boteler, R. J. Pirjola and H. Nevanlinna, "Effects of geomagnetic disturbances on electrical systems at the earth's surface," Advances in Space Research, vol. 22, pp. 17-27, 1998.

[5] R. S. Girgis, Chung-Duck Ko and D. J. Scott, "Analysis of transformer overheating due to geomagnetically induced currents," in Proceedings of the American Power Conference, 29 April-1 may 1991, 1991, pp. 1167-72.

[6] S. Lu, Y. Liu and J. D. L. Ree, "Harmonics generated from a DC biased transformer," IEEE Trans. Power Del., vol. 8, pp. 725-731, 1993.

[7] R. S. Girgis and C. Ko, "Calculation techniques and results of effects of GIC currents as applied to large power transformers," IEEE Trans. Power Del., vol. 7, pp. 699-705, 1992.

[8] J. G. Kappenman, "Geomagnetic Storms and Their Impact on Power Systems." IEEE Power Engineering Review, May 1996.

[9] R. Pirjola, "Space weather effects on technological systems on the ground," in Proceedings Asia-Pacific Conference on Environmental Electromagnetics. CEEM 2000, 3-7 may 2000, pp. 217-21.

[10] "Users guide: EMTDC," *Manitoba HVDC research center*, Canada, Apr. 2005.

[11] "Doccument C-15, Procedures for Solar Magnetic Disturbances Which Affect Electric Power Systems." NPCC Inc. 2007. Available online www.npccc.org.

Chapter 6 Determination of the Frequency Spectrum of the Magnetization Current of a Saturated Transformer

6.1 Introduction

When a transformer becomes saturated harmonic currents are generated due to the non-linear behaviour of the transformer magnetizing reactance. When that saturating current is a low frequency oscillating current, such as, a geomagnetically induced current [1-4] or the post fault behaviour of some FACTS devices [5], the currents generated by the saturated transformer fall not only on the harmonics of the system fundamental frequency but also on the sidebands of those harmonic frequencies. The ability to predict these sideband frequencies is necessary since they may excite resonances within the network. If any of the several frequencies coincides with the network resonant frequencies there may be undesirable amplification of this frequency component. This may potentially result in faulty operation of FACTS controllers or relays. In the case of interactions with FACTS devices it may be necessary to design filters to reject frequencies generated by saturated transformers at the voltage or current measurement inputs in order to avoid undesired operation [6].

In this chapter a technique is presented to predict not only the frequencies but the magnitudes of the harmonics generated. This is done by performing an accurate polynomial regression of the transformers B-H curve and a Fourier analysis of the resulting function. Section 6.2 describes the transformer saturation model, while section 6.3 presents the proposed technique for determination of the frequency spectrum of a saturated

transformer. The technique is validated in section 6.4 for a test study system. In section 6.5, the results from a Hydro Quebec system [5] are correlated with those predicted from the proposed technique. Section 6.6 extends the proposed technique to predict both magnitudes and frequencies. This extended technique is tested in section 6.7. Finally, section 6.8 concludes the paper.

6.2 System Model

The saturation characteristics of the transformer are central to the study of the impacts of GIC on transformer operation. The typical *B-H* curve of an iron-core transformer is shown in Figure 6.1. This can be approximated by a linearized *B-H* characteristic depicted in Figure 6.2. This saturation characteristic is defined in terms of the asymptotes that shape the final curve. The unsaturated magnetizing impedance (X_m) defines the slope in the unsaturated region. The slope of the saturated region represents the air core reactance ($X_{aircore}$). The intercept of this slope's asymptote with the y-axis provides the knee voltage (V_{knee}) [7]. The classical equivalent circuit of a transformer modified with a saturating current source that injects saturating current following the *B-H* property of Figure 6.2 is depicted in Figure 6.3.

The non-linearity of the B-H curve causes a non-linear current draw resulting in harmonic injection by the transformer.

6.3 Proposed Technique for Prediction of Frequencies Only

This technique is presented for predicting the spectrum of frequencies which could be emanated by a transformer when saturated by an oscillating current of another frequency. This technique does not predict the magnitudes of the various harmonic components.
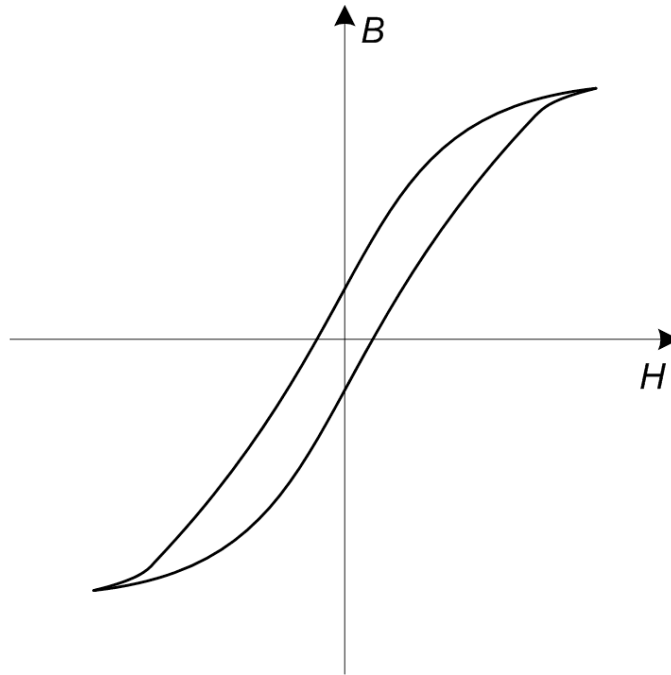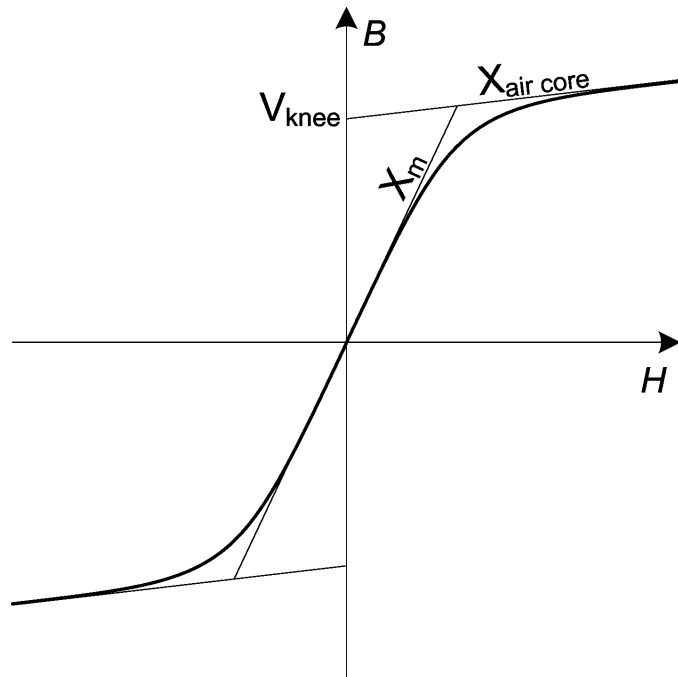
Figure 6.1: Typical B-H Curve

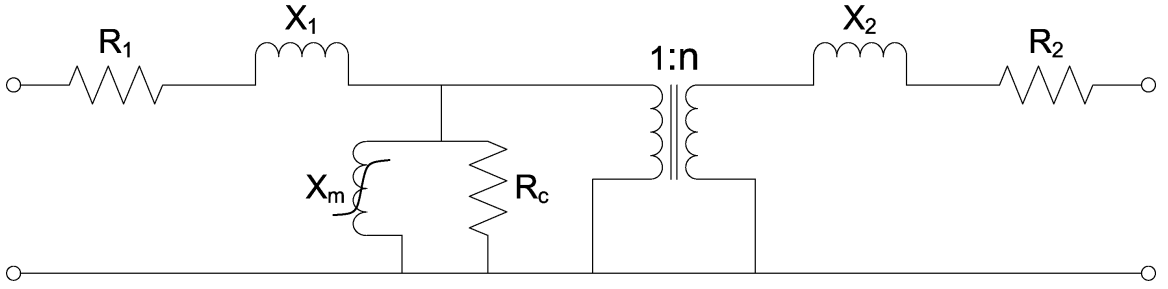
Figure 6.2: Simplified B-H curve

Figure 6.3: Transformer model with saturation incorporated

In a typical transformer, the saturated reactance is orders of magnitude smaller that the unsaturated reactance. For instance, a typical EHV transformer saturated reactance (X_m) may be 250 p.u. whereas the saturated reactance ($X_{aircore}$) may be 0.2 p.u. The actual slopes of the B-H curve may be replaced with arbitrary slopes k and l, since this technique in its present form focuses only on the prediction of frequencies (not magnitudes) of the harmonics generated. With the above approximations, a simplified general *B-H* function is obtained as below:

$$
\begin{aligned}
B = \quad & lH + V_{knee}, && H \geq \frac{V_{knee}}{k-l} \\
= \quad & kH, && -\frac{V_{knee}}{k-l} < H < \frac{V_{knee}}{k-l} \\
= \quad & lH - V_{knee}, && H \leq -\frac{V_{knee}}{k-l}
\end{aligned}
\tag{1}
$$

This derives a generalized B-H curve that should be applicable to any transformer. A curve fitting technique is now employed to approximate the generalized *B-H* curve. Different order polynomial functions are considered to obtain the closest fit, and desired resolution. The third, fifth and seventh, and ninth order odd polynomial approximations of the *B-H* curve are illustrated in Figures 6.4, 6.5, 6.6 and 6.7, respectively.
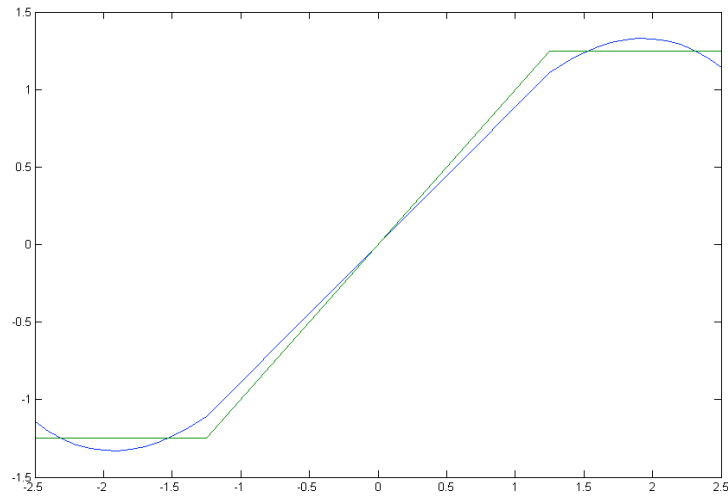
Figure 6.4: Simplified B-H curve with 3rd order polynomial approximation
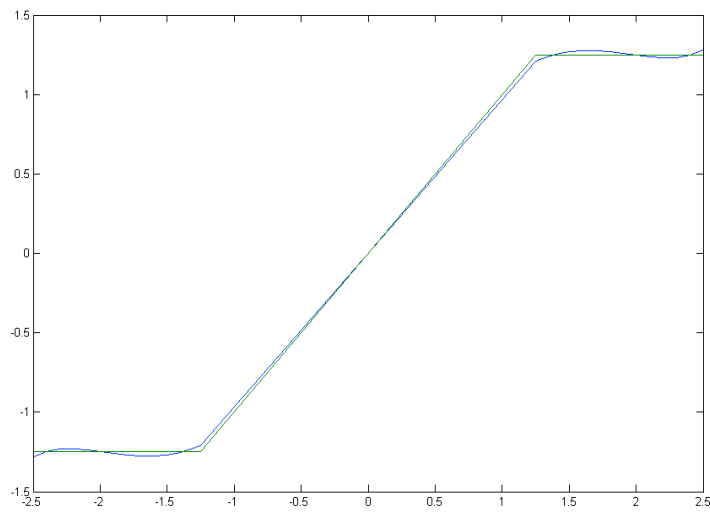

Figure 6.5: Simplified B-H curve with 5th order polynomial approximation
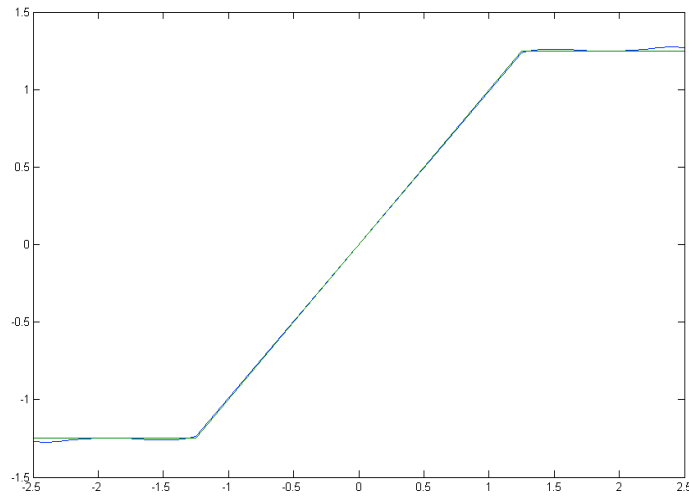
Figure 6.6: Simplified B-H curve with 7th order polynomial approximation
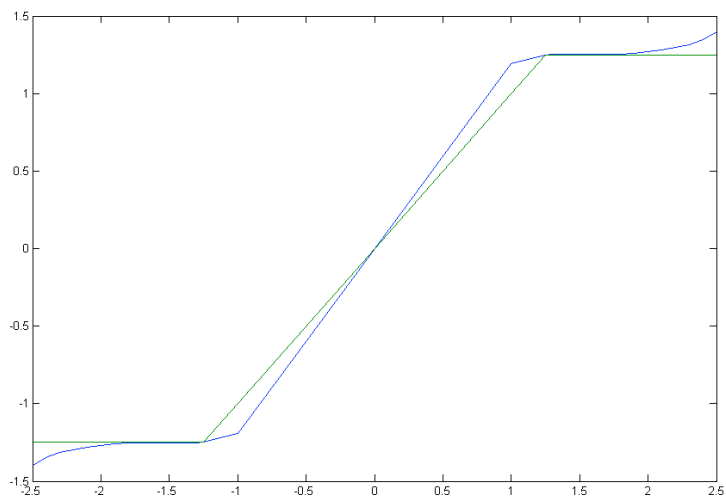
Figure 6.7: Simplified B-H curve with 9th order polynomial approximation

The degree of the approximating polynomial chosen will determine the number of frequencies obtained in the solution, the highest harmonic represented by the solution being the degree of the approximation used. The accuracy in terms of magnitude is not relevant here since this technique does not predict the magnitude of the harmonics. If the magnitude were to be considered, the knee point, saturated, unsaturated reactances and the expected operating range of the transformer would be important to determining the polynomial approximation.

For this example, the 5th order polynomial approximation, shown in (2), is used to represent the B-H curve of a given transformer. If more frequency resolution is desired, a higher order approximation may be selected. The input function, expressed in (3), is the sum of the power frequency (ω_1) component and a modulating frequency (ω_2) saturating function (typically having a low frequency).

$$f(x) \approx Ax + Bx^3 + Cx^5 \qquad (2)$$

$$x = Xe^{j\omega_1 t} + Ye^{j\omega_2 t} = a + b \qquad (3)$$

Substituting for x in (2) results in:

$$f(x) = Aa + Ab + Ba^3 + 3Ba^2b + 3Bab^2 + Bb^3 + \\ Ca^5 + 5Ca^4b + 10Ca^3b^2 + 10Ca^2b^3 + 5Cab^4 + Cb^5 \qquad (4)$$

When further expanded (substituting for a and b), this equation yields the frequencies shown in Table 6-1:

Table 6-1: Frequencies present in the general solution for a fifth order approximation

Band	Frequencies
Sub-harmonic	ω_2, $3\omega_2$, $5\omega_2$
1st Harmonic	ω_1-$4\omega_2$, ω_1-$2\omega_2$, ω_1, ω_1+$2\omega_2$, ω_1+$4\omega_2$
2nd Harmonic	$2\omega_1$-$3\omega_2$, $2\omega_1$-ω_2, $2\omega_1$+ω_2, $2\omega_1$+$3\omega_2$
3rd Harmonic	$3\omega_1$-$2\omega_2$, $3\omega_1$, $3\omega_1$+$2\omega_2$
4th Harmonic	$4\omega_1$-ω_2, $4\omega_1$+ω_2
5th Harmonic	$5\omega_1$

As observed from above, for a polynomial approximation of degree N, the number of sidebands (h) of any harmonic (n) is given by:

$$h = 1 + N - n, \quad n = 1, 2...N \tag{5}$$

Further, the odd harmonics have even multiples of modulating frequency as sidebands, whereas even harmonics have odd multiples of modulating frequency as sidebands.

6.4 Case Study I

6.4.1 Study System

The study system is shown Figure 6.8. The transformer of interest is a three-phase bank that consists of three independent single-phase autotransformers. This transformer type is selected because these are most vulnerable to saturation by zero sequence currents [8]. The transformer of interest is supplied from the grid, which is represented by an ideal voltage source behind a delta connected ideal transformer. This delta connected transformer serves to block DC currents from either side. A DC current source injects current in each primary phase to simulate the GIC. The low voltage side of the transformer of interest supplies a constant power load of

100 MW which is its rated capacity. This load is isolated from the flow of low frequency current again with a delta connected ideal transformer. Detailed transformer specifications are provided in the Appendix. EMTDC/PSCAD software [9] is utilized to simulate the entire system.
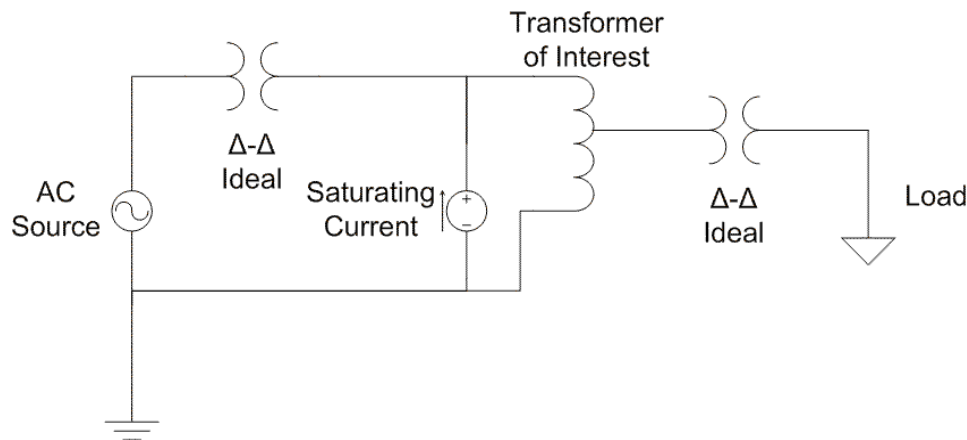
Figure 6.8: Single-phase transformer study system

6.4.2 Analysis

Figure 6.9 shows the resultant draw of the autotransformer studied when exposed to a GIC with a magnitude of 100 A (peak) and a frequency of 3 Hz.

The transformer real power P_{trans}, reactive power Q_{trans}, phase a current I_a, ground current I_g, transformer flux, load real power P_{load}, and load reactive power Q_{load} are depicted in Fig. 6.9. Each of these signals is superimposed with a spectrum of frequency components, except the load real and reactive power signals, which are constant. Although 3 Hz is much higher that the frequency of naturally occurring GIC, this value is selected to ensure that the modulation effects of the GIC signal are sufficiently distinct from the harmonics generated by transformer saturation to be easily identified.

Figure 6.9: Transformer with 100A oscillating (3Hz) saturating current per phase

Figure 6.10 illustrates the spectral analysis (by FFT with 1 Hz resolution) of the transformer phase current (on the high voltage terminal of phase A). In addition to the expected 3 Hz GIC and the 60 Hz AC fundamental, significant even harmonic modulation is see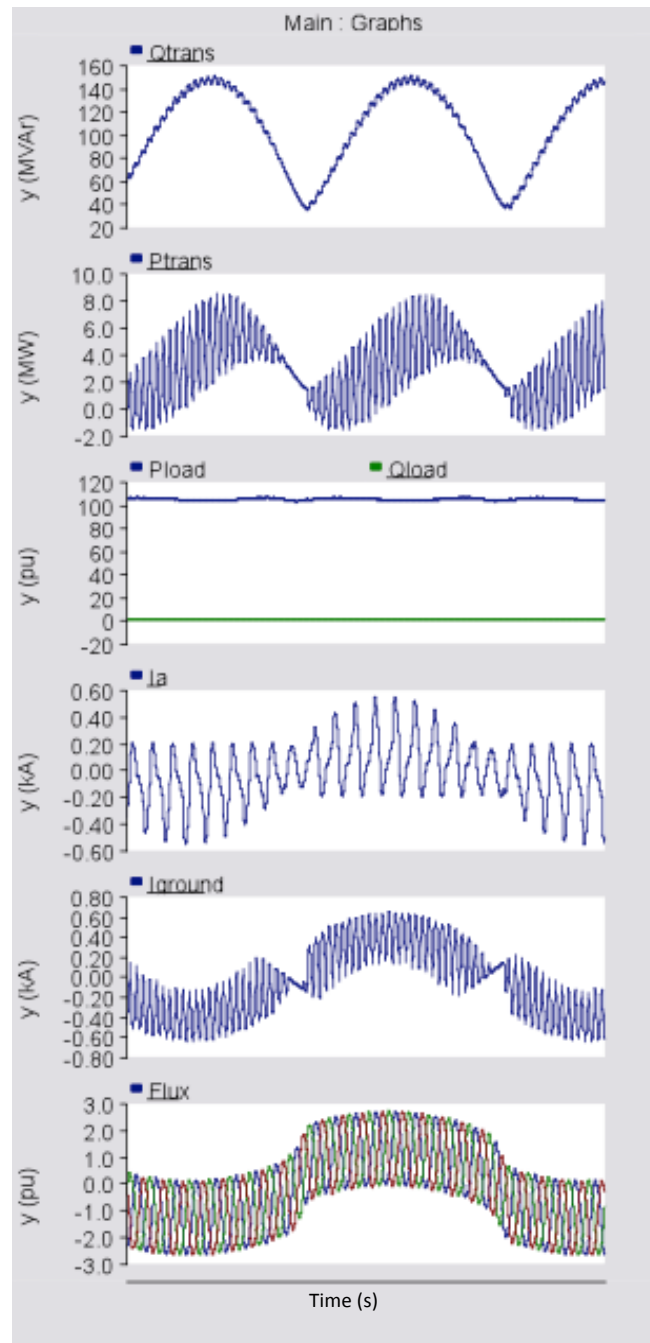n around the 60 Hz fundamental. The 2nd harmonic of the AC signal sees significant odd harmonic modulation (111, 117, 123, 129 Hz). The 4th harmonic of the AC (60 Hz) current sees some odd harmonic modulation (231*, 237, 243, 249* Hz). The 5th harmonic of the AC (60 Hz) current sees finite even harmonic modulation (288*, 294*, 300, 306*, 312* Hz). All the frequency components around the fundamental, second, fourth and fifth harmonic frequencies are predicted by the proposed technique. The asterisk (*) marked frequencies are not predicted by the model as the approximating polynomial is only of 5th order. A higher order polynomial approximation would have yielded the remaining harmonics.

It is seen in Figure 6.11 that the transformer neutral caries the triplen (3rd and 6th) harmonics of the AC current (60 Hz). These are blocked by the delta-delta isolation transformer and therefore flow into the transformer of interest only through the neutral. The third harmonic has significant even harmonic modulation (168, 174, 180, 186, 192 Hz etc.). The sixth harmonic sees odd harmonic modulation (351, 357, 363, 369 Hz).

Table 6-2, summarizes the results for both the neutral and phase currents. The predicted results, using the 5th and 9th order approximations are shown for comparison. Those frequencies marked with an asterisk (*) are present in the observed data but not predicted by the 5th order approximation, this is a limitation of lower order approximations. Those frequencies marked with a dagger (†) are predicted by the 9th order approximations but do not appear in the results at detectable levels, this extraneous data is a limitation of a higher order approximation.
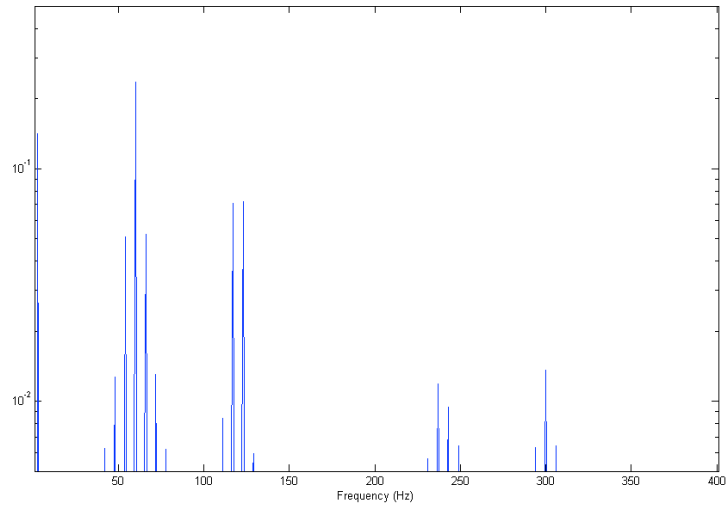
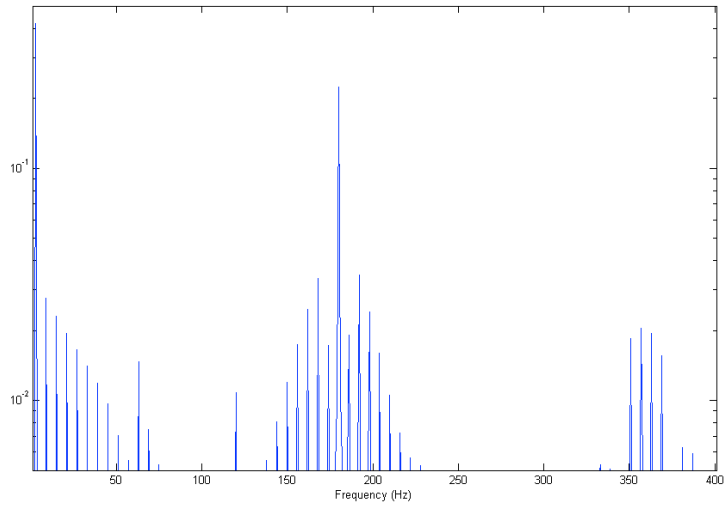**Figure 6.10: Spectral analysis of Transformer Phase A Current**

Figure 6.11: Spectral analysis of Transformer Neutral Current

Table 6-2: Harmonic currents generated by the test transformer

Band	Frequencies		
	Observed Results	Predicted by 5th Order	Predicted by 9th Order
Sub-harmonic	3, 9, 15 Hz	3, 9, 15 Hz	3, 9, 15, 21†, 27† Hz
1st Harmonic (60Hz)	48, 54, 60, 66, 72 Hz	48, 54, 60, 66, 72 Hz	36†, 42†, 48, 54, 60, 66, 72, 78†, 84† Hz
2nd Harmonic (120Hz)	111, 117, 123, 129 Hz	111, 117, 123, 129 Hz	99†, 105†, 111, 117, 123, 129, 135†, 141† Hz
3rd Harmonic (180 Hz)	168*, 174, 180, 186, 192* Hz	174, 180, 186 Hz	162†, 168, 174, 180, 186, 192, 198† Hz
4th Harmonic (240Hz)	231*, 237, 243, 249* Hz	237, 243 Hz	225†, 231, 237, 243, 249, 255† Hz
5th Harmonic (300Hz)	288*, 294*, 300, 306*, 312* Hz	300 Hz	288, 294, 300, 306, 312 Hz

Despite the limitations described above, this technique is able to reasonably well predict the frequencies generated.

6.5 Case Study II

6.5.1 Study System

In the early 1990s, Hydro Québec implemented an extensive network of 33 series compensators on their 735 kV transmission system. Included in this network were eleven Static VAr Compensators with capacities of +300/-110 MVAr each, installed at 6 substations [5].

In fault studies of the system, shown in section 4 of [5], the following results are obtained. With series compensation in place (creating the post fault resonance at 11 Hz), instead of the harmonic current injections from a saturated transformer at odd and even harmonics of the system fundamental frequency, side bands around those harmonics are seen, as shown in Figure 6.12.
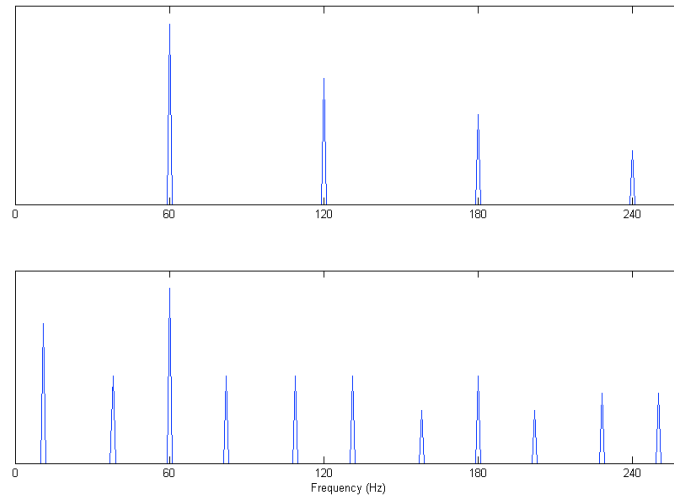
Figure 6.12: Spectrum of transformer magnetizing current at fault clearing without series compensation (top) and with series compensation (bottom), from [5]

6.5.2 Analysis

Using the 5th order analysis described in this paper, current injections are expected at the frequencies shown in Table 6-3. All the frequencies predicted by the proposed technique (except marked by asterisk) are found to be present in the actual waveforms measured in the Hydro Quebec system. It could perhaps be that these frequencies are likely present, but fall at a level below the detection threshold used by the original authors.

Table 6-3: Frequencies present in the solution for a fifth order approximation for the Hydro-Québec series compensator

Band	Frequencies
Sub-harmonic	11, 33*, 55* Hz
1st Harmonic	16*, 38, 60, 82, 104* Hz
2nd Harmonic	87*, 109, 131, 153* Hz
3rd Harmonic	158, 180, 202 Hz
4th Harmonic	229, 251 Hz
5th Harmonic	300* Hz

6.6 Extension of Technique to Predict Both Magnitudes and Frequencies

In order to predict the magnitudes of frequencies generated by a saturated transformer, a detailed knowledge of both the expected operating conditions of the transformer (magnitudes of both power frequency and saturating voltage) and the magnetization characteristic of the transformer are needed. Figure 6.13 shows the magnetization characteristic of a transformer represented in terms of power frequency voltage and current. The relationship between current (i) and voltage (v) is given by (6).
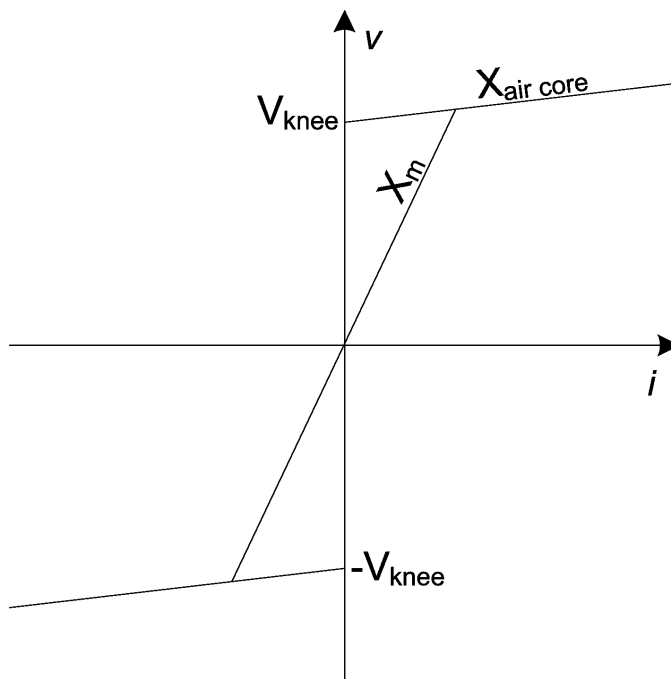

Figure 6.13: V-I magnetization characteristic of a transformer

$$i = \frac{v - \sqrt{2}v_{knee}}{x_{aircore}}, \qquad v > \frac{\sqrt{2}v_{knee}}{1 - \frac{x_{aircore}}{x_m}}$$

$$= \frac{v}{x_m}, \qquad \frac{-\sqrt{2}v_{knee}}{1 - \frac{x_{aircore}}{x_m}} \leq v \leq \frac{\sqrt{2}v_{knee}}{1 - \frac{x_{aircore}}{x_m}} \qquad (6)$$

$$= \frac{v + \sqrt{2}v_{knee}}{x_{aircore}}, \qquad v < \frac{-\sqrt{2}v_{knee}}{1 - \frac{x_{aircore}}{x_m}}$$

In order to use (6) for frequencies other that the power frequency (f_0), it is necessary to calculate an equivalent magnitude (v'_{sat}) of the saturating voltage (v_{sat}) to account for the increased susceptibility of the transformer core to saturation by lower frequencies [10]:

$$v'_{sat} = v_{sat} \frac{f_0}{f_{sat}} \qquad (7)$$

The polynomial approximation of the *i-v* characteristic of the transformer is taken over the expected operating voltage range (peak to peak of the combined power frequency (v_0) voltage and saturating (v_{sat}) voltages). The time varying voltages are substituted into the polynomial, which is simplified and the Fourier transform taken to give the expected spectrum.

The case study below shows the technique using a fifth order polynomial approximation for a transformer (specified in the Appendix) operating at $v_0 = 1.4$pu with no saturating function ($v_{sat} = 0$). While this example is oversimplified, it serves to illustrate the technique.

6.6.1 Case Study III

A fifth order polynomial approximation is selected for the purposes of this illustration. A fifth order approximation will only predict the fundamental, 3rd and 5th harmonic. A significant degree of error will be attributable to the low degree of the approximation. However, the principles developed can be extended to a higher degree of polynomial and to multi-frequency scenarios

The fifth order polynomial approximation of (6) using the values given in the appendix is taken over the range:

$$-1.4\sqrt{2} \le v \le 1.4\sqrt{2} \tag{8}$$

This approximation is:

$$i = 0.1719v^5 - 0.4298v^3 + 0.2002v \tag{9}$$

Substituting in the exciting voltage gives:

$$
\begin{aligned}
i &= 0.1719\left(1.4\sqrt{2}\cos(2\pi 60t)\right)^5 - 0.4298\left(1.4\sqrt{2}\cos(2\pi 60t)\right)^3 + 0.2002\left(1.4\sqrt{2}\cos(2\pi 60t)\right) \\
&= 0.1719(1.4)^5\sqrt{2}^5 \frac{10\cos(2\pi 60t) + 5\cos(3\times 2\pi 60t) + \cos(5\times 2\pi 60t)}{16} \\
&\quad -0.4298(1.4)^3\sqrt{2}^3 \frac{3\cos(2\pi 60t) + \cos(3\times 2\pi 60t)}{4} + 0.2002(1.4)\sqrt{2}\cos(2\pi 60t) \\
&= 1.1632\cos(2\pi 60t) + 0.8004\cos(3\times 2\pi 60t) + 0.3269\cos(5\times 2\pi 60t)
\end{aligned}
\tag{10}
$$

Taking the Fourier transform of the above functions gives:

$$I(\omega) = 1.1632\delta(\omega - 2\pi 60) + 0.8004\delta(\omega - 3\times 2\pi 60) + 0.3269\delta(\omega - 5\times 2\pi 60) \tag{11}$$

Taking a fast Fourier transform (FFT) of the current signal calculated using the original piecewise linear BH function gives a point for comparison. This same technique is repeated with 15th degree polynomial approximation, for which only the results are shown in Table 6-4. An electromagnetic transient analysis of a similar transformer is also shown as a reference.

Table 6-4: Results of approximation of frequency and magnitude

f	Electromagnetic Transient Simulation	Original Function	5th Order Approximation	15th Order Approximation
60	0.9546	1.1417	1.1632	1.1451
180	0.6616	0.7754	0.8004	0.7789
300	0.2835	0.3000	0.3269	0.3035
420	0.0654	0.0205	---	0.0168
540	0.0786	0.0937	---	0.0896

As expected the higher order approximation yields a more accurate result. However, the 5th order approximation still yields a result within 2.5% (0.025pu) on all frequencies.

Total Harmonic Distortion (THD) is a more comprehensive indicator of the accuracy of an approximation than comparing individual harmonics piecemeal and is therefore computed for the next study. Table 6-5 shows the THD for the previously described study system calculated based on the actual results as well as using approximations varying from the 5th to the 21st order. Total Demand Distortion (TDD) may not be used since the capacity is not defined with the model used.

Increased accuracy, as well as greater frequency content of the solution is seen as the degree of the approximation increases. This occurs, however, at the cost of computational intensiveness.

Table 6-5: Calculated THD using various order approximations

	THD
Original Function	0.5396
5th Order Approximation	0.5681
7th Order Approximation	0.5917
9th Order Approximation	0.5412
11th Order Approximation	0.5232
13th Order Approximation	0.5321
15th Order Approximation	0.5447
17th Order Approximation	0.5445
19th Order Approximation	0.5387
21st Order Approximation	0.5370

6.6.2 DC Saturating Function

Where the saturating function is either DC or of such a low frequency that it may be considered DC, the previously described method does not work because (7) is indeterminate. In this case, it is necessary to use an equivalent v_{sat} based on the flux in the transformer core due to the DC saturating current. Once this offset in flux is established, it is added to the upper and lower bands of the power frequency operating voltage in order to create an offset operating range for the transformer. The method previously described is repeated over the offset operating region. Table 6-6, shows the results of a 5th and 15th order regression for a sinusoid with v_0 = 1.0 pu and v_{sat} = 0.25.

Table 6-6: Magnitude results of approximation of frequency and magnitude

f	Magnitude		
	Original Function	5th Order Approximation	15th Order Approximation
60	0.0933	0.0766	0.0942
180	0.0770	0.0590	0.0780
300	0.0586	0.0370	0.0596
420	0.0370	---	0.0381
540	0.0171	---	0.0138

As was the case with an oscillatory saturating function, when a DC saturating function is used, the technique yields a good correlation, and accuracy improves as a higher degree of approximation is used.

6.7 Application of the Proposed Technique for Determining Both Frequency and Magnitude

The technique for predicting the magnitudes and frequencies generated by a saturated transformer is examined in the case of the transformer specified in the Appendix exposed to a power frequency voltage (v_0) of 1.0 pu plus a saturating voltage (v_{sat}) of 0.01pu at frequency (f_{sat}) of 3 Hz. The effective saturating voltage is 0.2 pu according to (7).

Six cases are considered. The frequency spectrum for the base case with a transformer exactly as specified is shown in Figure 6.14. Frequency spectra for transformers with two alternative magnetizing reactances (x_m) of 500 pu and 100 pu) are displayed in Figures 6.15 and 6.16, respectively. Frequency spectra for transformer with two variations in air core reactance ($x_{aircore}$) of 0.5 pu and 0.1 pu are presented in figure 6.17 and 6.18. Finally the effect of an elevated knee point (v_{knee}) of 1.25 pu on the frequency spectrum is depicted in figure 6.19.

All of the presented results (Figures 6.14 to 6.19) show an excellent correlation between the original function and the 15th order polynomial approximation. The 15th order approximation is selected to show sufficient detail in the sidebands around the higher harmonics of 60 Hz.
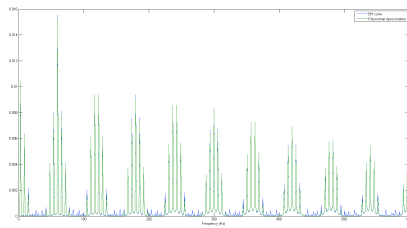
Figure 6.14: Frequency spectrum for normal operating conditions

Figure 6.15: Frequency spectrum with increased magnetizing reactance of 500 pu

Figure 6.16: Frequency spectrum with reduced magnetizing reactance of 100 pu

Figure 6.17: Frequency spectrum with increased saturated reactance of 0.5 pu

Figure 6.18: Frequency spectrum with reduced saturated reactance of 0.1 pu

Figure 6.19: Frequency spectrum with increased knee point of 1.25 pu

Of interest is the effect of manipulating the transformer characteristics on the magnitude and harmonic distortion of the magnetizing current. Decreasing the magn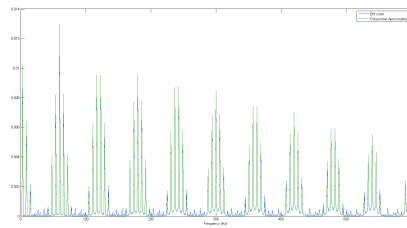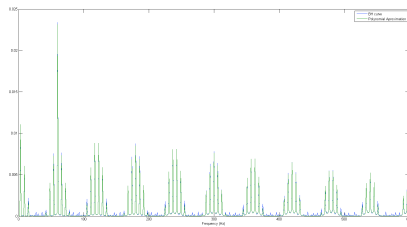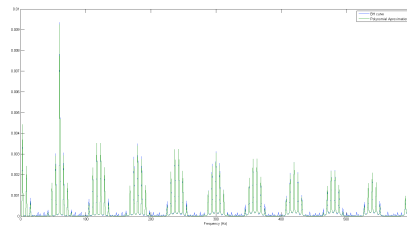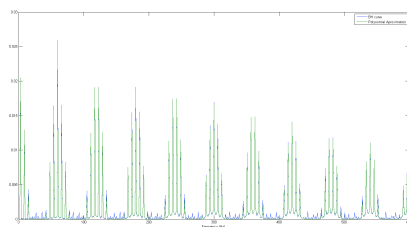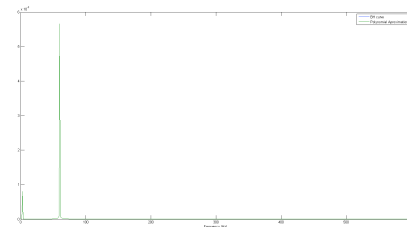etizing reactance serves to increase the point at which the transformer transitions to the saturated regions, see (6). This will cause the transformer to show less saturation for the same saturating function. Reducing the saturated reactance has the expected effect of increasing the magnetizing current and harmonics when saturated. Finally the case with the elevated knee point shows no signs of saturation since the new $v_{knee} = 1.25$ pu is greater than the voltage peak of 1.2 pu.

6.8 Conclusion

A simple technique is proposed to predict the spectrum of frequencies generated by a transformer due to its saturation by the injection of an oscillating current. This technique can be applied even without the detailed knowledge of the B-H characteristic of the transformer.

This technique is further extended to provide detailed estimations of the magnitudes of the frequencies generated. This may be useful in applications where electromagnetic transient simulation is unavailable, or undesirable due to computational intensiveness.

The modulated frequencies from saturated transformers may cause undesired interactions with network resonances of the system, resulting in magnification of some of these harmonics.

Higher order approximations yield more frequencies, however some of these may prove extraneous. Lower order approximations, on the other hand are limited in the their resolution. In some cases, it may not be necessary to

predict high frequency components as they may not cause undesired operation of FACTS devices such as Static VAr Compensators [6].

In the case of GIC, operators and system designers need to be aware of the potential for interaction between a saturated transformer and nearby reactive components. A harmonic overcurrent in a compensating capacitor could cause the tripping of protective systems and thus removing essential voltage support during a GIC event.

It should be noted that in the case of the extremely low frequency injection (1/10ths of Hz or less) of current seen during typical GIC events, the side bands will, within the resolution of most measuring equipment, merge into the harmonic frequencies.

The purpose of the study presented in this Chapter is to be able to eventually prepare for the operator a ready source of reference (a Lookup Table) that can predict the expected TDD with respect to a given level of GIC for a specific transformer. This TDD generation can be correspondingly related to the expected heating of the transformer.

Appendix: System data for the Study Transformer

Transformer type: three-phase autotransformer bank, each phase is on a separate core.
Base MVA: 100
Base Frequency 60 Hz
Leakage Reactance 0.001 pu
V1: 500 kV (ll, RMS)
V2: 230 kV (ll, RMS)
Neutral Connection: Grounded (0Ω)

Saturation Characteristics:

Air core reactance: 0.2 pu

Inrush Decay time constant: 1.0 s

Knee Voltage: 1.1 pu

Time to release flux clipping: 0.001 s

Magnetizing current: 0.004 pu

References

[1] D. H. Boteler, "Geomagnetic hazards to conducting networks," Nat. Hazards, vol. 28, pp. 537-561, 2003.

[2] V. Albertson, J. Kappenman and B. Damsky, "The influence of geomagnetically induced currents (GIC) on transmission systems," in Proceedings of the American Power Conference, 1990, pp. 311-15.

[3] D. H. Boteler, R. J. Pirjola and H. Nevanlinna, "Effects of geomagnetic disturbances on electrical systems at the earth's surface," Advances in Space Research, vol. 22, pp. 17-27, 1998.

[4] R. Pirjola, "Geomagnetically induced currents during magnetic storms," IEEE Trans. Plasma Sci., vol. 28, pp. 1867-1873, 2000.

[5] G. Sybille, L. Gérin-Lajoie, p. Giroux, "Interaction Between Static VAr Compensators and Series Compensation on Hydro-Québec 735 kV Network." Canadian Electrical Association, Power System Planning and Operation Section, March 1992.

[6] R. M. Mathur and R. K. Varma, *Thyristor-Based FACTS Controllers for Electrical Transmission Systems*, New York: Wiley-IEEE Press, 2002.

[7] R.A. Walling, A.H. Khan, "Characteristics of Transformer Exciting-Current during Geomagnetic Disturbances." IEEE Trans Power Del., vol. 6, no 4, pp. 1707-1714, 1991.

[8] N. Takasu, T. Oshi, F. Miyawaki, S. Saito and Y. Fujiwara, "Experimental analysis of DC excitation of transformers by geomagnetically induced currents," IEEE Trans. Power Del., vol. 9, pp. 1173-1182, 1994.

[9] EMTDC/PSCAD User Manual, HVDC Research Center, Manitoba, 2003.

[10] S. J. Chapman. *Electric Machinery Fundamentals, fourth Edition.* New York, NY: McGraw Hill: 2005. pp. 134-135.

Chapter 7   Conclusions and Future Work

This thesis deals with the impact of Geomagnetically Induced Currents (GIC) on electrical power systems from the perspective of power transformers. Power transformers act as the interface of GICs flow between the power network and earth. Furthermore, the two chief causes of problems arising from GIC are increased reactive power absorption and harmonic currents. These are caused due to the saturation of transformers by low frequency GICs. The research performed and the conclusions of each chapter are presented below. Each of the chapters correspond to a paper either published or being communicated for publication.

7.1   Chapter Summary

7.1.1 A Software Simulator for Geomagnetically Induced Currents in Electrical Power Systems

This chapter describes the development and testing of a software simulator to calculate the flow of Geomagnetically Induced Currents (GIC) in an electrical power transmission grid. In this chapter, a new technique for mapping the location of transmission equipment for the purposes of GIC simulation is proposed. The DC modeling of autotransformers for the purpose of GIC studies is discussed. The simulator models the electrical power system as an admittance matrix. GIC results for two study systems as obtained from the developed simulator are compared with those obtained from the Electromagnetic Transients Program (EMTP). Finally, the simulator is applied to the entire Hydro One 500/230 kV transmission system to calculate

the distribution of GIC in the network for a given set of electric field and earth modelling assumptions.

7.1.2 Determination of Geomagnetically Induced Current Flow in a Transformer from Reactive Power Absorption

This chapter proposes a novel technique to estimate Geomagnetically Induced Currents (GIC) in a transformer winding by measuring its absorbed reactive power. GIC is induced in electrical transmission lines by changes in the earth's magnetic field caused by solar magnetic disturbances and flows into transformers through neutral grounding connections. Assessment of GIC from readily available reactive power measurements is an attractive alternative to the installation of dedicated GIC monitoring equipment on every transformer of an HV transmission network. This technique is verified with PSCAD simulations and shows good agreement with the historical records captured in Hydro One's GIC detection network during the May 15 2005 SMD event.

7.1.3 Laboratory Validation of the Relationship Between Saturating Current and Transformer Absorbed Reactive Power

This chapter shows the results of laboratory work to confirm the linear relationship between Geomagnetically Induced Current (GIC) flowing through a transformer's windings and the reactive power absorbed by that transformer's core. This relationship is confirmed for various levels of GIC under different loadings.

7.1.4 Modelling and Mitigation of Geomagnetically Induced Currents on a Realistic Power System Network

This chapter uses the technique developed in Chapter 3 to correlate the magnitude of Geomagnetically Induced Current (GIC) with the reactive power absorbed by the transformer's magnetizing reactance to model the impacts of GIC in load flow studies (performed in PSS®E). A portion of an actual 500 kV power system segment is modeled and the impacts of a GIC event are considered on the voltage profile of the segment. What-if scenarios are considered and a potential operational mitigation strategy is proposed.

7.1.5 Determination of the Frequency Spectrum of the Magnetization Current of a Saturated Transformer

This chapter develops a technique to model the harmonic response of a saturated transformer. This technique is used to determine the range of frequencies of harmonic currents that will be generated when a transformer experiences saturation due to an injection of typically low frequency currents. This chapter examines the case when a power transformer is saturated due to geomagnetically induced currents (GIC). The proposed technique is validated for a study system utilizing EMTDC/PSCAD simulations. This technique will be useful in understanding the impact of transformer saturation on neighbouring equipment and as well as on FACTS controllers. Further this technique can be utilized to relate the GIC going through a transformer with the expected THD and consequent expected heating of the transformer.

7.2   Major Contributions

This thesis makes the following major contributions:

- A linear relationship between GIC flowing through a transformer core and the transformer reactive power absorption is demonstrated.

Previous work has shown a correlation, but has not sought to systematically define it.

- The linear relationship between GIC and reactive power absorption by a transformer core is proposed as the basis of a simple technique to measure GIC by employing measurements from reactive power meters normally already deployed in the network.

- The relationship between GIC and reactive power absorption is utilized to model the effects of GIC on bus voltages in a load flow study.

- The relationships between GIC and transformer reactive power absorption, and GIC and generation of harmonic currents by a saturated transformer, will allow utilities to easily assess the impact of a GIC event on their transformers. Until now there has been no method to directly measure the impact of GIC on system health and survivability.

- A method has been developed to explain and predict the frequencies of harmonic currents generated when a transformer is saturated by a low frequency oscillating voltage. This method has been extended to also predict the magnitude of these currents.

It is expected that this thesis will be of value to utilities like Hydro One in planning mitigation measures against GICs.

7.3   Future Research Directions

7.3.1 Correlation Between GIC and Transformer Reactive Power Absorption

The data presented in Chapter 3 for Hydro One's Essa TS, is the only viable data that could be taken from what was a relatively minor GIC incident.

Essa's configuration as three single-phase transformers, makes it particularly vulnerable to the effects of GIC since very little DC current is needed to result in a fairly high flux, compared to three-phase core configurations which have a higher reluctance to DC flux. When data becomes available for more extreme events in future, the work in Chapter 3 should be repeated using different transformers at higher levels of GIC.

The electromagnetic transient simulation work in Chapter 3 was done only for a bank of single-phase autotransformers. The poly-phase transformer models in PSCAD are not designed to handle DC flux and do not appear to behave correctly. These models should be extended, or new models created, to handle DC flux, including flux paths outside of the core iron, and the studies repeated.

7.3.2 Impacts of Harmonic Generation on Transformer Heating and Survivability

This research establishes a relationship between transformer absorbed reactive power and GIC, and TDD due to GIC. This relationship can be extended to relate expected transformer heating to GIC levels. With this relationship it is possible to set alarm levels to warn of excessive transformer spot heating due to harmonic generation. Work needs to be done to establish working limits for TDD in transformers. Once these limits are established they can be represented as reactive power absorption levels for those transformers. The limits can be used to inform system operation to protect transformers from damage in the case of a GIC event.

7.3.3 GIC Mitigation Strategies

The strategy of reducing the impact of GIC by removing lines from service was introduced in Chapter 5. While this strategy proved effective in reducing

the net GIC on the system, the impact on the flow of power was not treated in detail. A detailed investigation of the impacts in terms of power flow capacity, contingency planning and system stability can be undertaken to determine the practicality of this method. The possibilities of load shedding or system islanding to allow lines to be removed from service to mitigate GIC can be investigated.

Vitae

NAME:	Jonathan Eric Berge
PLACE of BIRTH:	Mississauga, Ontario, Canada
EDUCATION:	The University of Western Ontario London, Canada 2006-2011, Ph.D.
	The University of Western Ontario London, Canada 2004-2006, M.E.Sc.
	The University of Western Ontario London, Canada 2000-2004, B.E.Sc.
WORK EXPERIENCE:	Lecturer The University of Western Ontario 2011
	Teaching Assistant The University of Western Ontario 2004-2010
HONOURS and AWARDS:	National Sciences and Engineering Research Council of Canada (NSERC) Industrial Post Graduate Scholarship II September 2007 to August 2010

PUBLICATIONS:

Peer Reviewed Conference Papers:

[1] **J. Berge**, R. K. Varma. "Determination of the Spectrum of Frequencies Generated by a Saturated Transformer", Accepted to Proc. of 2011 Canadian Conference on Electrical and Computer Engineering, Niagara Falls, Ontario, Canada.

[2] **J. Berge**, R. K. Varma, W. Litzenberger. "Bibliography of FACTS 2009/2010 Part I: IEEE Working Group Report", Accepted to Proc. of IEEE PES General Meeting 2011, Detroit, Michigan, USA.

[3] **J. Berge**, R. K. Varma, W. Litzenberger. "Bibliography of FACTS 2009/2010 Part II: IEEE Working Group Report", Accepted to Proc. of IEEE PES General Meeting 2011, Detroit, Michigan, USA.

[4] **J. Berge**, S. S. Rangarajan, R. K. Varma, W. Litzenberger. "Bibliography of FACTS 2009/2010 Part III: IEEE Working Group Report", Accepted to Proc. of IEEE PES General Meeting 2011, Detroit, Michigan, USA.

[5] **J. Berge**, S. S. Rangarajan, R. K. Varma, W. Litzenberger. "Bibliography of FACTS 2009/2010 Part IV: IEEE Working Group Report", Accepted to Proc. of IEEE PES General Meeting 2011, Detroit, Michigan, USA.

[6] R. K. Varma, **J. Berge**, W. Litzenberger. "Bibliography of FACTS 2009 Part I: IEEE Working Group Report", Proc. of IEEE PES General Meeting 2010, Minneapolis, Minnesota, USA.

[7] **J. Berge**, R. K. Varma, W. Litzenberger. "Bibliography of FACTS 2009 Part II: IEEE Working Group Report", Proc. of IEEE PES General Meeting 2010, Minneapolis, Minnesota, USA.

[8] **J. Berge**, R. K. Varma, W. Litzenberger. "Bibliography of FACTS 2009 Part III: IEEE Working Group Report", Proc. of IEEE PES General Meeting 2010, Minneapolis, Minnesota, USA.

[9] R. K. Varma, **J. Berge**, W. Litzenberger. "Bibliography of HVDC Transmission 2007-2008 Part I: IEEE Working Group Report", Proc. of IEEE PES General Meeting 2009, Calgary, Alberta, Canada.

[10] **J. Berge**, R. K. Varma, W. Litzenberger. "Bibliography of HVDC Transmission 2007-2008 Part II: IEEE Working Group Report", Proc. of IEEE PES General Meeting 2009, Calgary, Alberta, Canada.

[11] **J. Berge**, R. K. Varma. "A Software Simulator for Geomagnetically Induced Currents in Electrical Power Systems", Proc. of 2009 Canadian Conference on Electrical and Computer Engineering, May 3-6, 2009, St. John's, Newfoundland, Canada.

[12] **J. Berge**, R. K. Varma. "Real Time Digital Simulation of a Static VAr Compensator (SVC) for Load Compensation", Proc. of 2007 Large Engineering Systems Conference on Power Engineering (LESCOPE), October 10-12, 2007, Montréal, Quebéc, Canada.

[13] R. K. Varma, W. Litzenberger, **J. Berge**, "Bibliography of FACTS: 2001 – Part I – IEEE Working Group Report." Proc. of IEEE PES General Meeting 2007, Tampa, Florida, USA.

[14] R. K. Varma, W. Litzenberger, **J. Berge**, "Bibliography of FACTS: 2001 – Part II – IEEE Working Group Report." Proc. of IEEE PES General Meeting 2007, Tampa, Florida, USA.

[15] R. K. Varma, W. Litzenberger, **J. Berge**, "Bibliography of FACTS: 2002 – Part I – IEEE Working Group Report." Proc. of IEEE PES General Meeting 2007, Tampa, Florida, USA.

[16] R. K. Varma, W. Litzenberger, **J. Berge**, "Bibliography of FACTS: 2002 – Part II – IEEE Working Group Report." Proc. of IEEE PES General Meeting 2007, Tampa, Florida, USA.

[17] R. K. Varma, W. Litzenberger, **J. Berge**, "Bibliography of FACTS: 2003 – Part I – IEEE Working Group Report." Proc. of IEEE PES General Meeting 2007, Tampa, Florida, USA.

[18] R. K. Varma, W. Litzenberger, **J. Berge**, "Bibliography of FACTS: 2003 – Part II – IEEE Working Group Report." Proc. of IEEE PES General Meeting 2007, Tampa, Florida, USA.

[19] R. K. Varma, W. Litzenberger, S. Auddy, **J. Berge**, A. C. Cojocaru and T. Sidhu. "Bibliography of HVDC 2004-2005 IEEE Working Group Report", Proc. of IEEE PES General Meeting 2006, Montreal, Quebéc, Canada.

[20] R. K. Varma, W. Litzenberger, S. Auddy, **J. Berge**, A. C. Cojocaru and T. Sidhu. "Bibliography of FACTS 2004-2005 Part I: IEEE Working Group Report", Proc. of IEEE PES General Meeting 2006, Montreal, Quebéc, Canada

[21] R. K. Varma, W. Litzenberger, S. Auddy, **J. Berge**, A. C. Cojocaru and T. Sidhu. "Bibliography of FACTS 2004-2005 Part II: IEEE Working Group Report", Proc. of IEEE PES General Meeting 2006, Montreal, Quebéc, Canada

[22] R. K. Varma, W. Litzenberger, S. Auddy, **J. Berge**, A. C. Cojocaru and T. Sidhu. "Bibliography of FACTS 2004-2005 Part III: IEEE Working Group Report", Proc. of IEEE PES General Meeting 2006, Montreal, Quebéc, Canada.

[23] **J. Berge**. "Real Time Digital Simulation of a Static VAr Compensator (SVC) for Load Compensation", Poster-Paper Presented at IEEE PES General Members Meeting 2005, June 2005, San Francisco, California, USA.

Other Conferences:

[24] **J. Berge**. "Improving Wind Power Generation in Weak Electrical Power Systems: Static VAr Compensator Application for Voltage Control in Electric Grids Fed by Wind Farms" Earth Day Colloquium: 21 April 2008, University of Western Ontario, Canada.

Teaching Resources:

[25] **J. Berge**, R. K. Varma. "ECE 333b (Electrical Machines and Power systems II) Laboratory Manual", *University of Western Ontario, Department of Electrical and Computer Engineering.* 2006. (Revised 2007)

[26] **J. Berge**, R. K. Varma. "ECE 3333 (Electric Power Systems I) Laboratory Manual", *University of Western Ontario, Department of Electrical and Computer Engineering.* 2008. (Revised 2010)

Technical Reports:

[27] **J. Berge**, R. K. Varma. "Comparison of Two and Three Blade Helical, Vertical Axis Wind Turbines", Prepared for Spira Wind Energy. 2006.

[28] **J. Berge**, R. K. Varma. "SVC For Load Compensation", Prepared for Cos-Phi Inc. pursuant to a MMO interact grant. 2006.